UNIVERSITY OF NAPLES FEDERICO II
DEPARTMENT OF PHARMACY

PHD IN
*NUTRACEUTICALS, FUNCTIONAL FOODS AND HUMAN HEALTH* - XXXIV cycle

# NUTRACEUTICAL TO PREVENT URINARY TRACT INFECTIONS: PRECLINICAL STUDIES

PhD Thesis
**Marco Dacrema**

TUTOR:
PROF. MARIA DAGLIA

PHD COORDINATOR:
PROF. ALBERTO RITIENI

Academic Year 2021-2022

# Abstract

In the first and second year of my PhD course the aim was to find a new non-antibiotic candidate of plant origin, which could be use in the management of the UTIs. In the first phase, I selected five different plants, which were extracted to explore their potential against uropathogenic *E. coli*. According to the literature the plants selected for the studies were: *Camellia sinensis L.* (Leaves), *Punica Granatum L.* (Fruit), *Orthosiphon stamineus* (Leaves), *Morus alba L.* (Leaves), *H. Sabdariffa* (Flowers). All the plants were extracted, and the extracts screened to select the most promising plant extract according to their polyphenol concentration, antioxidant, and antimicrobial activities. Based on these results we selected only one of the most promising extracts (*H. Sabdariffa*) and we performed UHPLC coupled to IT-TOF profile assessing the main compounds and understanding the possible mechanism of action of these molecules against the uropathogenic *E. coli*. Finally, there was the evaluation anti-invasivity activity using bladder carcinoma cells (HT-1376). In the third year of the PhD course, which took place at the Leibniz-Institut für Lebensmittel-Systembiologie an der Technischen Universität München, a non-canonical approach was followed, with the final aim to update the literature on the TAS2R expression and the *in vitro* bioavailability of Cucurbitacin B, which is contained in *Momordica charantia L.* fruits. For this reason *M. charantia.* fruits were divided into seeds, pulp, and skin and these parts and the whole fruit were extracted three consecutive times using water, acetonitrile/water (70/30) and ethyl acetate. The extracts were characterized with an untargeted UHPLC-Tof-MS screening. After the metabolic profile assessment and the determination of cucurbitacins in the extracts, the next step was understood if cucurbitacin B, present in each part of the fruit, was able to reach the GU tract using the transwell system. Moreover, considering the poor

literature on TAS2R in CACO-2 cell line we decided also to explore their expression in this specific cell line and to treat the cells with bitter melon extract to understand if the treatment could change the expression of this receptor.

# Contents

# Introduction

## 1.1 Urinary tract infections

Urinary tract infections (UTIs) affect more than 150 million of people each year and are considered one of the most frequent bacterial infections. The American health care system in 2007 registered a record of 10.5 million visit for UTI symptoms and 2–3 million emergency department visits [1–3]. The average cost per year in the United States for the treatment of UTIs is estimated around US$3.5 billion per year. UTIs are considered frequent bacterial infections caused by Uropathogenic bacteria. In most cases the infection is determined by *Escherichia coli* (UPEC) (>85%) [4], but also other gram-negative, positive bacteria or even fungi (e.g., *Klebsiella pneumoniae*, *Staphylococcus saprophyticus*, *Enterococcus faecalis*, group B *Streptococcus* (GBS), *Proteus mirabilis*, *Pseudomonas aeruginosa*, *Staphylococcus aureus* and *Candida* spp.) [5-8] were isolated from patients with UTIs. The recurrence of UTI (RUTI), for definition, occur when the patient has more than two episodes in 6 months or three in 12 months. The incidence of UTI especially for women is very high, in fact the recurrence rate in women is about 2.6 infections per year, considering that one woman every two is affected by UTIs in her lifetime against the lifetime prevalence in men of 13.7% [9]. From clinically point of view UTIs are divided in uncomplicated and complicated (Fig.1). In the first case there are no neurological urinary abnormalities, and these types of infections cause cystitis (lower UTIs) or pyelonephritis (upper UTIs). Different risk factors are associated to the uncomplicated UTIs such as: obesity, diabetes, sexual activity, female gender, vaginal infections, and genetic susceptibility [11, 10]. The complicated UTIs instead are related to the urinary tract impairment due

to the renal transplantation, urinary obstruction, immunosuppression, pregnancy, renal failure, and neurological disease. Sometimes also calculi or foreign bodies or the use of the catheters could eventually promote the complicated UTIs development. The catheter associated UTIs are also called CAUTIs, and the prolonged catheterization, diabetes, older age and female gender are risk factors that promotes also the bloodstream infections [12].

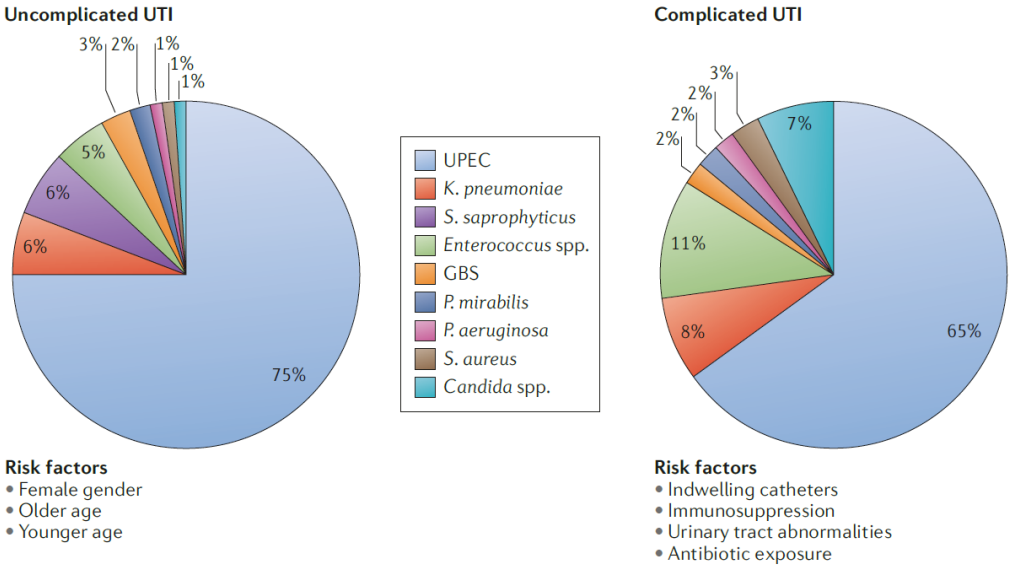


Fig.1 Gram-positive, gram-negative bacteria or fungi can cause uncomplicated or complicated UTIs. The most common pathogen for both is uropathogenic *Escherichia coli* (UPEC). However, the prevalence of the other bacteria for uncomplicated UTIs are: *Klebsiella pneumoniae*, *Staphylococcus saprophyticus*, *Enterococcus faecalis*, group B *Streptococcus* (GBS), *Proteus mirabilis*, *Pseudomonas aeruginosa*, *Staphylococcus aureus* and *Candida* spp. Instead, the complicated UTIs are determined by: *Enterococcus* spp., *K. pneumoniae*, *Candida* spp., *S. aureus*, *P. mirabilis*, *P. aeruginosa* and GBS.

## 1.2 Pathophysiology, adherence and colonization

Only the distal urethra is normally colonized by the genital and cutaneous flora, but the urinary tract is normally sterile and there are different mechanisms able to prevent the bacteria ascension such as the urethra and the osmolarity, pH and organic content of urine. Moreover, the urination process promotes the elimination of bacteria which could eventually develop the infection (Sobel, 1997). If these physiological barriers fail to prevent the bacterial colonization the urothelial cells can produce inhibitors of bacterial adhesion promoting an anti-inflammatory and anti-bactericidal effect inducing the exfoliation process of the infected cells. *E. coli* urinary tract colonization is influenced by the production of different adhesins, different strains of this bacteria can colonize the urinary tract (Fig. 2):

1) The type 1 adhesin promote the interaction between the pathogen and the low urinary tract.

2) The type P induces pyelonephritis due to the binding with glomerulus and endothelial cells inducing a modification of ureteral peristalsis. [14, 15].

3) The non fimbrial *E. coli* promotes the adherence to the urinary tract and colonization of the urinary tract thanks to the presence of extracellular matrix proteins [16].

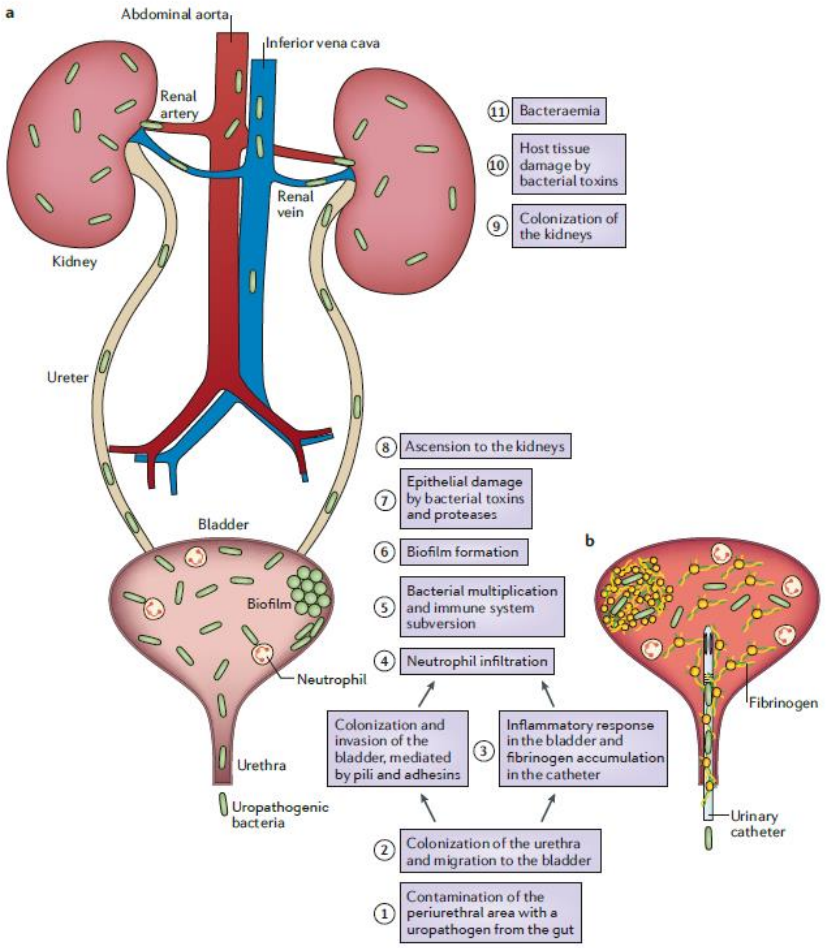


Fig.2 Gut uropathogen can contaminate the periurethral area promoting the colonization of the urethra. The next step is the migration to the bladder ant the interaction between the pili and adhesins expressed on the surface of umbrella cells. The inflammation induced from the neutrophil infiltration determine the elimination of the extracellular bacteria. The survival of some bacteria to the immune reaction causes the multiplication and the biofilm formation. The lower urinary tract infection can evolve in high urinary tract infection after the production of toxins and proteases with consequent cell damage. At the end the ascension and kidney colonization result in host tissue damage with the born of complicated UTI. B The catheterization process induces the bladder colonization and the production of fibrogen on the catheter, the bacteria starts to produce fibrogen binding protein. The formation of the biofilm

is consequent to the bacteria division; the infection can also in this case promote epithelial damage and proceed to the kidney inducing tissue damage.

The survival of the uropathogens is related to their invasion in the bladder epithelium, they can produce toxins inducing cell death and promoting the release of nutrients from the host cells. Another essential factor is the absorbtion of iron after the synthetization of siderophores. After the colonization bacteria start the division, which promotes the invasion of the kidney and the colonization of renal epithelium after the production of damaging toxins. The uncomplicated UTI are determined by the interaction between the pathogen and the bladder epithelium. The bladder epithelium, which is composed by basal cells, intermediate cells and umbrella cells can be invaded by UPEC bacteria (17) thanks to the expression of uroplakins and $\alpha_3\beta_1$ integrins, which are generally expressed on the uroepithelial cells (18,19). The complicated UTI instead, are usually determined by a physical obstruction or by the catheterization process. *P. mirabilis*, *P. aeruginosa* and *Enterococcus* spp. can cause complicated UTI more frequently; the formation of biofilm in this case is very common with the consequent persistence of the infection (20, 21).

## 1.3 Antibiotic treatment and resistance

The activity of antibiotics is decreasing and becoming a problem, in fact the resistance of amoxicillin in *E. coli* isolated from UTI patients is now 100% in some Africa countries. Moreover, the main common antibiotics, generally prescribed to the patients who suffer of UTIs or RUTIs, start to be ineffective all over the world. Lord O´Neil

has prepared a recent modeling to predict the possible consequences for the antimicrobial resistance, the model predicts 10 million of deaths per year and a loss of US$100 trillion by 2050 (Fig.3) (22, 23).

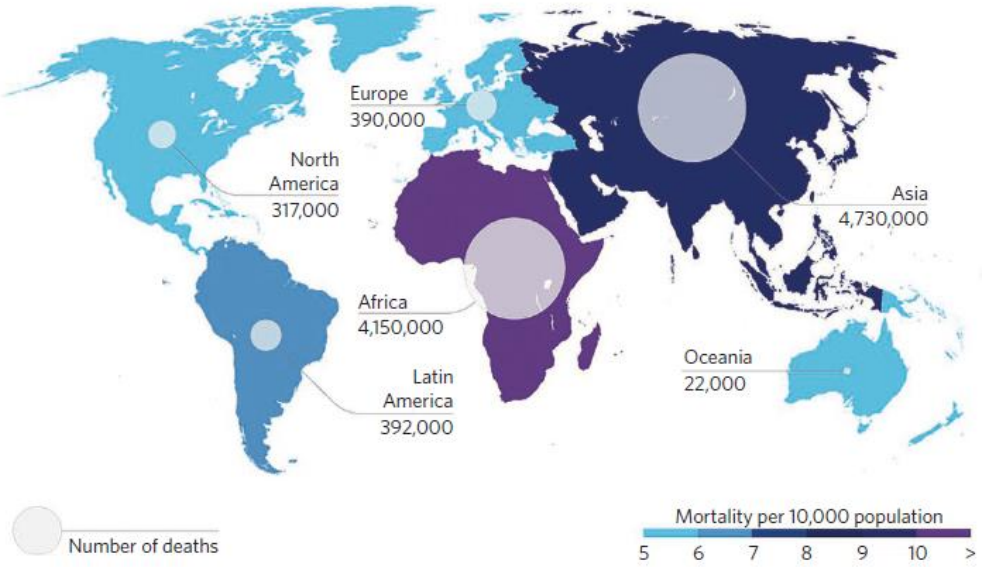


Fig.3 Deaths attributable to the antibiotic resistance by 2050.

The antibiotic resistance is a natural phenomenon and to slow down the spread of new resistance strain alternative therapies and diagnostics are needed together with prevention and control measures. The inappropriate use of antibiotics in human and animals but also the hygiene and basic sanitation should be improved to prevent the incidence of infectious disease and our antibiotics need. Until now low dose antibiotic remains the keystone for the prevention of RUTI, however this type of therapy works only in 85% of cases if compared to the placebo patients [24]. This type of strategy induces the born of new multi-drug resistant organism and increase the health care system. For all the reasons cited above is becoming more important the development of new non-antibiotics options.

## 1.4 Non antibiotic treatment

### 1.4.1 Vaccines

The aim of the vaccines to prevent UTI is to protect the host stimulating the immune response against the pathogen. The vaccine available until know are surface antigen or inactivated bacteria both obtained from uropathogens to promote the production of antibodies able to react to the target [25]. The aim of the vaccine should be to target critical bacteria components involved in the bladder colonization such as: alfa-hemolysin, siderophores and fimbrial units [26]. Until know there are 4 different vaccine that are tested in control randomized trials: UroVaxom® , Urovac®, ExPEC4V and Uromune®. UroVaxom® is obtained from the extraction of 18 different UPEC strains and it can stimulate the innate immune systems [27]. It was tested on mouse models confirming the defense response within the bladder using *K. Pneumoniae*. Instead Urovac® seems to reduce the risk of RUTIs RR 0.75, 95% CI 0.63–0.89) [28, 29]. A second study highlight the efficacy of the treatment after the booster vaccination [26]. Several trials phase 1 and 2 was accomplished with ExPEC4V a vaccine, which present four different *E. coli* serotypes and it shows a good safety and immunogenicity [29-32]. Uromune® is a sublingual vaccine which can reduce the recurrence of infection between the 70% and 90% when compared to the antibiotic prophylaxis [33]. The administration for 3 months highlights the absence of UTIs for the next one year for 59 of 75 women, which received the treatment [34]. The result was similar for another prospective study of 784 women, which 65% had zero or only one UTI after the administration [35].

### 1.4.1.1 Vaccines targeting adhesion

The interaction between bacteria and urothelium allow to the bacteria to resist to the elimination process through the flow of urine in the bladder. The shaperone-usher pathway (CUP) is a critical virulence factor which promotes the between bacteria and the formation of the biofilm [36]. The irreversible bacteria attachment and invasion is driven the Type 1, P and S pili generally present in UPEC, the adhesion-host cell interaction with this pili should be blocked by vaccine canditates (Fig. 4). FimH is able to bind the mono-mannose present on the urinary tract receptors [37], in 2000 Langermann et al. develop a vaccine which protects cynomolgus monkeys from cystitis [38], while poggio et al. [39] showed the cystitis protection after the intranasal and intramuscular administration. A good response for *E. coli* and *P.mirabilis* was obtained after the transurethral instillation of a recombinant protein MrpH.FimH of two different adhesins [40]. The P fimbra is the major subunit of PapA and minor of PapD, PapE, PapF and PapG, only 1000 subunits of this protein can induce the hemagglutination of erytrhrocytes (Riegman et al., 1988). However, the vaccine generation based on P fimbra was not effective like the other one, only in 2004 Roberts et al. obtained a good result with a vaccine purified on PapDG.

### 1.4.1.2 Vaccines targeting capsule

The use of capsules is promising for the vaccine strategy; in particular, the capsule should protect the bacteria from the immune system engulfment and bactericidal effect

[42] and at the same time on the surface of the capsule are expressed receptor ligand able to bind the target tissue. One of the first study a subcutaneous, intraperitoneal or bladder injection was performed in rhesus monkeys to show the protection from pyelonephritis [43-45]. However, the vaccine target capsule formulation is a challenge also considering the huge heterogeneity of *E. coli* serotypes, moreover, is very hard evade the immune response using the molecular mimicry and for these reasons there are no studies on humans yet.

### 1.4.1.3 Vaccines targeting toxins

The UPEC toxins can induce the signaling cascade promoting the inflammatory process, cell death and the invasion of the bacteria in different tissues. The most studied toxins are α-hemolysin (HlyA) (Fig. 4), which can lyse erythrocytes through the pore formation and at the same time is able to promote the exfoliation of epithelial bladder cells [42]. Instead, the necrotizing factor 1 (CNF1) is able to interfere with the phagocytosis and induce apoptosis in the host cells [46]. This toxin is also able to assess the entrance of the bacteria in the host cell, their use in the vaccine production could be useful to protect bladder and kidney from damage tissue but at the same time are not the best candidates for their immediate bacteria removal (Fig. 4) [47]. An interesting target could be the outer membrane vescicles (OMVs), which contain non protein antigens, adhensins and enzymes. Their formation is related to the bacteria division but the knowledge on this vescicles is still very limited [48]. Alternative Therapeutics in Urinary Tract Infections

### 1.4.1.4 Vaccines Targeting Iron Metabolism

Another essential factor for the bacteria survival is the absorption of the iron, *E. coli* uses this element to carry out numerous actions (eg. Peroxides metabolism, DNA synthesis, storying oxygen and electron transport) however its availability is limited in the host environment (Fig.4). The production of siderophores such as yersiniabatin, aerobactin, enterobacterin, and salmochelin [42] promote the iron absorption. The antibodies against yersiniabactin receptor and FyuA were studied for the first time by Brumbaugh et al. [49] and both had a good protection for kidney infections in mice. The same author in another study also underlined the efficacy of IreA and IutA antibodies for the kidneys and Hma for the intranasal immunization [50].

## 1.4.2 Small compounds

The small molecules approach allows inhibiting the capacity of adhesion of the UPEC blocking the assembling process of the pili. Small molecules, which are generally used from bacteria for the pili production are used as mimic molecules to block the adhesion process. The target in general are the fimbriae, in particular the P-fimbriae and the Type 1 [51]. These pilicide molecules present ring-fused 2-pyridone backbone which can interact directly with the hydrophobic substrate binding sites of the assembly chaperone [52]. In the 2014 Greene et al. [53] tested for the first time the most potent inhibitor of type 1 piliation, the pilicide ec240, able to block the biofilm formation with a strong reduction 70–80%) of fimbriae density [54] with a decrease of the Type 1 pilus on biofilms [55]. Even if study related to the pharmacokinetic and

pharmacodynamics are needed there are promising studies in mice which sustain also a reduce of the virulence *in vivo* [56]. Another target for small compounds is the enzyme able to catalyze the urea, which is essential to promote the urine alkalinization and production of struvite and carbonate apatite [57]. This process could contribute to the pyelonephritis and promote the biofilm formation [58,59], the bacterial and host cysteine protease [60] are the most studied inhibitors. Unfortunately, these molecules present a mutagenic power, and the research was stopped even if the first results were promising [61, 62]. Until now no *in vivo* or clinical trials have been conducted and due to the poor hydrolytic stability, these molecules have a very short half-life [63]

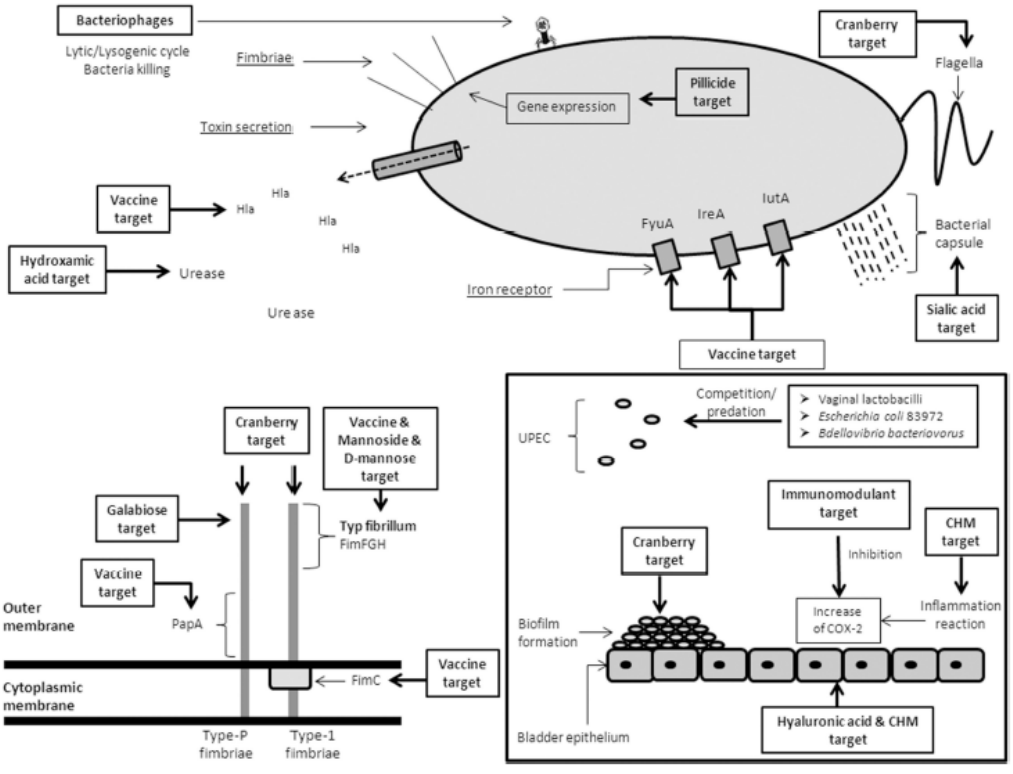


Fig.4 Alternative therapeutic method scheme for the treatment of UTI.

Another interesting strategy is the use of polysaccharide capsule, very effective in the UPEC virulence for their role in the biofilm formation [64, 65]. The use of these capsules is still limited for their antigenicity and low bioavailability [66] even if the mice studies were promising (Fig. 4) [67].

### 1.4.3 Probiotics

In the vaginal flora the lactobacilli are dominant [68] and can interfere with the adherence process and colonization of UPEC restoring the normal bacterial homeostasis (Hardy et al., 2013) (Fig. 4). Until now the mechanism of action of lactobacilli remains still unknown even if the literature highlights three different benefits against UPEC:

1) Competitive action against the uropathogens for nutrient and attachment sites [70].

2) Reducing of virulence thanks to the production of hydrogen peroxide and lactic acid with the consequent downregulation of the virulence genes and of the 1- and P-fimbrie genes in *E. coli* [71].

3) The bactericidal effect induced by the production of peptides called bacteriocins. These molecules are strain specific and some of the have been already identified against *E. coli*. [72-74].

A clinical study underlines the anti-inflammatory and immune-regulatory activities [75] of the lactobacilli for 252 post-menopausal women with RUTIs. The patients were treated with 480 mg of of trimethoprim sulfamethoxazole (TMP-SMX) daily for the prophylaxis treatment or capsules with $10^9$ CFU of *Lactobacillus rhamnosus* GR-1 and *Lactobacillus reuteri* RC-14 [76] Both treatments result equal and to the antibiotic treatment. *Lactobacillus rhamnosus* GR1 and *Lactobacillus reuteri* RC14 seems to be [77] effective for the treatment of 620 patients affected by UTI using intravaginal suppositories. The combination between *Lactobacillus acidophilus* PXN 35, *Lactobacillus plantarum* PXN 47 and cranberry extract (36 mg/d PACs) was tested by Korodia et al. in randomized, double-blind, placebo-controlled study with 81 premenopausal women [78] after the administration of Bio-Kult Pro-Cyan. The reduction of UTIs were significant in the treated group after the twice-daily administration for 26 weeks. Another strategy provides the use of the *E. coli* 83972, which is a non-virulent strain, able to interfere with the growth and colonization of the UPEC. Until know from 2000 to 2010 have been conducted 7 different clinical studies which underline the ability of the non-virulent strain to protect patients from UTI, however the bladder colonization remains complex to achieve.

### 1.4.4 Predatory bacteria

Predatory Bacteria can invade the intraperiplasmic bacteria space digesting their host. The most interesting predatory bacteria are Bdellovibrio and Micavibrio (Fig.4), they use the type IV pilus to interact with the host cell and penetrate inside. All this process requires only 2-3 hours and the main target of these deltaproteobacteria are: *E. coli*,

*Klebsiella spp.* and *Pseudomonas spp.* [79, 80]. Until know the *in vitro* and mouse models confirm the negative impact on human cell lines due to the presence of these bacteria, however more information and studies are essential to proceed with clinical studies.

### 1.4.5 Bacteriophages

The bacteriophages could be considered an alternative treatment especially for ostearticular infections, otitis, and infected burns [81, 82]. Until now, this type of strategy is not used in UTI even if there are some promising studies, which highlight the bactericidal effect. The combination of bacteriophage cocktails seem to be effective on *E. coli* ad *K.pneumoniae* strains and the lytic *in vitro* activity is between 66% and 93% [83]. The animal study conducted by Dufour et al. (2016) assess the reduction of *E. coli* and Pneumonia load in the kidney infection model [84]. The absence of adverse effect is reported by Ujmajuridze et al. [85] after the treatment of 9 patients with a commercial preparation of Pyo bacteriophage. The bacteria load decreses for 6 of the 9 treated patients. Interesting are two case reports, in the first one a patient with *P. aeruginosa* UTI is treated with a phage cocktail able to reduce the bacteria load in the urine of 10-fold after 5 days of treatment, in the other one is cured after 10 days of treatment with an intravescical bacteriophage treatment [86]. Also, in this case the literature is promising about the potential of bacteriophages, however more human studies are essential to define the real potential of this treatment.

## 1.4.6 Nutraceuticals

### 1.4.6.1 Cranberry and propolis

Fig 5. *Vaccinium macrocarpon* or cranberry fruits fruits (left), generally used to obtain the nutraceuticals for the treatment of UTIs. Propolis (right), which is a resinous bee product,

The health benefit of nutraceuticals are well known, food or food products can provided to the basic nutrition under medical form. A good example of effective nutraceutical for the treatment of UTI is the use of *Vaccinium macrocarpon* (Fig. 5), also called cranberry, which is very often use as prophylactic treatment to the RUTI [87]. Even if the mechanism of action remains still unclear the cranberry extract shows a very strong anti-adherence properties [88, 89] thanks to the inhibition of Type-I fimbriae. The A-type proanthocyanidin (PAC-A) can reduce the interaction between the bacteria and the host cells, moreover the extract also registered a reduction of motility and biofilm (Fig.6). Chan et al. [90] underline the reduction of biofilm formation on *E. faecalis*, moreover many other studies associate the reduction of adhesion of [91-93]; *E. faecalis*, *P. aeruginosa* and *E. coli*. In literature, the results of

clinical studies are difficult to interpret, Jepson et al compared placebo to control women with RUTIs and the conclusion was that the cranberry product was not useful to the reduction of symptomatic UTI. Also for Stapleton et al. the conclusion was that cranberry juice was not able to reduce the number of *E. coli* in urine [94, 95], however the different concentration of PAC-A used in the study could lead to misleading conclusions [96]. Another interesting consideration is also the variable effect of proanthocyanidins against different strains of *E. coli* as reported by [97].

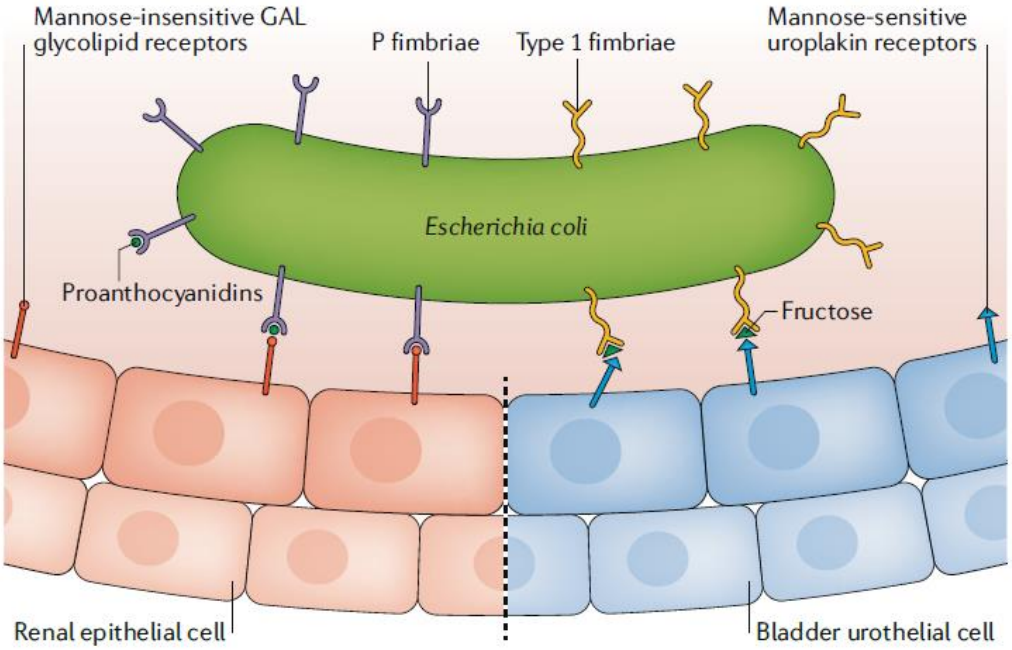


Fig.6 The proanthocyanins contained in the cranberry extract can interact with the P fimbriae interfering with the interaction of the glycolipid receptor present on the surface of the renal epithelial cell. In the same way, the fructose can block the interaction between the mannose uroplakin receptors on the bladder urothelial cells and the Type 1 fimbriae.

The effectiveness of cranberry can be enhanced thanks to the use of other natural products with antimicrobial properties. One example is propolis, which is a resinous

material collected by bees and mixed with was and enzymes. The propolis properties are well known and it is used also for gastrointestinal disorder, oral and dermatological health [98-103]. Ranfaing notice that the variable effect of cranberry between the *E. coli* strains was reduced or deleted when the cranberry extract was combined with the propolis [104]. Another study conducted by Bruyère confirmed the longer onset of cystitis for the women treated with propolis and cranberry if compared to placebo [105].

## 1.4.7 Glycosaminoglycan, hyaluronic acid, chondroitin sulfate and hyaluronic acid

Another possible alternative treatment is the use of Hyaluronic acid, the bladder cells can produce a protective layer of polysaccharide sulfated polysaccharide glycosaminoglycan (GAG), which is damaged during the infection process after the secretion of virulence factors (Fig. 7) [106].

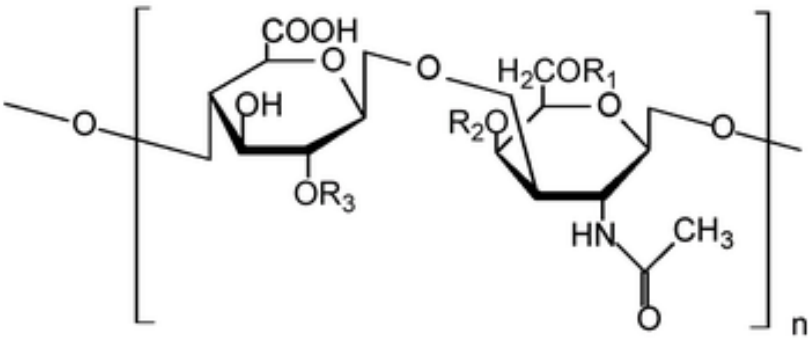

Fig.7 Glycosaminoglycans are constituted long linear polysaccharides consisting of repeating disaccharide units

So, the use of chondroitin sulfate (CS) and hyaluronic acid (HA) in the bladder epithelium could be a new strategy for the management of the UTI. A study on 276 women (aged 18–75 years) were treated with HA and CS to treat the UTIs, the result show that there was not a significant difference considering the number of recurrences or the median time to first recurrence [107].

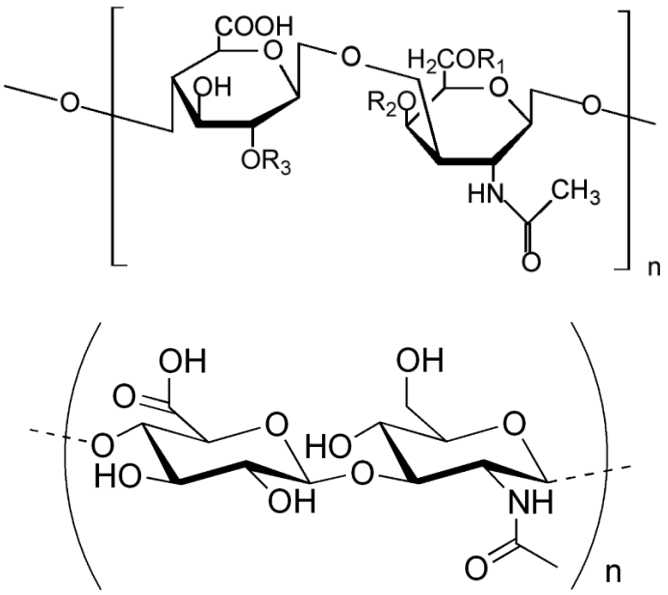


Fig.8 Chemical structure of CS and HA.

Loubet et al. find a reduction of 49% in recurrence rate in patients treated with HA + CS, in another similar study 157 women had a reduction in UTI recurrence [108]. The synergy between HA + CS could be present according to the study of 145 postmenopausal women with urogenital atrophy or recurrent UTI, in this study the participants were treated with

vaginal estrogen, oral HA + CS + vaginal estrogen and oral HA. The oral treatment together with the estrogen therapy was the more effective, however a positive response was registered also for the other treatments [109]. The intravescical administration of HA is more invasive but at the same time more performant if compared to the *os* one.

### 1.4.8 D-mannose, galabiose and vitamin C

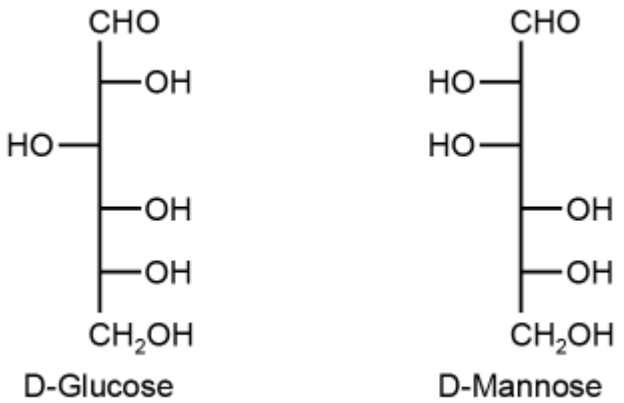


Fig. 9 Molecular structure of D-glucose and D-mannose.

The interaction between FimH and mannose-binding lectin domains present on the surface of mannosylated host cells are essential to start the infection and invasivity process (Fig. 9). There are two different strategies to block the interaction between the bacteria and the host:

1) Thanks to the similar molecular structure between D-mannose and glucose the D-mannose can block the adhesion between FimH and the host cell. The absorption is

fast and the require time for D-mannose to reach all the organs are around 30 min, moreover the elimination is through the urinary tract [110].

2) Mannosides are molecules able to block the FimH function and the *in vitro* biofilm formation growth [111, 112]. Mice studies highlight the decrease in bladder colonization after the *os* administration of mannosides for the prevention of chronic and acute UTI [113, 114]. Kranjcec et al. compare the risk of recurrence between a group treated with nitrofurantoin ad a group treated with D-mannose powder. The risk between groups were similar considering a strong side effect reduction in the D-mannose group [115].

Another important interaction between the host and the bacteria occurs between the P fimbriae and the PapG galabiose like receptor [116]. This type of receptor can promote the ascension of the bacteria to the kidneys and for this reason some drugs are designed to target different variant of the PapG receptor (PapG II and PapG III) (Fig.10) [117]. The galabiose has a great potential for the reduction of UTI but at the same time any *in vivo* studies have been performed until now.

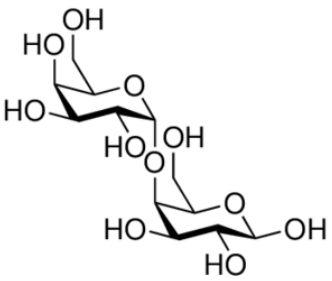


β-Galabiose
α-D-galactopyranosyl-(1-4)-β-D-galactopyranose

Fig. 10 Galabinose, which could be used for the treatment of UTIs, is a disaccharide based on two galactose residues.

Another important interaction between the host and the bacteria occurs between the P fimbriae and the PapG galabiose like receptor [116]. This type of receptor can promote the ascension of the bacteria to the kidneys and for this reason some drugs are designed to target different variant of the PapG receptor (PapG II and PapG III) [117] (Fig. 10). The galabiose has a great potential for the reduction of UTI but at the same time any *in vivo* studies have been performed until now. Vitamin C presents antimicrobial and antioxidant activities. The release of reactive oxygen species (ROS) during the infection process are limited by the vitamin C through killing or deactivation of the microorganisms. The level of ROS is reduced thanks to the essential role of vitamin C in the oxidative stress pathways [118], moreover vitamin C (Fig. 11) can also decrease the colonization and adhesion of the bacteria involved in the CAUTI. In the 2007 Ochoa-Brust et al. confirmed the efficacy of 110 pregnant women treated with 100 mg ascorbic acid for 3 months reducing the incidence of UTIs from 29.1 to 12.7% [119].

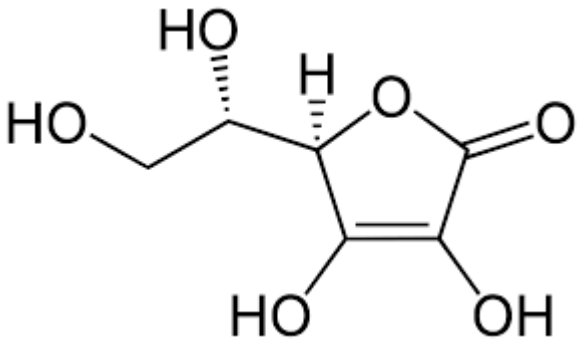


Fig. 11 Molecular structure of vitamin C

## 1.5 Extraoral bitter taste receptor (T2R) a new target for UTIs

### 1.5.1 Bitter taste receptor

Bitter taste receptor belongs to the G protein-coupled receptors (GPCR) family, which are activate by the presence of bitter substances [120-122]. This response induces the activation of the GPCR subunit called Gα-gustducin, the receptor is activated by different substances such as: amarogentin, caffeine, N-phenylthiourea, 6-propyl- 2 thiouracil, picrotin, salicin, denatonium, phenylthiocarbamide, procainamide and cycloheximide [123, 124]. The signal transduction of T2R is related also the signaling molecules cascade of sweet and umami receptors (i.e., T1Rs; 125-129). The activation of Gα-gustducin induces the dissociation of α, Gnat3, and βγ subunits promoting the activation of PLCβ2 and the consequent release of Ca2+ from InsP3-sensitive Ca2+. All this cascade determines the biological response through the Na+ influx TRPM5 channels and the depolarization of the cells with the release of ATP thanks to CAL HM1 ion channels [130-131] (Fig. 12). The ATP induce the activation of purinergic receptor with the transmission of the nervous impulse to the central nervous system with the perception of bitter taste [132, 133]. However, the extraoral T2R presents different mechanisms to promote their biological roles according to their location.

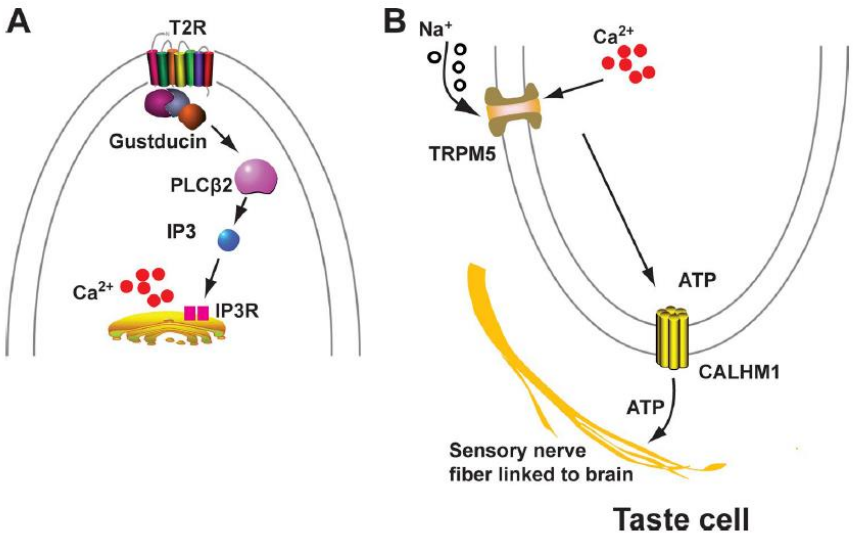


Fig. 12 Representation scheme of the oral bitter taste cascade in the taste cell. The extraoral tissue present different signal cascade according to their localization.

The 25 bitter receptors are present in murine and humans, where are localized on chromosome 12, 7 and 5 and are very well characterized. In mice instead the 35 different subtypes are localized on chromosomes 15, 6 and 2 [134]. TAS2R were discovered also in fish, primates and insects and they were detected for the first time in bud cells where their function was to detect the poisonous compounds [135-137]. Then, the research discovered their presence also in small intestine, colon and stomach, where these receptors were able to play different roles than sensing bitter substances. The presence of these receptors was discovered for the first time in the respiratory tract in the twenty-first century, in this case the activity of the receptor was related again to the perception of poisonous substances. The response mediated by activation of TAS2R in the respiratory tract induces the elimination of the harmful substances and the protection of nasal respiratory epithelium. In 2009 Shah et al. found three different

autonomous regulation of T2Rs for the human airway epithelia (cell-autonous regulation, endocrine and paracrine), which were controlled by a dose-dependent response of Ca2+ and ciliary beat frequency. This mechanism is not even now well established but probably there is a correlation between the beat frequency of ciliary cells via a cyclic nucleotide-dependent manner [138]. Another interesting phenomenon is the relaxion of the smooth muscle thanks to the membrane hyperpolarization induced to the activation of Ca2+-activated K+ (BK) channels.

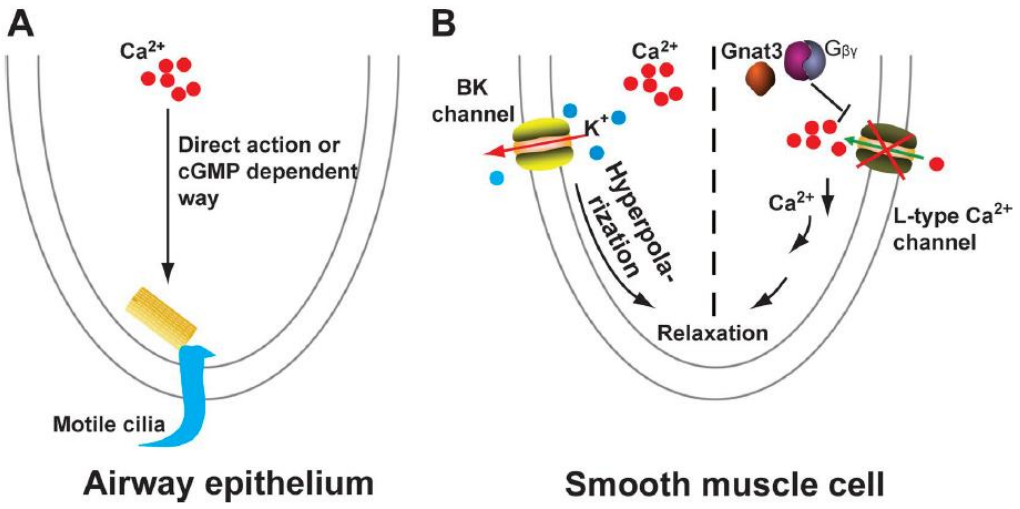


Fig. 13 (A) The T2Rs behave in different way according to their localization, bitter substances can promote the cilia beat frequency in the airway epithelium. (B) In the smooth cell the interaction between T2Rs and bitter molecules induces the relaxation of airway smooth muscle cells.

The βγ subunits of gustducin seems essential to promote the relaxation of airway cells thanks to their ability to turn off the L-type voltage-dependent $Ca2^{+}$ decreasing $Ca2^{+}$ levels (Fig. 13A) [139]. The T2Rs have also paracrine role in the small intestines, in

fact the release of activity peptide hormone cholecystokinin (CCK) induced by the activation of T2Rs and the increase of $Ca2^{+}$ promote the activity of multidrug resistance protein 1 (ABCB1) to remove from the cells the bitter substances (Fig 14 A) [140]. The vagal nerve is stimulated through the release of CCK1 receptors expressed on the sensory fibers after the T2Rs activation. (Fig. 14 B) [141]. The release of acetylcholine as registered after the use of bitter chemicals or bacterial signal from solitary chemosensory cells (SCCs) placed in the nasal and vomeronasal cavity.

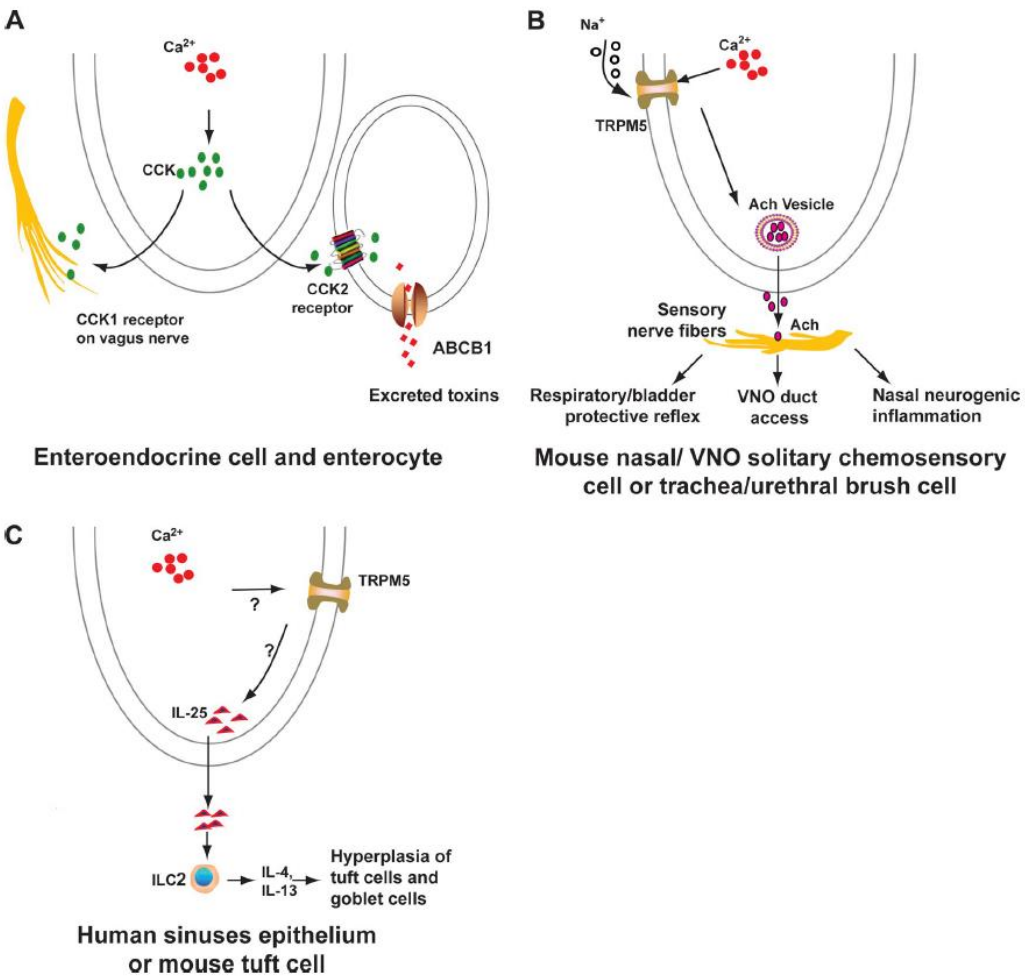

Fig. 14 (A) The bitter toxins are pumped out from the enterocytes after the activation of the T2R receptor with the consequent release of the peptide hormone CCK, which can promote the activity of the ABCB1 in the neighboring cells. The CCK could also activate the CCK1 receptor expressed on the vagus nerve sending to the brain the signal to limit food intake. (B) A similar signal cascade can be found in the SCC nasal organ or in the trachea and bladder brush cells. Here bitter compounds like N-acyl homoserine lactones produced by bacteria promote the release of acetylcholine, which promotes the contraction of bladder and the decrease of respiratory rate. (C) In tuft cell the cascade is activated thanks to the parasites able to also induce the release of the IL-25 and the increase the level of ILC2s, IL-13 and IL-4.

The acetylcholine can induce the decrease of the breathing rate and the closure of the vomeronasal organ (VNO) after the interaction with nicotinic receptors (Fig. 14 B; 130; 142-145]. This is a protective mechanism which can be found also in the bladder [146], but also in the gut after the parasitic infection which lead to hyperplasia (Fig. 14 C) [147-149]. So, the T2Rs were detected also in extraoral tissue such as: brain, pancreas, thymic epithelial cells, blood cells (macrophages), but also in all genitourinary system (kidney, urethra, bladder, ureter, ovary, endometrium, myometrium, placenta, vagina, cervix, prostate, testis [150-154], and even spermatozoa [151]. The last discoveries suggest a strong correlation between the T2Rs activation, and the release of the quorum sensing molecules produce by pathogenic microbes. These molecules in fact could be involved in the T2Rs activation and to the host response defense, considering that N-acyl homoserine lactone, which are produce by gram-negative like *Pseudomonas aeruginosa* are essential to control the virulence factor expression, biofilm formation, virulence factor expression and the production of secondary metabolites involved in the adaption process and bacterial competition.

The activation mechanism between quorum sensing molecules and T2Rs still remain unknown as the anti-inflammatory response.

### 1.5.2 Bitter taste receptors of genitourinary tract

As mentioned before the extraoral T2Rs can be found also in the genitourinary tract and increasing evidence highlight the function of T2Rs as immune sensors to recognize toxins and microbes promoting a protective mechanism against the aggression [155–158]. The presence of these receptor was determined for the first time by Deckmann et al. in 2014, their research underlined the inflammatory response mediated by pathogenic *E. coli* and bitter substances in urethra, bladder, ureter, and renal pelvis. This type of response could prevent the development of genital urinary tract infection. TAS2Rs were found also in the placenta, also in this case their functions are related to the inflammatory responses and to the poison prevention in fact these receptors could be involved also in the chorioamnionitis and villitis. The T2Rs can also induce the contraction of uterine environment to prevent the infection from pathogens, for example chloroquine can induce the increase of $Ca2^{+}$ level inducing the contraction of the muscle [159]. A confirmation of this intracellular response is due to the inhibition of $Ca2^{+}$ level after the deletion of α-gustducin. The knockdown of T2R14 in myometrial cells determine the inhibition of chloroquine for the rise of oxytocin. A murine study confirms the positive action of chloroquine in the prevention of preterm birth determine by lipopolysaccharide, moreover chloroquine seems to be even more effective than tocolytics [159]. All this evidence suggest a strong relationship between the intrauterine infections and the T2Rs activation, the pathogenic ligand such as

quorum sensing molecules are the main actor able to induce the host defense response. These signaling molecule are essential for the microbes communication and are generally produced by virus, parasites, gram negative and positive bacteria [160, 161]. The quorum sensing molecules are involved in many different processes, in fact they control between 10-50 % of microbial genome and more than 80% of pathogen motility. In fact, these molecules are also involved in the production of virulence factors [160–163] which are involved in the counter defense of the host [164]. The 182 quorum sensing molecules are available in the database SigMol (http://bioinfo.imtech.res.in/manojk/sigmol) [162] and these molecules are divided in different classes. The gram negative produces a series of molecules called autoinducers synthesized from fatty acids, S-adenosylme-thionine, and anthranilate, S-adenosylme-thionine, and anthranilate through a series of enzymatic reactions. These molecules are divided in class: acyl AHSLs, DSFs, alkylquinolones, α-hydroxyketones, and AIs. The oligopeptides, called autoinducing peptides (AIPs), are produced by gram-positive and can regulate the density in the host [165]. The AI-2 instead are produced by both gram-positive and gram-negative [166]. The quorum sensing molecules when reach high concentration can interact with the receptors located in the cytoplasm and on the cell surface promoting the signal cascade which regulate gene expression and transcription factors.

### 1.5.3 Signal transduction of TAS2R in genitourinary system

The genitourinary cells (GU) and the epithelial brush/neuroendocrine cells can detect bitter substances and microbial metabolites to promote reflexes and the production of

neurotransmitters or hormones due to the pathogenic aggression [146]. However, this type of response is promoted also from some polyphenols or other pharmacological molecules such as: chloroquine, quinine, chloramphenicol, thiamine, noscapine [167–170]. The canonical activation of the T2R on the surface of GU cells induces an increase of $Ca2^{+}$ level and the formation of complexes with calmodulin (Fig. 15). The L-arginine (L-Arg) is converted to NO and L-citrulline [171, 172]. In the same way, the concentration of microbial quorum signal sensing promotes the stimulation of the G-protein α-gustducin inducing the same response, the high concentration of NO is useful to destroy microbes [173].

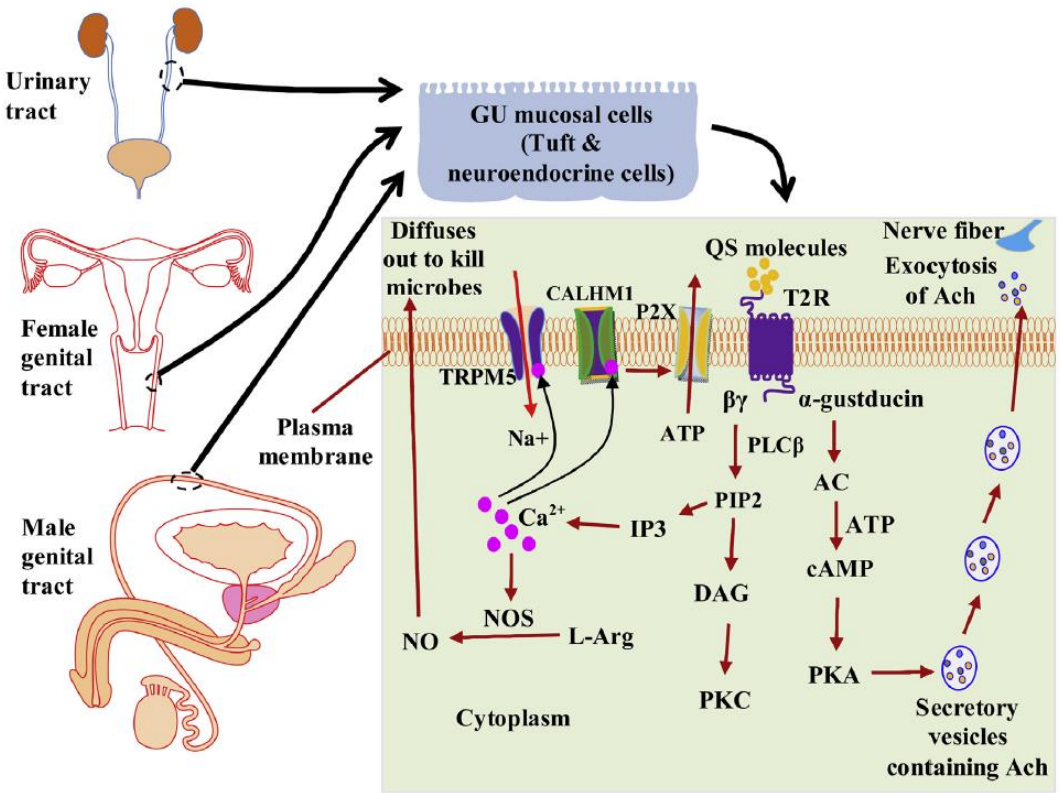


Fig. 15 The image represents the signal transduction of T2R for the GU mucosal cells. T2Rs can detect bitter substances produced from the microbes, these quorum sensing molecules are able to interact with homomer, heteromers or oligomers functionally expressed on the cell membrane surface of the GU tract. Microbial quorum sensing after the interaction with the

T2Rs induce the dissociation of the α-subunit gustducin from the βg subunits with the production of the guanine triphosphate (GTP) after the activation of the adenylate cyclase (AC). The PKA is activated after the increase of cAMP level, this event induces the release of the acetylcholine and other mediators in the GU tract. The activation of phospholipase Cβ (PLCβ) promotes the production of diacylglycerol (DAG) and 1,4,5-inositol trisphosphate (IP3) starting from PIP2 after the separation of the βg subunits. The protein kinase C (PKC) at the end of the signalling cascade phosphorylates different intracellular targets. The IP3 increase allow to the to activate the $Ca2^{+}$-dependent kinases and transcription factors (CALHM1 and TRPM5). The quorum sensing molecules increase the nitric oxide (NO) production after the increase of $Ca2^{+}$, which activate calmodulin complex and oxide synthase (NOS). Detection of AHLs at physiological concentration leads to nitric oxide (NO) production via Ca2+ -dependent mechanism. Ca2+ ions bind to calmodulin to form Ca2+ -calmodulin complex, which activates NOS. Thanks to this enzyme L-arginine (L-Arg) is converted to NO and L-citrulline.

Grekov et al. (2017) discovered this defense mechanism against the parasite *Leishmania promastigotes* thanks to the NO synthesis [173]. The increase of NO also promotes the activation of protein kinase G and guanylyl cyclase inducing the phosphorylation of microvilli proteins with the increase of beat frequency [146,174]. The GU neuroendocrine cells are immune sentinels that play an essential role to detect the harmful substances and microbes, this interaction leads to the host response inducing the elimination of the invasion [146].

## 1.5.4 Signal transduction of TAS2R in bladder and myometrial smooth muscles

The release of NO in the myometrium promotes the production of (cyclic guanosine monophosphate or cGMP) GMP after the activation of guanylate cyclase [175] which lead to the smooth muscle relaxation (Fig. 15B). This event is caused by the membrane hyperpolarization after the activation of the voltage- and Ca2+-activated K+ or Big Potassium (BK) channel. The muscle relaxation is promoted thanks to the βg-subunits, which can interact with ion channels and regulate the potential. According to these preliminary studies the T2Rs should be able to induce the bladder contraction, for example Deckmann et al. [146] demonstrated the bladder contraction after the T2R activation. This hypothesis is sustained also thanks to the high expression of BK channel in the human detrusor smooth muscle, which is essential to regulate the activity of the bladder [176] (Fig. 16A). The myometrium presents the expression of T2Rs, and the dysregulation of these receptor suggest that they should play a main role for bladder myositis and myometriosis even if the literature data are limited.

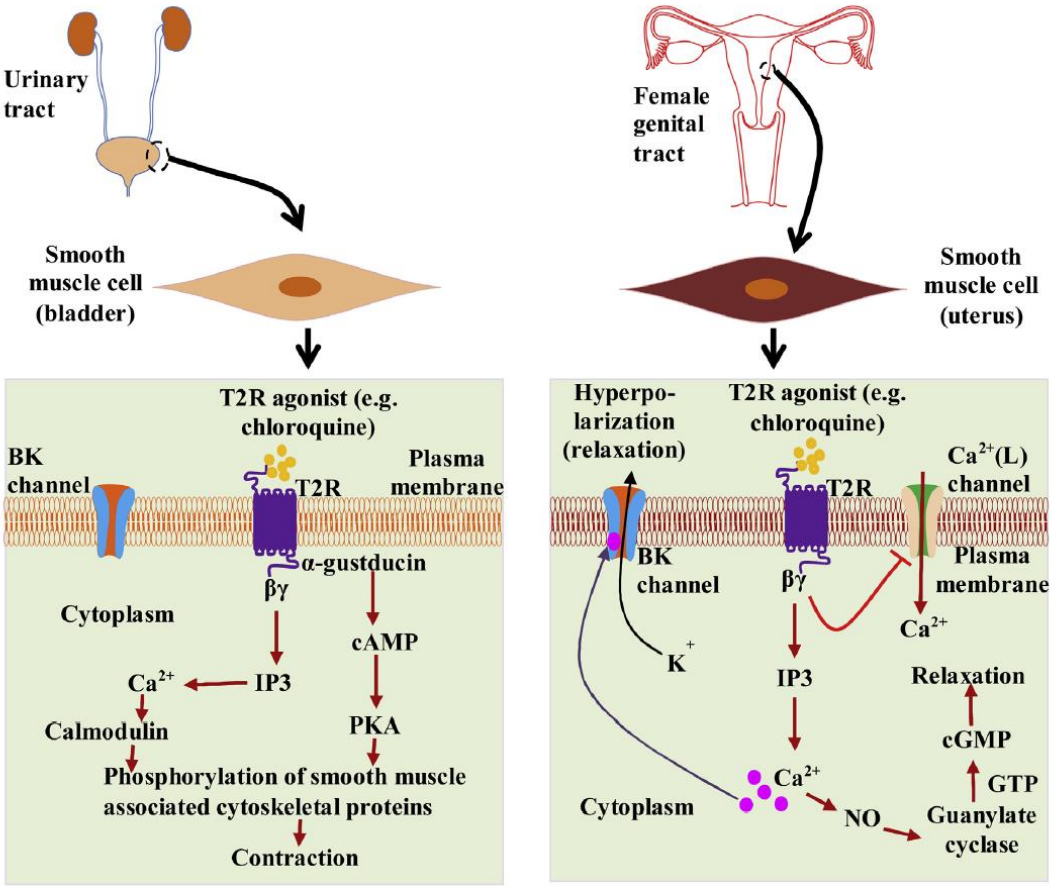


Fig. 16 The signal cascade of bladder and uterine e smooth muscle for T2R is different even if the final biological response is contraction of the relaxation of the smooth muscle. A The agonist such chloroquine or quinine induces the separation of the βg-subunits from the α-gustducin, the first one induces the increase of IP3 and $Ca2^{+}$ level with the phosphorylation of smooth muscle associated cytoskeletal proteins thanks to the activation of calmodulin. The same event is promoted by α-gustducin which induces the increase of cAMP with the consequent activation of PKA. The activation of BK channel calcium can also cause muscle contraction in the smooth muscle bladder. B Also in this case agonist such chloroquine or quinine, interacting with the T2R can induce the activation of the βg-subunits, which from one side inhibits the opening of the L-type calcium channel and from the other promotes the increase of $Ca2^{+}$ level. This take to the opening and hyperpolarization of BNK channel but also to the production of NO and activation of guanylate cyclase.

### 1.5.5 TAS2Rs and inflammation for bladder and uterine contractions

In genitourinary infection the bitter taste is also related to the anti-inflammatory response even if the knowledge remains still limited. The research data obtained until now sustain the non-canonical signaling which involve PKC/PI3-K/Akt/NF-kB (Fig. 17) [146,177-179]. The increase of Ca2+ remain essential also in this signaling cascade, this event leads to the PKC activation and then the consequent PI3-K stimulation after the increasing level of phosphatidylinositol-4,5-bisphosphate (PIP2) [178, 179]. The activation of mTORC1 is determined by the PDK1, recruited after the activation of PI3-K and the phosphorylation of Akt [180, 181]. FOXO, SIRT1, which are regulated by mTORC1 controls the production of inflammatory cytokines and chemokines [182-186]. Zhou et al. were able to correlate the defect of α-gustducin and PLCβ2 to the uncontrolled increased of ROS and the activation of inflammasome [187].

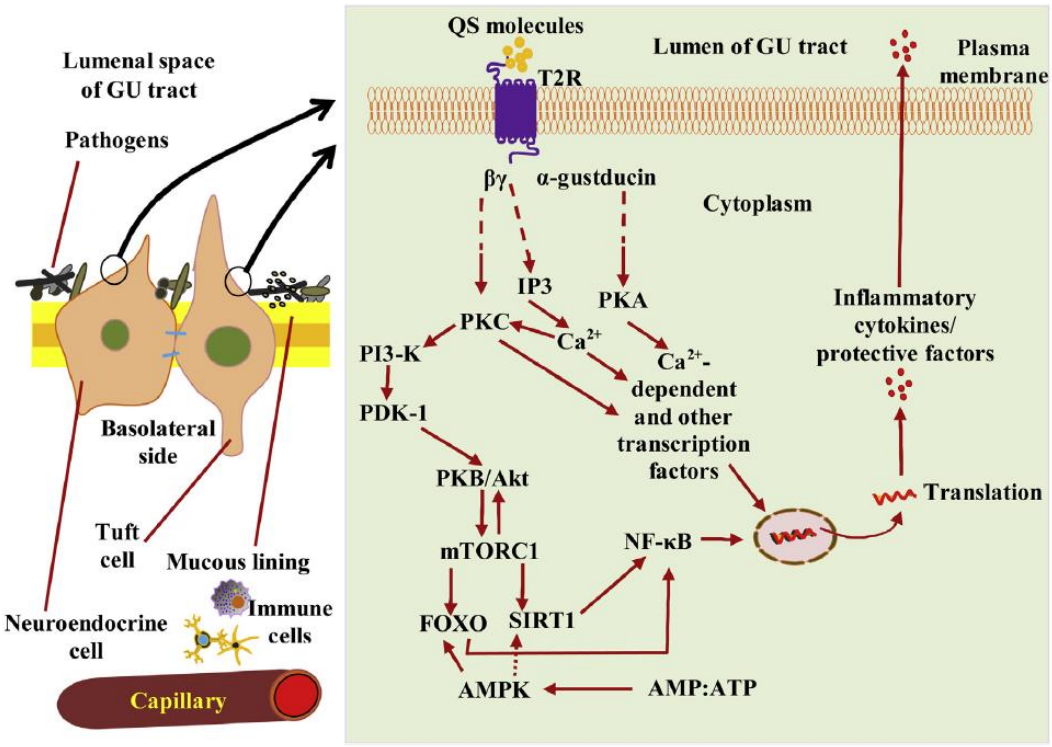


Fig. 17 Also, in this case the quorum sensing produced by the pathogen can activate the signaling cascade in the neuroendocrine cell in the GU tract. The final response in this case is the regulation of the inflammatory response thorough PKC/PI3-K/Akt/NF-kB. This The production of inflammatory cytokines and protective factor should promote the elimination of the pathogens after their proliferation in the GU tract.

## 1.6 *Hibiscus sabdariffa L.* and *Momordica charantia L.* and their potential in the UTIs management

### 1.6.1 *H. sabdariffa* origin, distribution, and traditional medicine

Fig. 18 Flowering stage (Left) and mature calyces (Right) of *H. sabdariffa*

*H. sabdariffa* presents more than 300 species and is commonly cultivated in subtropical regions and only in early date was cultivated also in Africa [188]. The common English name is roselle and it belongs to the Malvaceae family, the flower at the beginning is white and yellow with a dark spot on the base but they become red when the fruits mature (Fig. 18). The time required is six month and the flower are 1-2 cm wide to the base enlarging to 3-3.5 cm. The plant is generally cultivated in the rainy season [189, 190] and the flower thanks to their phytochemical, pharmacological and toxicological properties [191]. The leaves are eaten raw in with fish or meat or cook in Sudan with vegetables [192]. In India re used in the rainy season for prepare chutney [193], instead seed are used to prepare the oil or as substitute of coffee in Africa [194]. The dried flowers are used in the tea, sauces, jellies, jam or wines for the presence of anthocyanins [192, 194-196]. Also, their use in salad is very common or in pudding and ice-cream. In Pakistan the calices are consumed in the fruit-preserving industry while in Africa are consumed with peanuts [197]. In sud-America the flowers are used freezed to prepare lemonade or other bevarages and the same is for China and India [198,193]. The traditional medicine uses this plant for treat colds, toothaches, urinary tract infections and hangovers. The thai colture for example use it for kidney

and urinary bladder stones [198] but also Mexicans prepare infusion to treat hypertension [199]. The drinks in general are used to treat fever, liver disease but also hypercholesterolemia, hypertension, antispasmodic and antimicrobial agent [200–202]. However, their anti-inflammatory, anti-microbial and diuretic properties shown in literature suggest the potential of roselle also in the management of the UTIs.

### 1.6.2 *H. sabdariffa* chemical composition and UTIs

The studies on the possible use of *H. sabdariffa* in the prevention of UTIs still remains limited Chou et al. [203] investigated for the first time this possible application only in the 2016 conducting an observation guided transcriptomic study. The treatment with a concentrated drink of roselle with 4.84 μg/ml of delphinidine-3-sambubioside down-regulates the cytokine network and pro-inflammatory products in dose-depend manner in mice treated with LPS. *H. sabdariffa* seems to be effective also against the UTIs in residents with urinary catheters in long-term care reducing the incidence by 36%. Very interesting is also the study conducted by Ali et al. [204], the aqueous extracts reduce the severity of the chronic kidney disease (CKD) in mice in dose dependent manner reducing also in this case the inflammatory cytokines but also the oxidative stress. The main compounds present in the roselle are polysaccharide, flavonoids (antocyanins) and organic acid [205-208]. The extract of roselle leaves are antioxidants, which are generally water soluble and organic acid [209]. The beneficial effects of this plant are related to the polyphenols fraction. The phenolic content of the plant is due to the presence of β-sitoesterol and ergoesterol [209-211] or flavonoids like hibistecin or gossypetine. The main anthocyanins are 3-sambubioside, delphinidin-3-glucoside,

cyanidine- and sambubioside [212, 213]. Finally, we also have flavonoids such as eugenol, protocatechuic acid and hibiscetin, while the the color of the extract is generally related to the presence of flavylium or 2-phenylbenzopyrylium. All the anthocyanins are sensitive to pH, light, enzyme and temperature or metals [214]. The major anthocyanins of *H. sabdariffa*. are cyanidine-3-sambubioside and delphinidine-3-sambubioside, while the minor are cyanidine-3-glucoside and delphinidine-3-glucoside [209, 215]. These compounds were found also in other studies [217, 218], for example Tsai et al. [219] assessed that the 85% of anthocyanins comes from delphinidine-3-sambubioside, which is the main antioxidant actor of this extract.

### 1.6.3 *H. Sabdariffa* and the antimicrobial activities

Alshami et al. was the first to underline the antifungal activity and anti-biofilm activities of Hibiscus sabdariffa. The methanolic extract used in a concentration of 0.5 to 2.0 mg/ml against 6 strains of fluconazole-resistant C.albicans seems to be effective at all level and useful in the prevention of urinary tract infections [220]. Abdallah et al. was able to evaluate the activity of calyces against the multidrug-resistant (MDR)-Acinetobacter baumanni, the results underline the high activity of roselle extract against MDR strains compared to the gentamicin [221]. Borras-Linares et al. reported the activity of ethanolic extract against 25 varieties of Mexican roselle used to obtain ethanolic extracts against gram-positive and gram- negative bacteria [222]. Jabeur et al. assess that the antimicrobial activity of hydroethanol or infusion is 10 mg/mL against gram positive and gram-negative bacteria but also against *Trichoderma viride* and four different strain of Aspergillus. However, the anti-microbial effect was

registered only for the hydroethanol extract, a similar result was obtained also for the anti-fungal activity. The properties of the roselle extract are related to the flavonoid and their ability to form a complex with the bacteria cell wall, these interactions could lead to the leakage of bacterial cells after the increase of membrane permeability [223]. Finally Hashimi studied the activity of *H. sabdariffa* against the P-fimbriae bacteria, underline the ability of proanthocyanidins to inhibit the adhesion to the uroepithelium promoting also the inhibition of the *in vitro*.biofilm formation [224].

### 1.6.4 *M. charantia* origin, distribution, and traditional medicine

Fig. 19. *M. charantia* fruit (Left). Skin pulp and seed (right).

*M. charantia*, called also bitter gourd or bitter melon grow in tropical and sub-tropical region (Fig. 19). This plant belongs to Cucurbitaceae family, and the fruit is rich of interesting phytochemicals useful to promote healthy effects [225]. The plant was used since the ancient time in traditional medicine and present a lot of different applications such as: cancer, AIDS, obesity, hypertension, bacterial and viral infections. The pharmacological properties are related especially to the unripe fruits [226] for this

reason the juice is used to treat joint pain, chronic fever, liver illness, jaundice and to promote diuretic, laxative and anti-helmintic actions. It is also used to treat burns, skin disease, rashes, and boils, for example in the Turkish traditional medicine the fruit is macerated with in olive oil warmed by the sun and combined with honey to treat the gastric ulcers [226, 227]. In Africa is very used to treat inflammation (fruits, seeds, and leaf juice), menorrhea (leaves), syphilis, skin disease (roots), rheumatism and fever. Chicken pox, malaria, gonorrhea, measles, and scabies are other illness treat with momordica preparations. In the Caribbean the leaf or the juice is used to treat diabetes. The decoction leaves are also used for worm infections, malaria, dysentery, and high pressure [225].

### 1.6.5 *M. charantia* chemical composition

The properties of bitter melon are related to the presence of cucurbits, moreover it is a good source of minerals, vitamins, carbohydrates, fibers, and protein. The fruit is composed by 93.2 % of water, followed by the protein and lipids around 18.02 and 0.76 % respectively [228]. Bitter melon also presents a high content of Vitamin A and C but also, niacin, thiamine, and riboflavin. [229]. The lipids are present especially in the seeds, which are constituted by 45% of polyunsaturated fatty acid and for the remaining 63-68% by eleostearic acid [230]. The oil present different bioactive compounds such as sesquiterpenes, phenylpropanoids and monoterpenes (Nyam et al., 2013). The antioxidant damage potential is in the stem, leaves, aril and pericarp while the fruit and the steam are a good source of cucurbitance-type triterpenoids and cucurbitacins are the main one [230].

## 1.6.6 Cucurbitacins and TAS2R

A common feature of the cucurbitacins is the presence of the 5, [231] double bond and the ring skeleton 19-(10→9β)-abeo--10α-lanost-5—ene. The basic structure of these molecules changes according to the position of the methyl group located on C-9 or C-10. The cucurbitacin T and S present also an extra ring, which is cyclized between C—16 and C—24 [231-232]. All the different cucurbitacins could be distinguished also on the presence of acetoxy, hydroxyl and keto groups [233] or for the presence of different functional group on the A and C rings. Cucurbitacins are designated by the following letters: A, B, C, D, E, F, G, H, I, J, K, L, O, P, Q, R and S (Fig. 20) [234]. A special group of cucurbitacins were identified in *M. Charantia* fruits, these molecules are oxidized on the $C_{19}$ to an aldehyde group. Cucurbitacins are in general crystalline and are soluble in Chloroform, methanol, ethanol, ethylacetate and benzene. Cucurbitacin B according to literature activates TAS2R10 and TAS2R14 according to Meyerhof et al. 2010 respectively at 0.01 μM and 100 μM of human embryonic kidney [235].

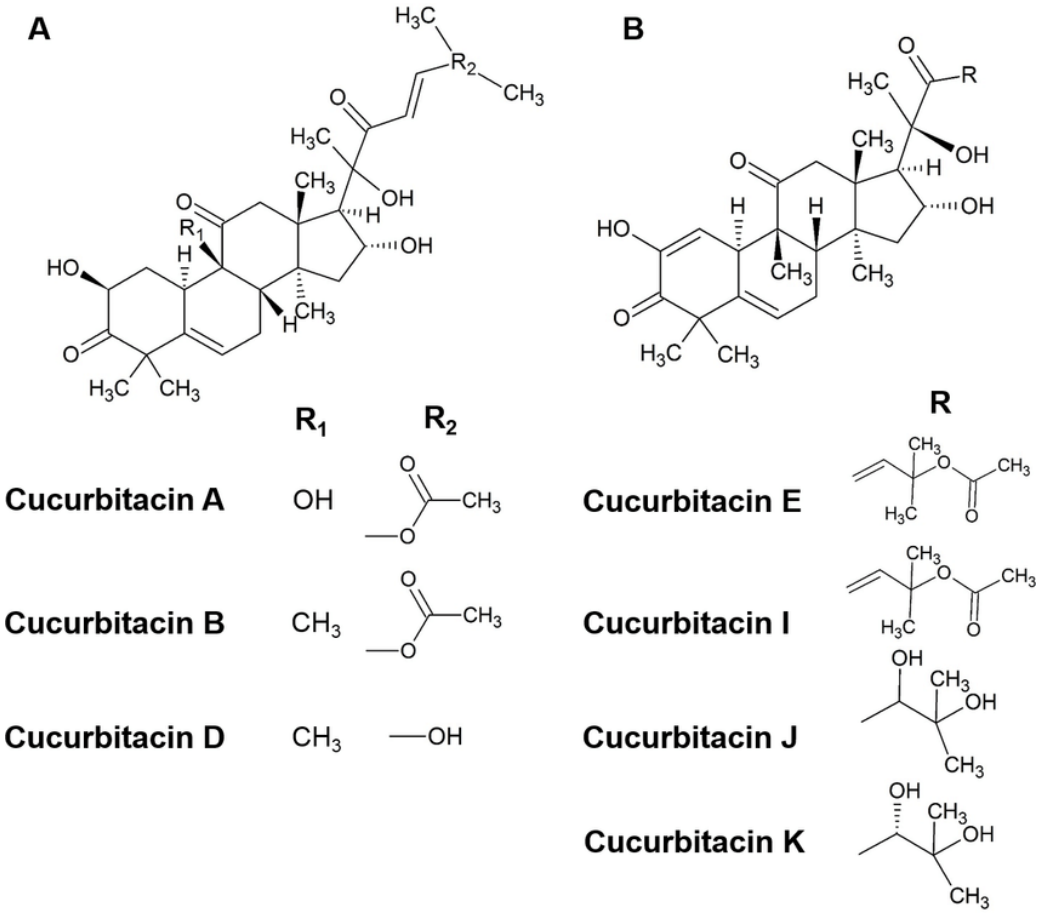


Fig. 20: The structure of cucurbitacins. (A) The skeleton of cucurbitacin A, B and D. (B) The skeleton of cucurbitacin E, I, J and K.

(HEK)-293T cells transfected with the chimeric G protein Gα16gust44. Stephan Born et al. 2013 underline the ability of TAS2R10 to accommodate numerous diverse ligands, among which cucurbitacin B [236]. Also, in this case the cells used were HEK)-293T cells transfected with the chimeric G protein Gα16gust44 using the site-directed mutagenesis to investigate the effects of different substitutions on the receptor's response profile. This study confirms the high response of TAS2R10 to the cucurbitacin B with a reduction of TAS2R10 responsiveness for all mutations in positions 175 and 178. One of the biological actions of cucurbitacin B is to induce the mediated GLP-1 secretion in H716 after the activation of AMPK through the -

gustducin and Gβγ-signaling of taste receptors. Also, in this case the research was focused on the TAS2R10, but the cell used were enteroendocrine L-cells. This study conducts by Yamamoto et al. (2018) highlight how cucurbitacin B could be used for the development of new therapeutics taking advantage of the TAS2Rs activation [237].

### 1.6.7 *M. charantia* anti-inflammatory and anti-oxidant activities

*M. charantia* can be used to treat several diseases such as cancer, obesity, dyslipidemia or T2DM [238-239] (Fig. 21).

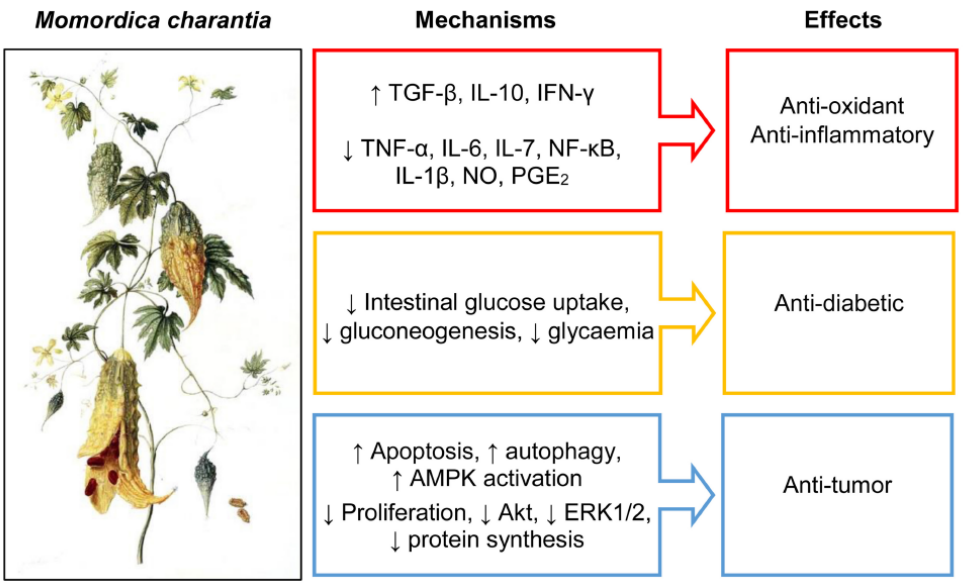


Fig. 21 *M. charantia* pharmacological effects.

The inflammation is a key process in diabetic patients and promote the increase of glucose in blood and cardiovascular problems. Moreover, the chronic inflammation could lead to different diseases, in fact the oxidative stress can play an essential role in the born of chronic inflammatory disease [240]. The capacity of bitter melon to

show antioxidant and anti-inflammatory activities push the scientist to study the mechanism of action of this extract [241]. Now there is a great correlation between the consumption of bitter melon and the regulation of NF-kB in RAW 264.7 cells treated with LPS. The treatment with bitter melon seems to reduce the activity of NF-kB with the consequent inhibition of p38, JNKs, ERKs as well as MAPKs [242]. In fact, the study registered a reduction in the expression of for IL-1a, IL-1b, and TNF-α, moreover it seems also that the treatment with bitter melon can reduce the production of NO synthase and IL-1b expression [243]. More recently, Svodobodva et al. were able to report a reduction in the expression of NO synthase and cyclooxygenase-2 (COX-2) after the treatment in the same cell model registering a suppression of suppressing NF-kB, and activator protein-1 [244]. Other research assesses also the downregulation of ERKs and Akt of [245-246], transcription factors related to the cell growth, survival, metabolism and protein synthesis. The triterpene purified from the fruit seems to have the same anti-inflammatory effect in FL83B cells through the inhibition of TNF-α induced expression [247]. C57BL/6 mice registered a loss of hyperglycemia and hyperlipidemia after the high fat diet supplemented with bitter melon extract [248]. Moreover, was shown also an important anti-inflammatory effect of TNF-α and IL-6 serum blood level [249]. Bai et al. [250-251] confirmed these evidence treating mice with an high fat diet supplemented with *M. charantia* reducing the systemic inflammation. Interesting is also the chemopreventive potential of bitter melon extract, in fact it seems the use of bitter melon in mice can determine the upregulation of mir-221/-222 and a downregulation of PI3K/Akt/NF- kB/IkB in TNF-a treated lung tissues in mice [252]. The antioxidant potential of this fruit was revealed in neuroblastoma cells treated with the extract to reduce the $H_2O_2$ stress after the

activation of JNKs, p38, and ERK1/2 MAPK [253]. The xanthine oxidase activity, which is involved in several inflammation diseases, is inhibited [254] from fruits and stem extracts [255]. Antioxidant compounds in pulp and seed inhibit the lipid peroxidation [256], moreover the oxidative damage induced by peroxynitrite seems to be reduced [257]. The antioxidant potential is reduced after the blanching process of the fruit together with the phenolic content [258]. A very interesting effect is the reduction of the inflammation determined by bacteria; bitter melon extract can reduce the skin inflammation in mice affected by Propionibacterium acnes promoted by THP-1 cells. The cucurbitane triterpenoids promotes the suppression of *Porphyromonas gingivalis* also reducing the production of IL-8, IL-6, and IL-1b levels [219]. In one randomized trial 38 patients were treated for 3 months with bitter melon supplementation obtaining a reduction in analgesic score but also in body weight, body mass index, and fasting blood glucose [259].

# 2 Aim of the research

In the first and second year of my PhD course the aim was to find a new non-antibiotic candidate of plant origin, which could be use in the management of the UTIs. In the first phase, I selected five different plants, which were extracted to explore their potential against uropathogenic *E. coli*. According to the literature the plants selected for the studies were:

1) *Camellia sinensis L.* (Leaves)
2) *Punica Granatum L.* (Fruit)
3) *Orthosiphon stamineus* (Leaves)
4) *Morus alba L.* (Leaves)
5) *H. Sabdariffa* (Flowers)

All the plants were extracted, and the extracts screened to select the most promising plant extract according to their polyphenol concentration, antioxidant, and antimicrobial activities. Based on these results we selected only one of the most promising extract (*H. Sabdariffa*) and we performed UHPLC coupled to IT-TOF profile assessing the main compounds and understanding the possible mechanism of action of these molecules against the uropathogenic *E.coli*. Finally, there was the evaluation of the anti-biofilm and anti-invasivity activities. Although *H. Sabdariffa* is currently used in Traditional Medicine to reduce the UTI symptoms, as until now its

real potential in the management of UTIs has not been explored and the data on this topic remain still limited, we decided to perform this study to improve the knowledge about its use in the prevention and treatment of UTIs.

In the third year of the PhD course, which took place at the Leibniz-Institut für Lebensmittel-Systembiologie an der Technischen Universität München, a non-canonical approach was followed, with the final aim to update the literature on the TAS2R expression and on *in vitro* bioavailability of Cucurbitacin B, which is contained in *M. charantia* fruits. This molecule is very interesting from a pharmacological point of view considering the multiple biological activities such as anti-proliferative, anti-inflammatory and pro-apoptotic. As reported in the introduction section TAS2R are also expressed in the GU tract and the activation of these receptors can activate a host defense response against uropathogenic bacteria. *M. charantia.* fruits were divided into seeds, pulp, and skin and these parts and the whole fruit were extracted. The extracts were characterized with an untargeted UHPLC-Tof-MS screening. After the metabolic profile assessment and the determination of cucurbitacins in the extracts, the next step was understood if cucurbitacin B, present in each part of the fruit, was able to reach the GU tract using the transwell system. This *in vitro* prediction bioavailability assay was performed to determine the Apparent Permeability (P app) of cucurbitacin B and to understand if this molecule, despite its low bioavailability, can cross the intestinal barrier to reach the bloodstream and eventually the bladder to interact with the T2Rs. Moreover, considering the poor literature on TAS2R in CACO-2 cell line we decided also to explore their expression in this specific cell line and to treat the cells with bitter melon extract to understand if the treatment could change the expression of this receptor. This preliminary

investigation was essential not only to increase the knowledge of this receptor, which play a main role in the GU host response, but also to understand if bitter compounds could alter the expression of this receptor in our body after a desensitization process. Despite the promising result obtained from this preliminary study, to understand and confirm the real potential of cucurbitacins in the GU tract further *in vitro* and *in vivo* studies should be conducted with the aim of defining the activation of TAS2Rs and the biological effect of cucurbitacins in the GU tract confirming the activation of the host mechanism against the uropathogenic bacteria.

# 3. Materials and Methods

## *3.1. Chemicals and reagents*

One batch (C-040919281119) of commercial *H. sabdariffa* (flowers), *Punica granatum* L. (fruits) (C-050419150419), *Morus alba* L. (G-140618150519) (leaves), *Orthosiphon stamineus* (leaves) (C-031019171219) were purchased from Minardi A. & Figli S.r.l (Ravenna, Italy), while *Camelia sinensis L.* (Hashiri Shincha leaves) was bought from from Naturalitea (Kinezuka, Japan). The HT-1376 CRL-1472™ cells and *Escherichia coli* (Migula) Castellani and Chalmers 25922™ were purchased from ATCC. Formic acid solution (1M), water, methanol, acetonitrile LC-MS grade, ethanol technical grade, HCl, sodium monobasic dehydrated phosphate ($NaH_2PO_4$ $2H_2O$)**,** gallic acid (≥98%), Folin-Ciocalteu, calcium carbonate ($CaCO_3$), ABTS [2,2-azinobis-(3-ethylbenzothiazoline-6-sulfonic acid)], Crystal violet ($C_{25}H_{30}N_3Cl$), potassium persulfate ($K_2O_8S_2$), dimethyl sulfoxide (DMSO), 0.22 µM PES membrane were sourced from Sigma-Aldrich, Merck KGaA (Milan, Italy). All the media and reagents for cell culture were purchased from Gibco (Milan, Italy). Chromatic™ detection, Brain Hearth Infusion (BHI) media, ampicillin, tryptic soy broth, were purchased from Liofilchem® (Roseto degli Abruzzi, Italy).

## 3.2 Extraction procedure

The extraction procedure was performed using 3g of starting material and 60 ml of a 50-50 ethanol/water solution, adding 0.1 % of HCl. The mixture is prepared in a becker and kept on a shaker with a stirring magnet bar for 2 hours, protected from light in

nitrogen atmosphere at 4 °C. To maximize the polyphenol extraction, the entire process was repeated three times. The supernatant obtained was centrifuged at 6000 rpm and was stored in a 50 ml falcon at 4 °C. The material obtained after centrifugation was newly extracted for two times. The precipitate was centrifuged at 6000 rpm for 10 minutes at 4 °C to recover the supernatant which was added to the others. The hydroalcoholic extract was filtered through Whatman filters. The ethanol occurring in the hydroalcoholic solution was evaporated using a rotary evaporator under reduced pressure at room temperature. The aqueous extract at the end of the evaporation process was freeze dried. Then the dried material was weighed to determine the extraction yield.

### *3.3.1 Determination of total phenolics*

The polyphenols concentration was assessed using the Folin Ciocalteu determination. Gallic acid was used as reference standard compound; the standard calibration curve was prepared weighting 10 mg of gallic acid in 10 mL of methanol/water 50-50 solution. The obtained stock solution was then diluted with different volumes of methanol/water 50-50 solution to build a 7 points standard curve (1000; 850; 700; 550; 400; 250; 100 µg/mL). The standard blank was prepared using only the buffer solution. Then, an aliquot of 10 mg of the extracts was dissolved in 1 mL HPLC water Millipore grade and then centrifuged at 16000 g for 10 minutes to obtain supernatants at the concentration of 10 mg/mL. At least, 10 µl of each sample was combined in this sequence with. 50 µl of FC, 200 µl of calcium carbonate ($CaCO_3$) and 740 µl of HPLC water to reach the final volume of 1 ml. The sample blank was prepared with the same

procedure but in the absence of each sample, which were replaced with HPLC water Millipore grade. All the samples were incubated at room temperature for 2 hours in dark conditions. At the end of the incubation time, 200 µl of the prepared solution were loaded into a 96 well plate and the absorbance was read at λ 750 nm using a microplate reader (BMG Fluo Omega Star).

### 3.3.2 *Trolox equivalent capacity (TEAC)*

The ABTS stock solution [2,2-azinobis-(3-ethylbenzothiazoline-6-sulfonic acid)] and potassium persulfate ($K_2O_8S_2$) stock solution were dissolved in water at the concentration of 7 mM and 140 mM respectively. Then 44 µL of $K_2O_8S_2$ was mixed with 2.5 mL of ABTS and the solution was left overnight at 4 °C dissolved in water and is kept in darkness by mixing 1.7 mmol L−1 of ABTS to 4.3 mmol. L−1 of potassium peroxydisulfate in water in the ratio of 5:1. The concentrated ABTS• is diluited with water to reach a final absorbance of 0.7 ±0.02 at λ 734 nm. The stock trolox solution was prepared in ethanol at the concentration of 1500 µM and then diluted to prepare a 6 points standard calibration curve (35; 30; 25; 20; 15 µM). Also in this case, 10 mg of all extracts were dissolved in 1 mL HPLC water Millipore grade and then centrifuged at 16000 g for 10 minutes to obtain supernatants at the concentration of 10 mg/mL. Then 100 µL of extract or standard was mixed with 1 mL of working solution and the absorbance is measured at λ 734 nm after 2.5 min against a blank. The TEAC was calculated correlating the decrease in absorbance of the sample with that of Trolox solution on molar basis. The % inhibition was expressed as {(OD ABTS – OD sample)/OD ABTS}*100

### 3.4.1 *Minimum Inhibitory Concentration (MIC) and Minimal Bactericidial Concentration (MBC) assessment*

Identification of *E. coli* was performed on with the Chromatic$^{TM}$ detection. The susceptibility test on *E. coli* was determined using the microdilution method system [35] and results were interpreted according to European Committee on Antimicrobial Susceptibility Testing (EUCAST version 7.1, 7 June 2017). E. coli was cultured in BHI at 37°C under aerobic conditions, for 24 hours on an orbital shaker at 200 rpm. Then the solution was adjusted to 0.2 McFarland standard turbidity scale and 100 µL of this solution were dispensed in a 96 well. Meanwhile, all the extracts were dissolved in water at 100 mg/mL, after centrifugation the supernatants was filtered with 0.22 µM PES membrane. Finally, 100 µL of extracts were added to each well to reach a final concentration of 50 mg/mL, 25 mg/mL, 12.5 mg/mL and 6.25 mg/mL. Positive and negative controls were added to the plate using BHI with bacterial suspension and BHI alone. Each MIC determinations were performed in triplicate. For the Minimal bactericidal concentration (MBC) 10 µL were taken from the well with an OD equal or lower to the MIC and spotted on BHI plates. The plates were incubated at 37°C for 24 hours. Only the concentrations which did not allow the colonies growth were considered as MBCs.

## *3.5 UHPLC-MS/MS analysis of H. sabdariffa extract*

50 mg of *H. sabdariffa* were dissolved in 1 mL of water to reach the concentration of 50 mg/mL. The separation of the sample was performed on a Shimadzu UHPLC coupled to IT-TOF using as a mobile phase: A) 0.01% CH3COOH in H2O, B) CH3COOH% in ACN. The injection volume was about 5 µL of extract and the detection UV/VIS λ was performed at λ 330 nm HRMS analysis was performed with Full MS (m/z 100-1000) and data-dependent acquisition (DDA), source parameters were: Interface and CDL temperature, 250 and 280°C, nebulizer, and drying gas 1.5 and 10 mL/min.Data were analyzed with MZMine2.

## *3.6 Invasion assay for E. coli*

The urinary bladder cells (HT-1376) were pretreated for 24 h with the extract of *H. sabdariffa* at the following concentrations: 50 mg/mL, 25 mg/mL, and 12.5 mg/mL. The positive control used were treated with Cranberry at the same concentration of *H. sabdariffa*. The cells were grown in Eagle's Minimum Essential Medium (n. 80520201) to reach 70% of confluence, then the cells were infected with the uropathogenic *E. coli* (ATCC 700928) for 4h (MOI $10^5$). The experiments were conducted at the same time with the two different treatments. At the end of the treatments, the cells were washed three times with PBS and treated with gentamycin (Merck; Italy) at bactericidal concentration (10 µg/mL) for 4h at 37°C. The cells were then detached with trypsin and lysed with 0.1% Triton-X100 at 4 °C. Finally, the cells

were diluited in PBS and plated using Chromatic$^{TM}$ detection and the colony were counted after 24h at 30 °C in triplicate using 10 µL to evaluate the CFU/mL.

# 4 Results

## *4.1 Yield and total phenolic concentration*

The extraction procedure was repeated three times from three different samples of the same batch, the media and the standard deviations of the dry residue obtained after the lyophilization process are reported in Tab. 1. All the measurement are expressed in % considering 3g of starting material.

| Plant extract | I extraction | II extraction | III extraction | Mean | Dev.st |
|---|---|---|---|---|---|
| *C. sinensis* | 29.66 | 25.66 | 25.66 | 27 | 2.3 |
| *P. granatum* | 43.66 | 46.66 | 46.66 | 45.66 | 1.73 |
| *O. stamineus* | 8 | 11.33 | 11.33 | 10.22 | 1.92 |
| *M. alba* | 23.33 | 28.29 | 28.29 | 26.63 | 2.86 |
| *H. sabdariffa* | 56 | 61.33 | 61.33 | 59.55 | 3.07 |

Table 1: Yield obtained after lyophilization, mean, and standard deviation obtained from three different samples of the same batch. All the measurement are expressed in % considering 3g of starting material.

To assess the polyphenol content of the extracts selected for the study Folin–Ciocalteu and aluminum chloride colorimetric methods, commonly used for the estimation of

total phenolic compounds and flavonoids, respectively, were performed. The results show that the highest concentrations of polyphenols are registered for *C. sinensis* with a mean of 201.12 ± 36.49 mg GAE g-1 of extract and *P. granatum* with 483.71 ± 105.63 mg GAE g−1 of extract. Java tea if compared to the green tea show a lower concentration of 66.57 ± 28.91 mg GAE g−1 of extract and the lowest concentrations are reported for *M. alba* and *H. sabdariffa* with 38.44 ± 6.96 and 31.40 ± 5.60 mg GAE g−1 of extract (Tab. 2).

| Plant extract | Total Polyphenols (mg GAE. g−1) | Standard deviation |
|---|---|---|
| *C. sinensis* | 201.12 | 36.49 |
| *P. granatum* | 66.57 | 28.91 |
| *O. stamineus* | 31.402 | 5.60 |
| *M. alba* | 38.44 | 6.96 |
| *H. sabdariffa* | 483.71 | 105.63 |

Table 2: Total polyphenol content expressed as mg GAE. g−1 of extract obtained from C. sinensis *P. granatum*, *O. stamineus*, *M. alba* and *H. sabdariffa*. The means and standard deviations were obtained from the data corresponding to three different extractions and each extract was analyzed in triplicate.

## *4.2. Trolox Equivalent Antioxidant Capacity (TEAC)*

As expected, the TEAC reflect the total phenolic concentration of the different extracts, the highest % of inhibition was registered for *P. granatum* and *C. sinensis* followed by *O. stamineus*, *M. alba* and *H. sabdariffa* which have a very similar antioxidant potential (Tab.3).

| Plant extract | ABTS (μmol TE g−1) | Standard deviation | % Inhibition |
|---|---|---|---|
| *C. sinensis* | 0.255 | 0.314 | 45.77* |
| *P. granatum* | 0.418 | 0.167 | 81.40* |
| *O. stamineus* | 0.031 | 0.085 | 45.10 |
| *M. alba* | 0.020 | 0.025 | 34.05 |
| *H. sabdariffa* | 0.019 | 0.040 | 45.59 |

Table 3: TEAC is expressed as μmol TE g−1 of extract obtained from *C. sinensis*, *P. granatum L.*, *O. stamineus*, *M. alba* and *H. sabdariffa*. The mean and standard deviation were obtained from three different extraction and each of them was used to obtain a technical triplicate. * The % inhibition of *C. sinensis* and *P. granatum* were obtained after 1:10 diluition.

## *4.3. Susceptibility Activity on UPEC*

Tab. 4 shows the values of MIC and MBC of the hydroalcoholic extracts against the UPEC *E. coli* ATCC 25922™. The most potent activity was registered for *H. sabdariffa* with a MIC of 6.25 mg/mL and a MBC of 12.5 mg/mL and for *P. granatum L.* with a MIC of 25 mg/mL and a MBC of 50 mg/mL (Fig. 22). For the other extracted was not possible register any type of antibacterial activity.

| *E.coli* ATCC 25922™ | | |
|---|---|---|
| Extract | MIC | MBC |
| *C. sinensis* | NA | NA |
| *P. granatum* | 25.00 | 50.00 |
| *O. stamineus* | NA | 50.00 |
| *M. alba* | NA | NA |
| *H. sabdariffa* | 6.25 | 25.00 |

Table 4: The minimum inhibitory concentration (MIC) and minimum bactericidial concentration (MBC) evaluated for the hydroalcoholic extract of *C. sinensis, P. granatum, O. stamineus, M. alba* and *H. sabdariffa* of UPEC *E. coli* ATCC 25922™. The highest

concentration evaluated was 50 mg/mL. NA means no inhibitory or bactericidal activity.

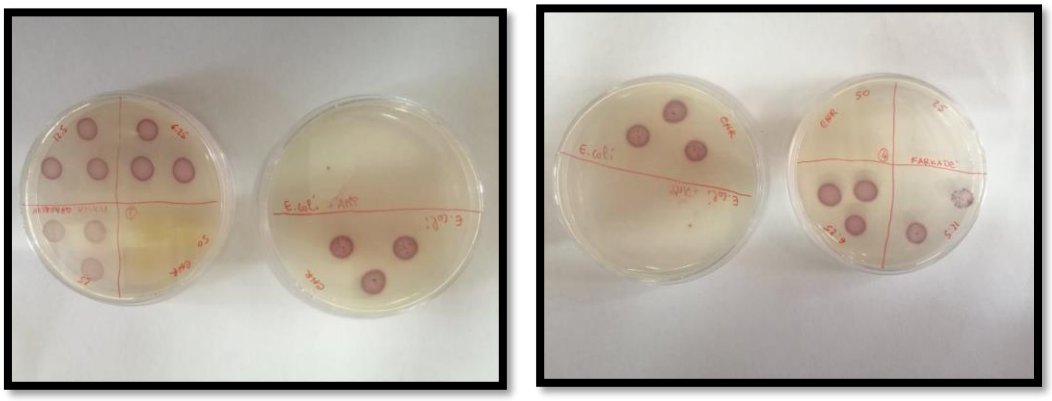

Fig. 22: In the first image (Left) is reported the plate after the treatment with *P. granatum*, in the second one (Right) with *H. sabdariffa L.*

## *4.4. Metabolic profile of H. sabdariffa extract*

The chromatogram reported in Fig. 23 was registered at λ 330 nm, the identification was determined thanks to the comparison between the data available in literature and the experimental data (RT, *m/z* and fragmentation) (Tab.5). The identified compounds are one organic acid, four phenolic acid and five flavonoids. Peak 1 represents hibiscus acid with *m/z* of 189.01 with the fragment 127 [MH–$H_2O$-$CO_2$] after the loss of water and $CO_2$ [14]. Peak 2 and 4 are chlorogenic acids with possible isomers with *m/z* 353.09 and the fragmentation pattern is 191, 179 and 191,173 for the isomer. The fragment at *m/z* 191 is the deprotonated quinic acid ($C_7H_{12}O_6$), fragment at *m/z* 179 is related to the dihydroxycinnamic acid ($C_9H_7O_4$) and fragment at *m/z* 173 is determined to the release of caffeic acid ($C_9H_8O_4$) [17]. Peak 3 at *m/z* 337.10 represent the P-coumaroylquinic acid, also in this case 91 is the deprotonated quinic acid ($C_7H_{12}O_6$), fragment at *m/z* 179 is related to the dihydroxycinnamic acid ($C_9H_7O_4$) as reported for

the chlorogenic acid [18]. Peak 5 and 7 are myricetin 3-arabinohexoside and myricetin 3-hexoside respectively. The examination of their respective MS2 fragmentation patterns allowed one main fragment ion to be distinguished at 317, which corresponds to the aglycone myricetin and the loss of an arabino-galactose moiety. Peak 6 is the 5-O-Caffeoylshikimic acid ($C_{16}H_{16}O_8$) and their fragments at *m/z* 161 and 135, the first one is determined from the loss of water from the deprotonated dihydroxycinnamic acid ($C_8H_7O_2$) $[179\text{-}H2O]^-$, while the second is derived from the deprotonated dihydroxycinnamic acid $[179\text{-}CO2]^-$ [20].

| ***Peak*** | ***RT*** | ***Compound*** | ***Mol.formula*** | ***m/z[M-H]-*** | ***Fragments*** | ***Error (ppm)*** |
|---|---|---|---|---|---|---|
| ***1*** | *0.59* | *Hibiscus acid* | $C_6H_5O_7$ | *189.01* | *127* | *1.30* |
| ***2*** | *2.38* | *Chlorogenic acid* | $C_{16}H_{17}O_9$ | *353.09* | *191/179* | *2.26* |
| ***3*** | *3.25* | *P-coumaroylquinic acid* | $C_{16}H_{17}O_9$ | *337.10* | *191/179* | *4.32* |
| ***4*** | *3.56* | *Chlorogenic acid isomer* | $C_{16}H_{17}O_9$ | *353.09* | *191/173* | *2.26* |
| ***5*** | *5.33* | *Myricetin 3-arabinohexoside* | $C_{26}H_{27}O_{17}$ | *611.11* | *316/271* | *5.01* |

| | | | | | | |
|---|---|---|---|---|---|---|
| ***6*** | *5.46* | *5-O-Caffeoylshikimic acid* | *$C_{16}H_{15}O_8$* | *335.08* | *161/135* | *3.62* |
| ***7*** | *5.67* | *Myricetin 3-hexoside* | *$C_{21}H_{20}O_{13}$* | *479.08* | *316/271/287* | *1.50* |
| ***8*** | *5.98* | *Quercetin 3-sambubioside* | *$C_{26}H_{27}O_{16}$* | *595.14* | *300/271/255* | *4.48* |
| ***9*** | *6.20* | *Quercetin 3-rutinoside* | *$C_{27}H_{29}O_{16}$* | *609.13* | *300/271/255* | *1.20* |
| ***10*** | *6.48* | *Quercetin 3-hexoside* | *$C_{21}H_{19}O_{12}$* | *463.10* | *301/271/255* | *0.60* |

Table 5: Identified compounds in the extract of *H. sabdariffa* according to the retention time (RT), Identified compounds in EAE according to the retention time (RT), *m/z* and fragmentation.

The loss of $C_{11}H_{18}O_9$ from the compound quercetin 3-sambubioside (peak 8) generates the fragments 300 after the loss of $C_6H_{10}O_4$ and the fragment ions at *m/z* 271 and 255 due to loss of $[Y\text{-}CHO]^-$ and $[CO+H2O]^-$, respectively. The same fragmentation pattern is followed by quercetin 3-rutinoside and quercetin 3-hexoside (peak 9 and 10) after the loss of $C_{12}H_{20}O_9$ and $C_{21}H_{19}O_{12}$.

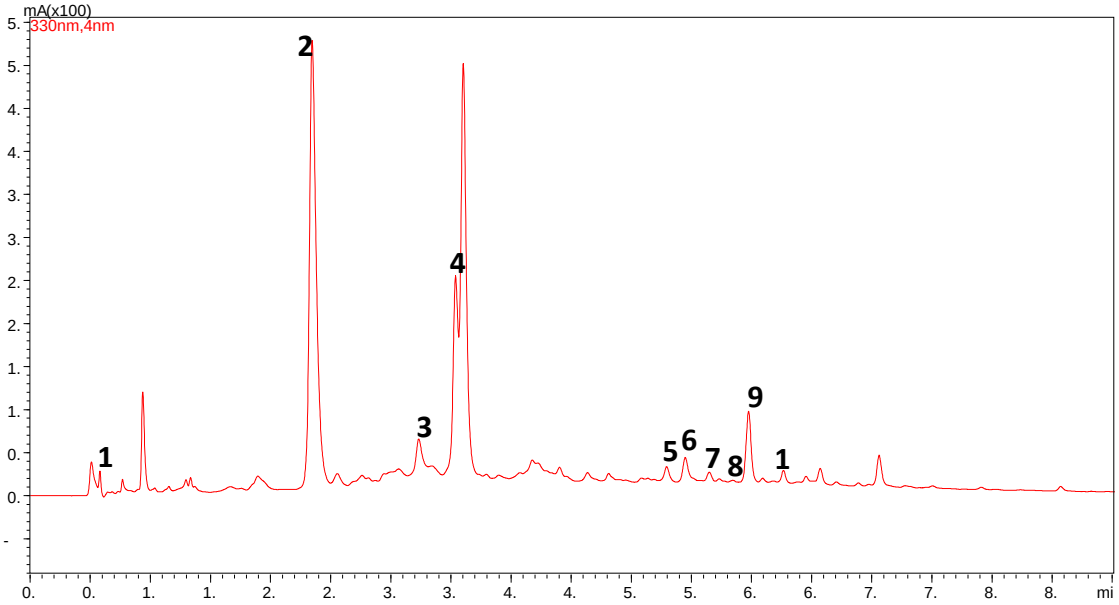


Fig. 23: Chromatogram obtained from the RP-HPLPDA analysis of EHS, registered at λ 330 nm. Peak 1: Hibiscus acid, peak 2: Chlorogenic acid; peak 3: P-coumaroylquinic acid; peak 4: Chlorogenic acid isomer; peak 5: Myricetin 3-arabinohexoside; peak 6: 5-O-Caffeoylshikimic acid; peak 7: Myricetin 3-hexoside; Peak 8: Quercetin 3-sambubioside; Peak 9: Quercetin 3-rutinoside; Peak 10: Quercetin 3-hexoside.

## *4.5. Invasion assay for E. coli with HT-1376 cells*

In Tab. 6 are reported the result obtained after the invasion assay. The experiment was repeated in duplicate and is possible to see a good dose response according to the CFU obtained. The highest activity for *H. sabdariffa* and *V. macrocarpon* against uropathogenic *E. coli* was registered at 50 mg/m however, is possible to see how the first extract seems to be more effective if compared to the second one for each concentration used in the assay.

| Treatment | CFU I | CFU II |
|---|---|---|
| Cells (HT-1376) | $4 \times 10^8$ | $3,5 \times 10^8$ |
| *H. sabdariffa* 50 mg/ml | $3,4 \times 10^5$ | $2,8 \times 10^5$ |
| *H. sabdariffa* 25 mg/ml | $1,8 \times 10^7$ | $2,1 \times 10^7$ |
| *H. sabdariffa* 12.5 mg/ml | $2,1 \times 10^8$ | $3,2 \times 10^8$ |
| *V. macrocarpon* 50 mg/ml | $6,7 \times 10^6$ | $5,7 \times 10^6$ |
| *V. macrocarpon* 25 mg/ml | $2,8 \times 10^7$ | $3,3 \times 10^7$ |
| *V. macrocarpon* 12.5 mg/ml | $5,2 \times 10^8$ | $4,7 \times 10^8$ |

Table 6: In table are reported the treatment used for the invasion assay with the correspond CFU (the experiment was performed in duplicate).

# 5. Discussion

The phytochemical profile of the *H. sabdariffa* extract revealed the presence of 10 secondary metabolites identified using RP-HPLPDA analysis. The analysis underlines the presence of different antimicrobial and anti-biofilm compounds. The hibiscus acid, studied from Torres et al., seems to show its MBC between 5 and 7 mg/mL against pathogenic *E. coli* strains effect. Moreover, at the same concentration, an alteration of the membrane permeability underlying the possible effect of this molecule against the pathogen was registered [260]. Ana et al (2020) assessed the MBC and MIC of different Hibiscus fractions against *E. coli* underlying the activity of the extracts between 25 and 500 mg/L for the extract and their fractions. Also, chlorogenic acid exhibits a similar effect against Gram negative, in fact according to Lou et al., this molecule with a MIC ranging from 20 to 80 μg/mL can bound the outer membrane and alter the intracellular potential inducing the pathogen to death [261]. A similar mechanism is mediated by p-coumaroylquinic acid with a MIC ranging from 10 to 80 μg/mL, in fact this molecule can bind the DNA double helix and affect the replication, transcription and expression also disrupting the bacterial cell [262]. The presence of all these compounds can explain the good MIC and MBC results obtained against uropathogenic *E. coli* and the good results obtained from the invasion assay.

# 6. Materials and Methods

## 6.1 Extraction procedure of *M. charantia* fruits

1 kg of fresh fruit was bought online (get-grocery.com), cleaned and chopped to divide individually skin, pulp, and seeds. The extraction material of each part of the fruit were obtained using five different fruits, three different consecutive extraction were performed using the ULTRA-TURRAX® (IKA) using water, water/acetonitrile (30/70) and ethyl acetate. For each extraction 45 mL of solvent were added to 9 g of starting material. At the end of the homogenization, the water solution was collected and discarded together with the polar compounds. The ethyl acetate and water/acetonitrile (30/70) were merged to remove the presence of the organic solvent using the rotary evaporator R100 (BÜCHI). The remained water solution was evaporated using the Speedvac DNA 120 (Thermo Fisher Scientific) at 30 °C at 1400 rpm for 15h to obtain the dried extract.

## 6.2 Caco-2 maintenance

Human adenocarcinoma cells Caco-2 were purchased from the German Collection of Microorganisms and Cell Cultures GmbH (DSMZ; ACC 169) and maintained in DMEM containing 10% (v/v) FBS with 1% penicillin and streptomycin (100 units/mL penicillin, and 100 µg/mL streptomycin). The cells were maintained at 37 °C in a humidified atmosphere of 5% CO2. The cells were used at passage 19–29 for all experiments. The cells were trypsinized at 70%-80% confluence using trypsin-EDTA after the PBS (w/o $Ca^{2+}$ and $Mg^{2+}$) wash step.

## 6.3 Viability assessment

To assess the cell viability avoiding the problems of the canonical viable test, a non-lytic, homogeneous, bioluminescent method was used. The RealTime-Glo was used to monitor the cell viability in real-time for six different time point (1, 2, 3, 4, 5, 6 h) at four different concentrations for Atropine (100, 10, 1, 0.1 µM), digoxine (100, 10, 1, 0.1 µM) and at five different concentrations for each part of the extract (500, 250, 125, 62.5, 31.25 µg/mL). The standards and the extracts were all prepared using the complete medium and at each point the luminescence was measured with an integration time of 0.5 second per well. The cells were seeded at 2500 per well in a 96 well and 2 days after the test was performed. At the end of the assay the luminescence was assessed on the multi plate reader infiniteM200 (Tecan). RealTime-Glo MT Cell Viability Assay were obtained from Promega Corporation. White 96-well assay plates were purchased from Corning, Inc. All reageant instead were purchased from Sigma.

## 6.4.1 Transwell seeding

Caco-2 were seeded at $3 \times 10^5$ cells/well into 12-well plates with Transwell® inserts and cultured for 21 days prior to transport experiments. The cells were seeded only when the percentage of viability was at least 98%, after the seeding the medium was changed only in the apical compartment between 6-16 hours after seeding to avoid the multilayer formation. The change medium was changed each two days for the maintenance and 12-24 h before the experiment to avoid the starved phenotype, during the experiment the filter were incubated under gentle shaking (100 rpm) to avoid the

unstirred water effect. Prior to start the experiment the filters were washed using Hanks' Balanced Salt Solution (HBSS) with $Ca^{2+}$ and $Mg^{2+}$ for 15-20 min at 37 °C in a humidified atmosphere of 5% CO2. The cell culture media, supplements, and reagents were obtained from Life Technologies.

### 6.4.2 Morphological studies of Caco-2 cells cultured on transwell system

To assess and verify the correct formation of the monolayer after the differentiation process a double staining was performed using first Alexa Fluor® 488 conjugate (Product # A27034; Thermofisher scientific; Germany) with secondary antibody Goat anti-Rabbit IgG (H+L) (Product # A-11008; Thermofisher scientific) and the HOECST 33342 to highlight the of ZO-1 and the nuclei presence. The medium was removed from the well and transferred to a new 12 well-plate, then the apical and the basolateral chamber were washed with 0.5 µL and 1.5 mL of HBSS respectively. The filters were stained with 3% paraformaldehyde/PBS to the apical side for 2 minutes at room temperature. The solution was removed and the filters washed 2 times with 500 µL of PBS for 10 minutes w/o $Ca^{2+}$ and $Mg^{2+}$, then the filter were treated with 0.1 % Triton X-100 in PBS w/o $Ca^{2+}$ and $Mg^{2+}$ for 1 min at 60 rpm on a plate shaker. The antibody solution was prepared diluting the stock solution 1:1000 in 0.2 % Triton X-100 PBS w/o $Ca^{2+}$ and $Mg^{2+}$ for 30 minutes. The antibody solution was removed, and the washing step repeat twice for 10 minutes with PBS w/o $Ca^{2+}$ and $Mg^{2+}$ for 30 minutes, after this the secondary antibody Goat anti-Rabbit IgG (H+L) was diluited 1:100 in the

same phosphate saline solution and 150 µL were added to each well for 30 minutes in the dark. The washing step was repeated twice for 10 minutes and finally the

HOECST 33342 was diluited 1:10000 in PBS w/o $Ca^{2+}$ and $Mg^{2+}$ for 5 minutes. At the end of the staining procedure the filter was washed 3 times and the membrane cut with a fine-pointed scalpel. The membrane was mounted on a microscope slide using two drops of Flourmont-G (Thermo fisher scientific). The slides were analyzed on the confocal microscope Zeiss LSM780 (Zeiss) and the image were processed using the ZEN software (Zeiss, Version 3.4).

### 6.4.3 Transport studies of Standards and *M. charantia* extracts

Caco-2 were seeded at $3 \times 10^5$ cells/well into 12-well plates with Transwell® inserts and cultured for 21 days prior to transport experiments. The cell culture media, supplements, and reagents were obtained from Life Technologies. The cells were seeded only when the percentage of viability was at least 98%, after the seeding the medium was changed only in the apical compartment between 6-16 hours after seeding to avoid the multilayer formation. The change medium was performed 12-24 h before the experiment to avoid the starved phenotype, during the experiment the filter were incubated under gentle shaking (100 rpm) to avoid the unstirred water effect. Prior to start the experiment the filters were washed using Hanks' Balanced Salt Solution (HBSS) with $Ca^{2+}$ and $Mg^{2+}$ for 15-20 min 37 °C in a humidified atmosphere of 5% CO2. Between 21-29 days, the cells were treated with standard solutions or with the extract to assess the permeability coefficient (Papp) of the interested compound.

### 6.4.4 Lucifer yellow assay

At the end of the assay to check the monolayer integrity was used the lucifer yellow, a solution of 1 mg/mL was prepared in HBSS and 400 µL of this solution were added in the apical compartment of each well for 1 h under gentle shaking (100 rpm). At the end 200 µL of basal compartment of each well were transferred in a 96 well plate and the plate was read with the multiplate reader infinite M200 (Tecan) excitation 485 nm/emission 535 nm.

## 6.5 Real-Time PCR (RT-qPCR)

Total RNA was extracted from Caco-2 cells using the RNeasy Plus Mini Kit (Qiagen) following the manufacturer's instructions. The quality and the quantity of RNA were checked using the Nanodrop 3.0 (Thermofisher Scientific), the reverse transcription was carried out using 800 ng of RNA using the iScript gDNA Clear cDNA Synthesis Kit (Biorad) according to the manufacture instructions. The primers (Eurofins Genomics) used in the qPCR assays were already validated and used to assess the presence of TAS2R in gastric parietal cells (Tab.7) [263]. The qPCR was performed using the SsoAdvanced Universal SYBR® Green Supermix (Biorad) following this cycling conditions: 30 s/98 °C (activation), 5-15 s/95 °C (denaturation), 15-30 s/60 °C (annealing and extension) with fluorescence measurement.

| Number | Name | Forward Primer Sequence | Reverse Primer Sequence |
|---|---|---|---|
| 1 | TAS2R1 | AAATGGCTCCGCTGGATCTC | GTGGCAAGCCAAAGTTCCAA |
| 2 | TAS2R3 | GGGACTCACCGAGGGGGTGT | CCTCAAGAGTGCCAGGGTGGTG |
| 3 | TAS2R4 | GCAGTGTCTGGTTTGTGACC | GCGTGATGTACAGGCAAGTG |
| 4 | TAS2R5 | ACACTCATGGCAGCCTATCC | CGAGCACACACTGTCTTCCA |
| 5 | TAS2R7 | GCAGGTGTGGATGTCAAACTC | TCTTGACCCAGTCCATGCAG |
| 6 | TAS2R10 | GCTACGTGTAGTGGAAGGCA | TCCATTCCCCAAAACCCCAA |
| 7 | TAS2R13 | GAAAGTGCCCTGCCGAGTAT | CCAGATCAGCCCAATTCTGGA |
| 8 | TAS2R14 | CCAGGTGATGGGAATGGCTTA | AGGGCTCCCCATCTTTGAAC |
| 9 | TAS2R19 | TCTTAGGACACAGCAGAGCA | AGCGTGTCATCTGCCACAAAA |
| 10 | TAS2R20 | ATTTGGGGGAACAAGACGCT | ACTACGGAAAAACTTGTGGGAA |
| 11 | TAS2R30 | GGCTGGAAAAGCAACCTGTC | ACACAATGCCCCTCTTGTGA |
| 12 | TAS2R31 | TTGAGGAGTGCAGTGTACCTTTC | ACGGCACATAACAAGAGGAAAA |
| 13 | TAS2R38 | CCCAGCCTGGAGGCCCACATT | TCACAGCTCTCCTCAACTTGGCA |
| 14 | TAS2R39 | TTCTGTGGCTGTCCGTGTTTA | GGGTGGCTGTCAGGATGAAC |
| 15 | TAS2R40 | CGGTGAACACAGATGCCACAGATA | GTGTTTTGCCCCTGGCCCACT |
| 16 | TAS2R41 | GCAGCGAATGGCTTCATTGT | TGGCTGAGTTCAGGAAGTGC |
| 17 | TAS2R42 | TCCTCACCTGCTTGGCTATC | GGCAAGCCAGGTTGTCAAGT |
| 18 | TAS2R43 | ATATCTGGGCAGTGATCAACC | CCCAACAACATCACCAGAATGAC |
| 19 | TAS2R46 | ACATGACTTGGAAGATCAAACTGAG | AGCTTTTATGTGGACCTTCATGC |
| 20 | TAS2R50 | CGCAAGATCTCAGCACCAAGGTC | GCCTTGCTAACCATGACAACCGGG |

| | | | |
|---|---|---|---|
| 21 | TAS2R8 | ATGTGGATTACCACCTGCCT | GGAAATGGCAAAGCATCCCAG |
| 22 | TAS2R9 | GCAGATTCGACTGCATGCTAC | TGCCTTTATGGCCCTCATGT |
| 23 | TAS2R16 | ATGGCATCACTGACCAAGCA | TTTCAACGTAGGGCTGCTCA |
| 24 | TAS2R45 | AGTACCCTTTACTGTAACCC | AGTAAATGGCACGTAACAAG |
| 25 | TAS2R60 | GGTGTTCAGTGCTGCAGGTA | CACCTTGAGGAACGACGACT |

Tab. 7: Forward and reverse primer sequences used in the qPCR assay.

# 7. Results

## 7.1 Monolayer integrity assessment and lucifer yellow permeability test

To assess and verify the correct formation of the monolayer after the differentiation process a double staining was performed using first Alexa Fluor® 488 conjugate

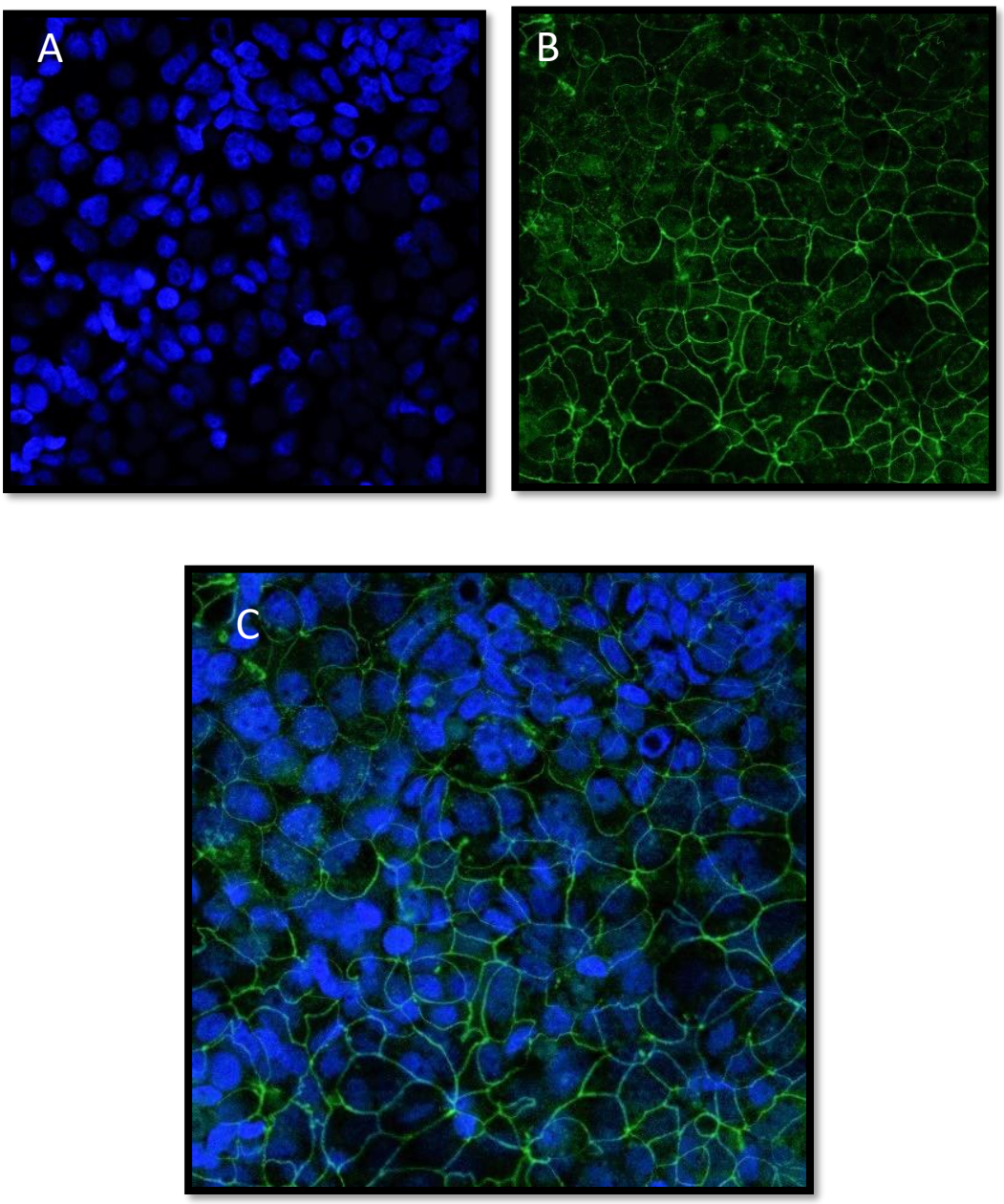

Fig. 24: Membrane integrity assessment using antibodies raised against the tight-junction protein ZO-1 (green) in Caco-2 cells. Cells were fixed with 3% paraformaladehyde/PBS for 2 min at room temperature. Cells were stained with ZO-1 primary antibody Goat anti-Rabbit IgG (H+L) #61-7300 at the concentration of 5 µg/mL for 1 hour at room temperature, and then incubated with the secondary antibody Goat anti-Rabbit IgG (H+L) Alexa Fluor® 488 conjugate (Product # A27034) at a dilution of 1:100 for 30 minutes hour at room temperature (Panel B). Nuclei (Panel A) were stained with Hoechst 33342 dye. The panel C represent the double staining used for the assay. Images were taken on Zeiss LSM780, confocal microscope system.

(Product # A27034) with secondary antibody Goat anti-Rabbit IgG (H+L)and the HOECST 33342 to highlight the presence of ZO-1 and the vitality of the cells. The Fig. 24 (A) represents the HOECST 33342 staining, while the panel B of the same figure the ZO-1 tight junction. The monolayer as shown in the panel C is intact, and the cells are vital, even after 6 hours in HBSS under gentle shaking (100 rpm). These conclusions are confirmed also from the permeability test with the lucifer yellow, for this test four well were monitored and were performed withdrawal from the basolateral compartment each 2h. Four negative controls were also prepared scratching the top of the filter with a tip or using toxic concentration of cucurbitacin B (1000 µM). The % permeability measured in the HBSS medium at each timepoint didn’t exceed the cut off value of 3 % for the control wells, while the negative control used in the same well revealed the lack of monolayer integrity (Fig. 25).

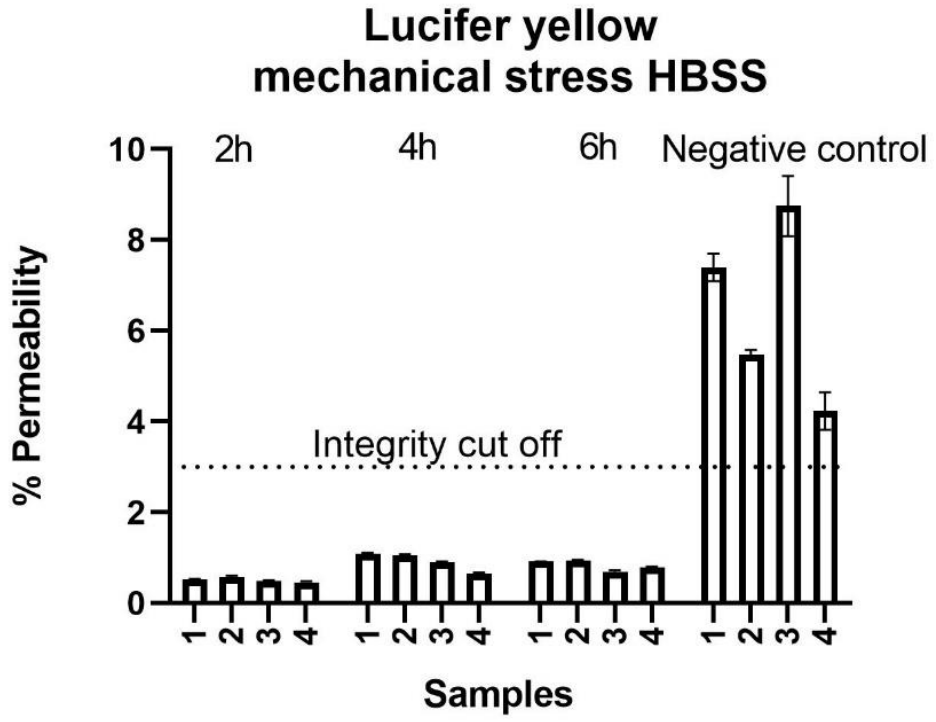


Fig. 25: HBSS is used to test the integrity of the membrane after 6 hours of shaking (100 rpm). Each value (RFU) is < than 3% if compared with negative control confirming the integrity of the membrane. Sample 1 and 2 of the negative control were prepared scratching the monolayer with a tip, while the 3 and 4 using a citotoxic concentration of Cucurbitacin B (1000 µM). The negative control values were obtained after 1h from the starting of the experiment.

## 7.2 Vitality assay

The results obtained from the RealTime-Glo MT Cell Viability Assay reveal that the treatment with skin (Fig. 26) reduce the vitality of Caco-2 cells with a good dose-response, only the concentration of 31.25 µg/mL seems to be comparable to the not treated control.

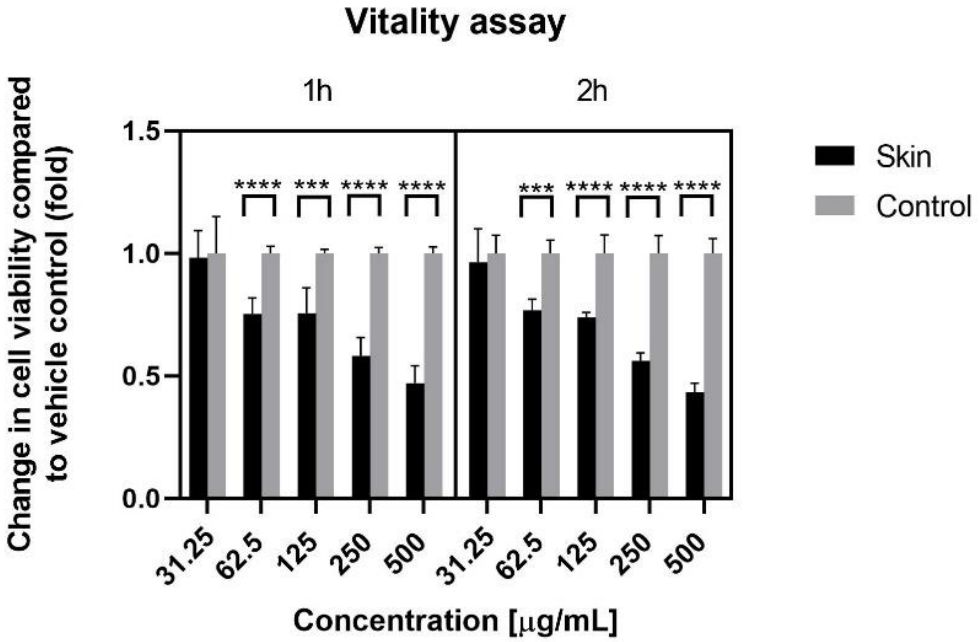


Fig. 26: Viability of caco-2 cells using the RealTime-Glo™ MT (mean ± std.dev; n=4) treated with the skin extract from 500 to 31.25 µg/mL for 2h. On the y axis is reported the cell viability compared to the vehicle control (medium + DMSO), while on the x axis is reported the µM concentration of the standard used for the treatment (**p<.01; ***p<.001; ****p<.0001).

A similar pattern is followed by the pulp treatment, in fact also in this case only the concentration of 31.25 µg/mL seems to be comparable to the not treated control. All the other concentrations reduce the vitality of the treated cells (Fig. 27).

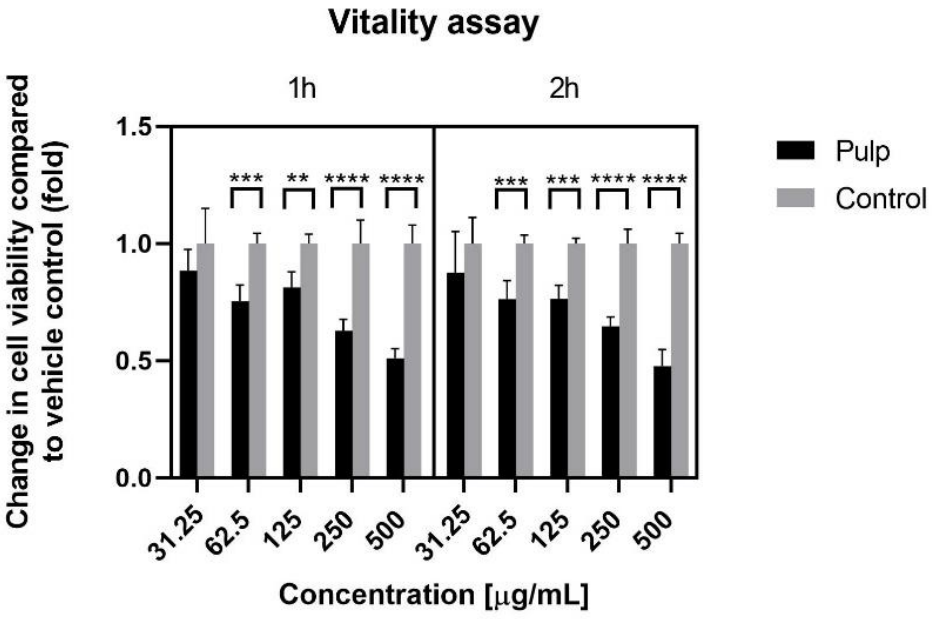


Fig. 27: Viability of caco-2 cells using the RealTime-Glo™ MT (mean ± std.dev; n=4) treated with pulp extract from 500 to 31.25 µg/mL for 2h. On the y axis is reported the cell viability compared to the vehicle control (medium + DMSO), while on the x axis is reported the µM concentration of the standard used for the treatment (**p<.01; ***p<.001; ****p<.0001).

A vitality difference between the control and the treated cells were registered only for 250 and 500 µg/mL concentration for the extract obtain from the whole fruit (Fig. 28).

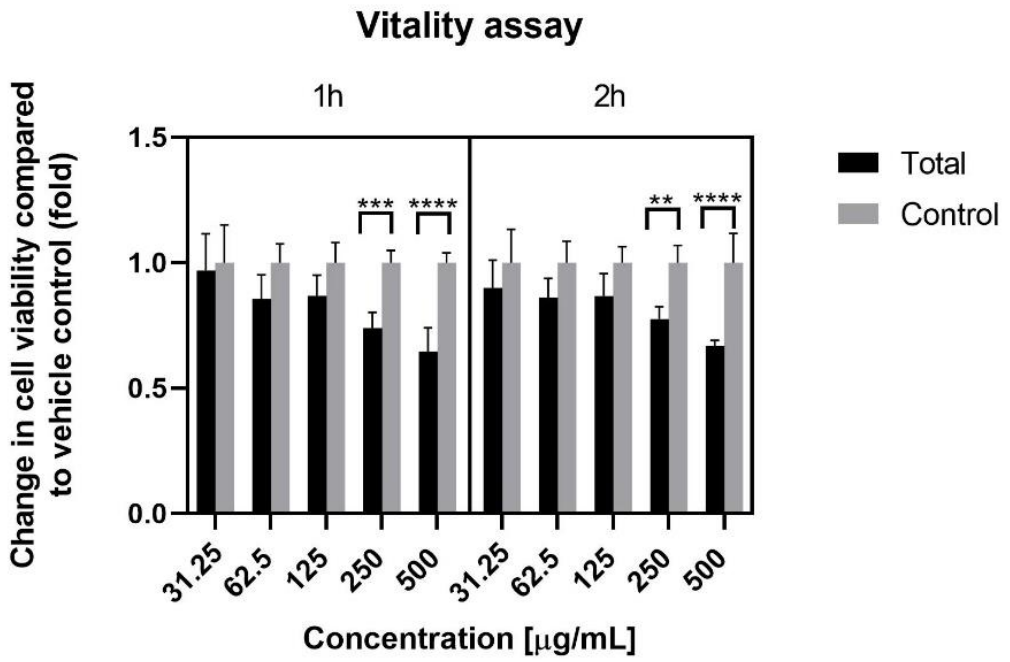


Fig. 28: Viability of caco-2 cells using the RealTime-Glo™ MT (mean ± std.dev; n=4) treated with whole extract from 500 to 31.25 µg/mL for 2h. On the y axis is reported the cell viability compared to the vehicle control (medium + DMSO), while on the x axis is reported the µM concentration of the standard used for the treatment (**p<.01; **p<.001; ****p<.0001).

For the seed treatment there was a difference between the treated and the control cells also at the 125 µg/mL. Considering the results obtained from the vitality assay the transwell were treated for 2h at the concentration of 31.25 µg/mL for each of the 4 extracts tested (Fig. 29).

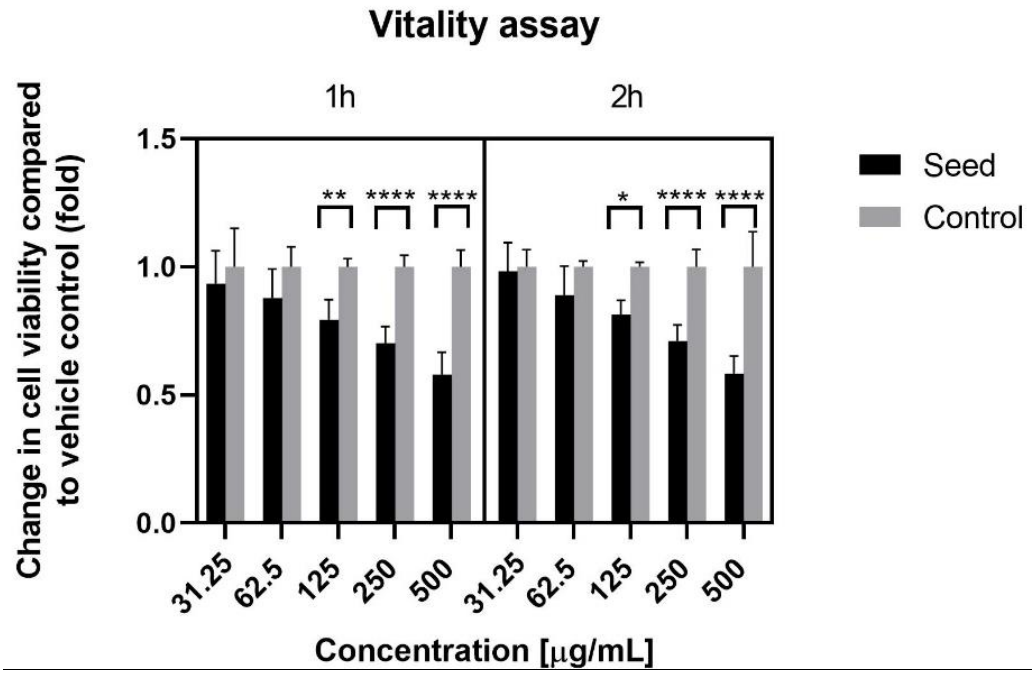


Fig. 29: Viability of caco-2 cells using the RealTime-Glo™ MT (mean ± std.dev; n=4) treated with different part of extract (Total, Skin, Pulp, Seed) from 500 to 31.25 µg/mL for 2h. On the y axis is reported the cell viability compared to the vehicle control (medium + DMSO), while on the x axis is reported the µM concentration of the standard used for the treatment (**p<.01; **p<.001; ****p<.0001).

The atropine and digoxin mixes are not changing the vitality of the cells if compared to the control, even at the highest concentration of 100 µM (Fig. 30).

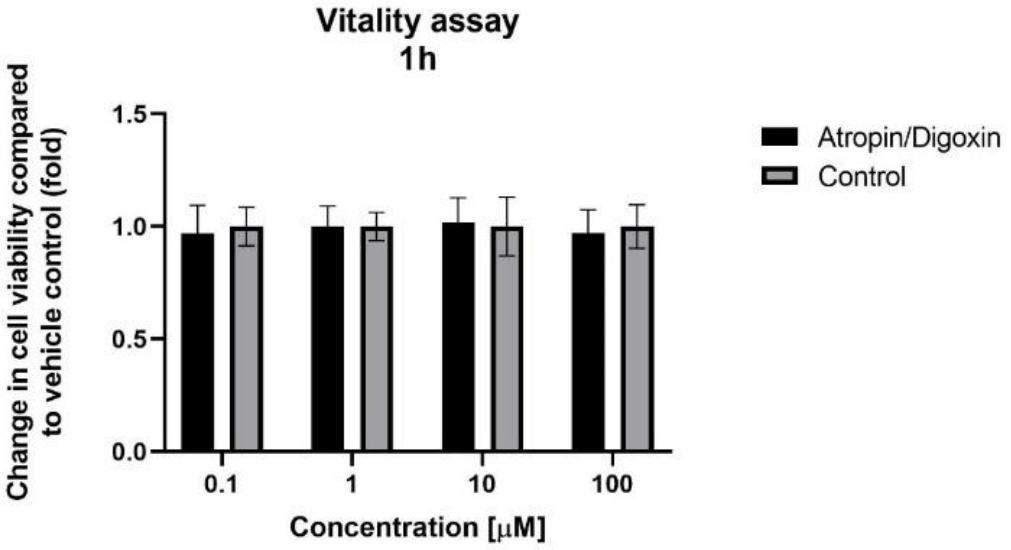


Fig. 30: Viability of caco-2 cells using the RealTime-Glo™ MT (mean ± std.dev; n=4) treated with Atropin + Digoxin starting from 0.1 to 100 µM for 1h. On the y axis is reported the cell viability compared to the vehicle control (medium + DMSO), while on the x axis is reported the µM concentration of the standard used for the treatment (**p<.01; ****p<.001).

Different is the case of the cucurbitacin B. Even at the concentration of 1 µM the cucurbitacin B seems to affect the vitality of the cells if compared to the control, it is possible to see a clear dose response at the following concentration of 10 and 100 µM for 1 h and 2 h.

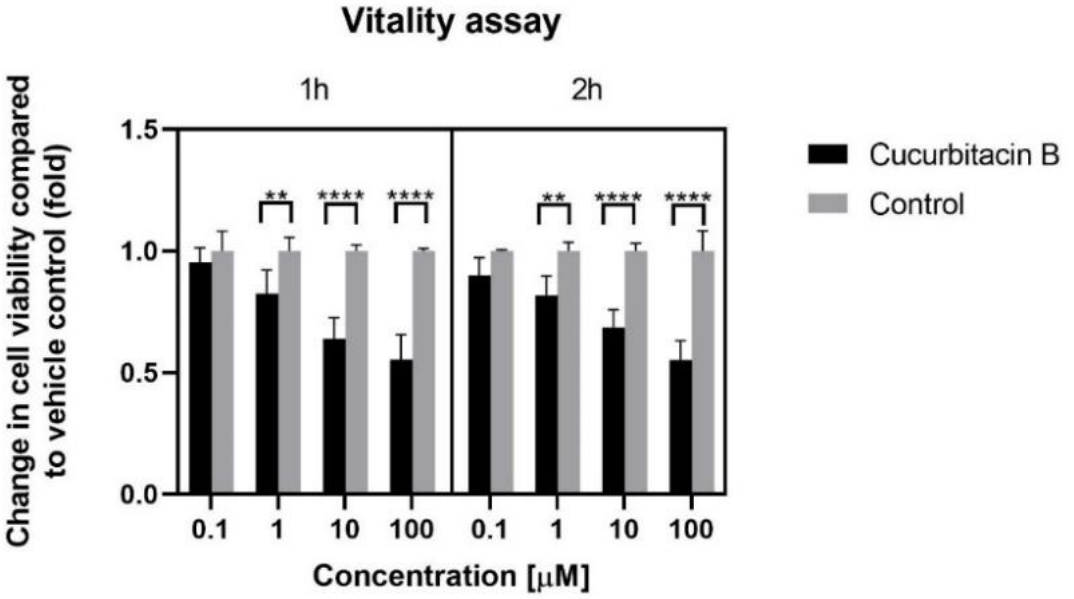


Fig. 31: Viability of caco-2 cells using the RealTime-Glo™ MT (mean ± std.dev; n=4) treated with Cucurbitacin B starting from 0.1 to 100 μM for 1h. On the y axis is reported the cell viability compared to the vehicle control (medium + DMSO), while on the x axis is reported the μM concentration of the standard used for the treatment (**p<.01; ****p<.001).

## 7.3 Cucurbitacin B treatment and effect on Caco-2 monolayer

The confocal microscope images obtained after the treatment of the transwell monolayer with the cucurbitacin B after 2 hours reveal the pharmacological activity of the cucurbitacin B well established from literature. In Fig. 32 is possible to see a clear alteration of nuclei morphology and cell shape.

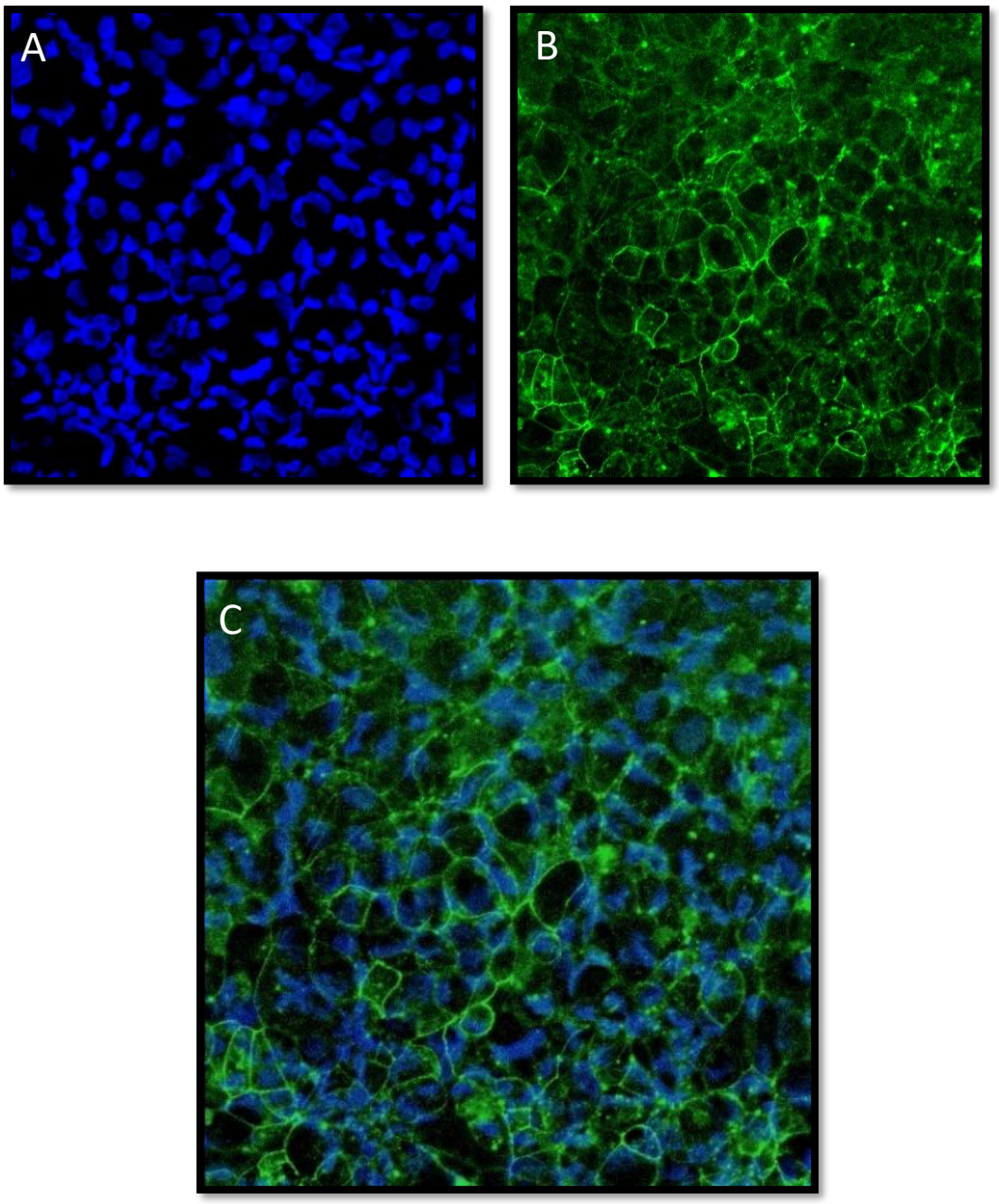


Fig. 32: Monolayer integrity and morphology assessment after the treatment of Caco-2 differentiated cells with 1000 µM of Cucurbitacin B standard solution in HBSS after 2 hours of treatment.

The alteration of the nuclei is very clear also at the concentration of 100 µM even if is not so pronounced, is it possible again to see holes in the membrane and alteration of cell morphology. Cells shape and ZO-1 distribution is more organized (Fig. 33).

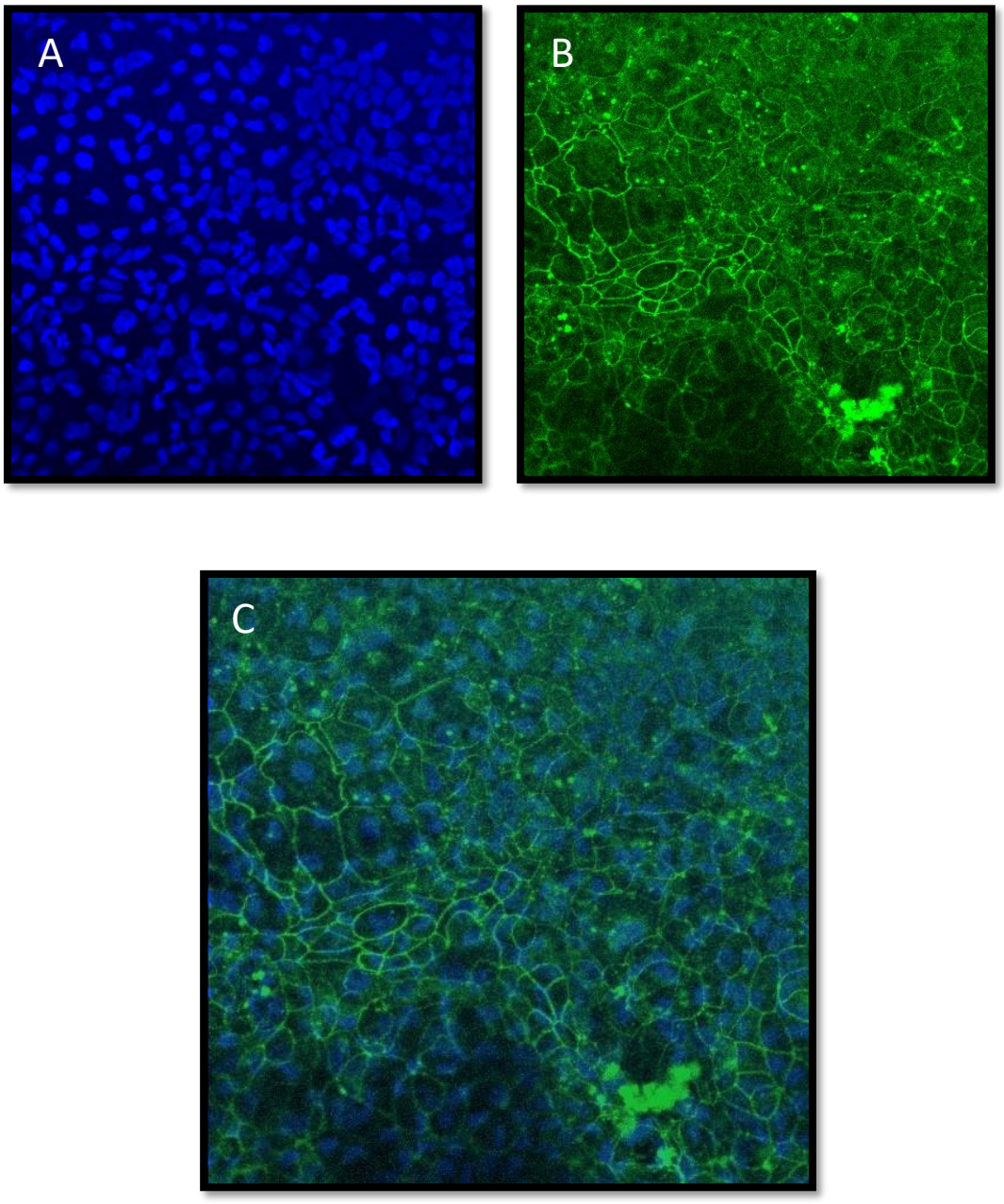


Fig. 33: Monolayer integrity and morphology assessment after the treatment of Caco-2 differentiated cells with 100 µM of Cucurbitacin B standard solution in HBSS after 2 hours of treatment.

In Fig. 34 (Panel A) is possible to see slight alterations from the nuclei shape start at the concentration of 10 µM- However, also according to the vitality assay, the cucurbitacin B is still affecting the monolayer integrity promoting the apoptosis process and the formation of big gaps which are very visible in the panel B.

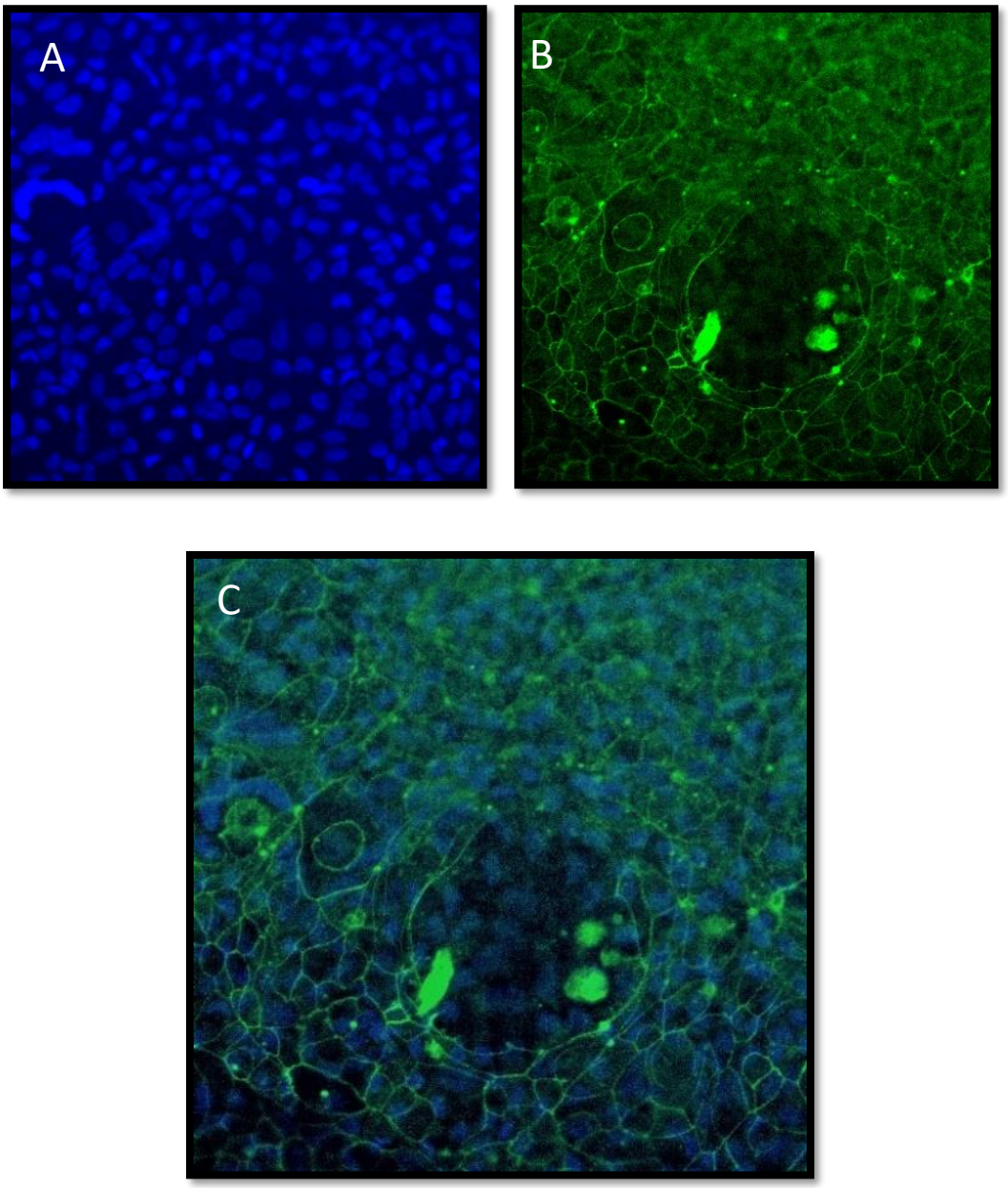

Fig. 34: Monolayer integrity and morphology assessment after the treatment of Caco-2 differentiated cells with 10 µM of Cucurbitacin B standard solution in HBSS after 2 hours of treatment.

At the concentration of 1 µM the nuclei come back to have a normal shape (Fig 35). The structure of the monolayer is very well organized even if it is possible to see some

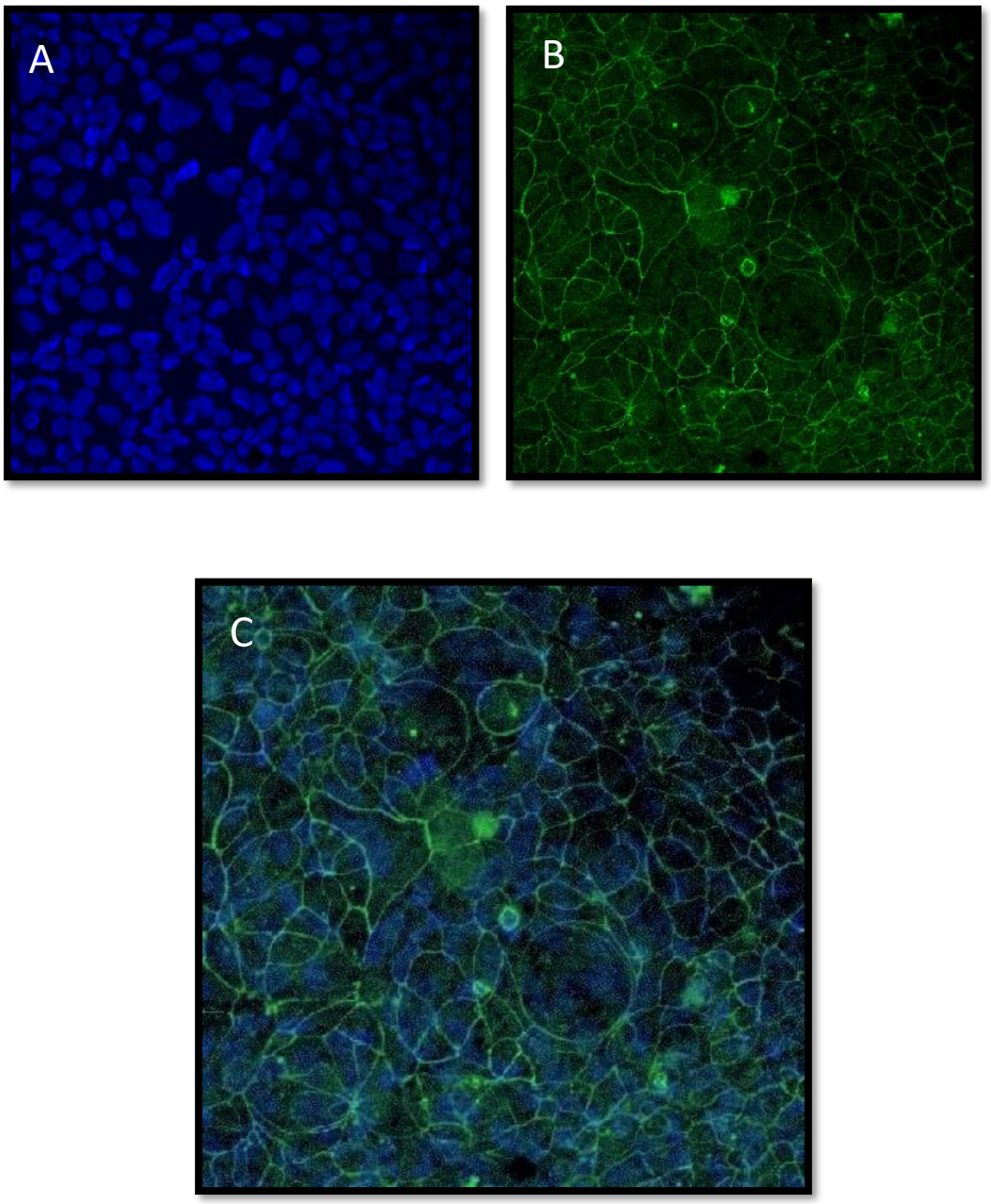

Fig. 35: Monolayer integrity and morphology assessment after the treatment of Caco-2 differentiated cells with 1 µM of Cucurbitacin B standard solution in HBSS after 2 hours of treatment.

holes and gaps between cells; according to the vitality assay this concentration is still lower if compared to the control.

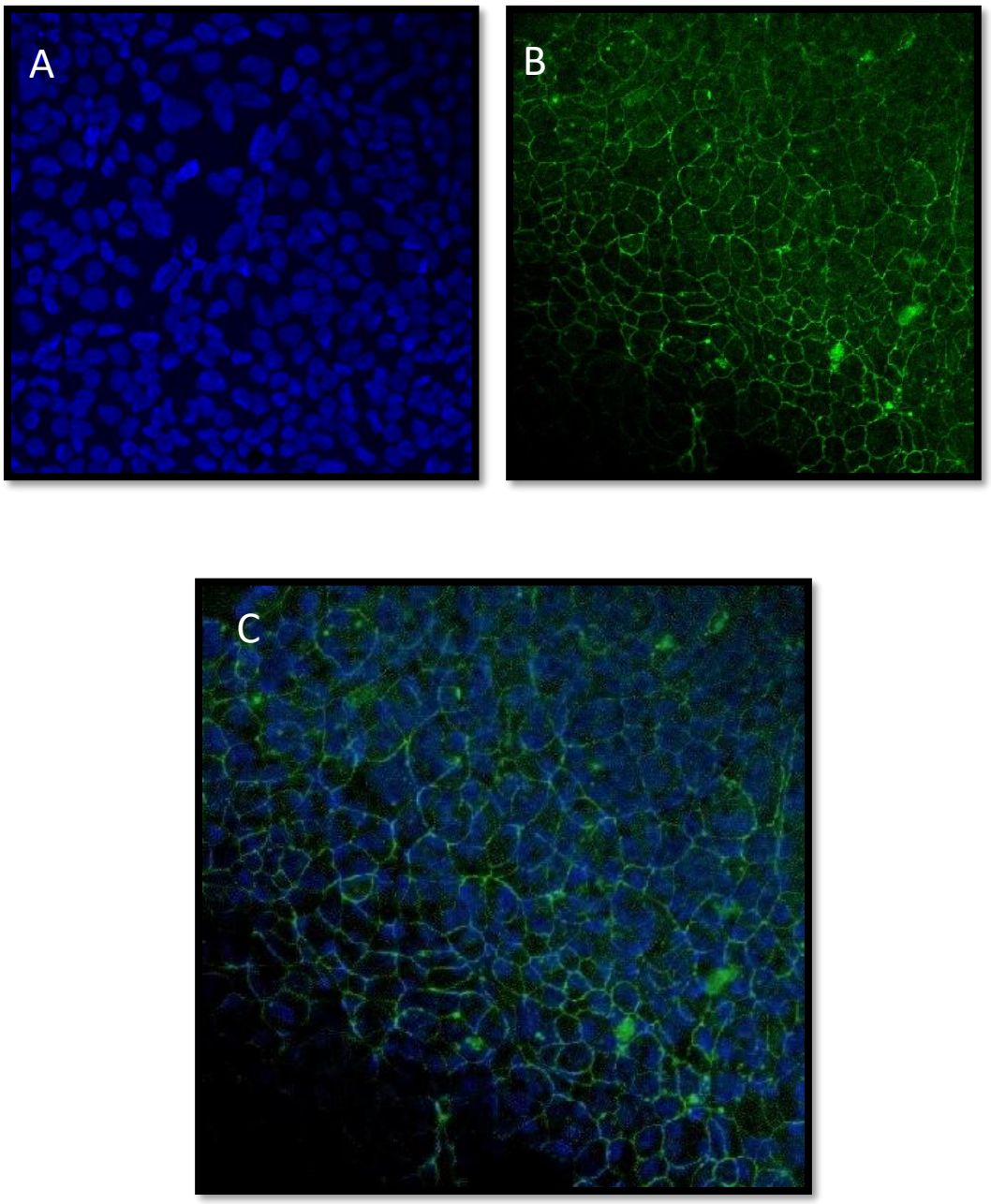

Fig. 36: Monolayer integrity and morphology assessment after the treatment of Caco-2 differentiated cells with 0.1 µM of Cucurbitacin B standard solution after 2 hours of treatment.

At this concentration the vitality assay and the confocal microscope confirm the activity of cucurbitacin B on the cells. Finally, at the concentration of 0.1 µM the shape of the nuclei and the organization of the cells seems to be more precise and without any type of alteration, these types of images are in fact comparable to the non-treated control (Fig. 36).

## 7.4 TAS2R expression in Caco-2

Using quantitative reverse transcription PCR (RT-qPCR), we screened the expression profile of all 25 TAS2R genes in human in Caco-2 (DSMZ ACC169; LOT 19). We found that TAS2R14 and TAS2R31 were the most abundantly expressed genes, with a mean ct level of 28.28 and 29.31. The expression levels of TAS2R5, TAS2R19 are similar followed by TAS2R42, TAS2R4, TAS2R20, TAS2R45, TAS2R3, TAS2R10, TAS2R46, TAS2R60. Fourteen TAS2R genes (TAS2R1, TAS2R7, TAS2R8, TAS2R9, TAS2R16, TAS2R30, TAS2R38, TAS2R39, TAS2R40, TAS2R41, TAS2R41 and TAS2R60) were not expressed according to the experimental conditions used (Tab. 8).

| Target | Cq | Mean -ΔCq expression *1000 ± Dev.st |
|---|---|---|
| **TAS2R1** | NA | NA |
| **TAS2R3** | 31.37 ± 0.43 | 0.46 ± 0.13 |
| **TAS2R4** | 31.48 ± 0.16 | 0.79 ± 0.09 |
| **TAS2R5** | 30.33 ± 0.39 | 1.94 ± 0.33 |
| **TAS2R7** | NA | NA |
| **TAS2R8** | NA | NA |
| **TAS2R9** | NA | NA |
| **TAS2R10** | 32.21 ± 0.42 | 0.377 ± 0.084 |
| **TAS2R13** | 33.56 ± 0.56 | 0.21 ± 0.08 |
| **TAS2R14** | 28.28 ± 0.11 | 5.64 ± 1.02 |
| **TAS2R16** | NA | NA |
| **TAS2R19** | 30.09 ± 0.59 | 2.33 ± 0.59 |
| **TAS2R20** | 31.62 ± 0.80 | 0.46 ± 0.06 |
| **TAS2R30** | NA | NA |
| **TAS2R31** | 29.31 ± 0.1 | 3.55 ± 0.29 |

| | | |
|---|---|---|
| **TAS2R38** | NA | NA |
| **TAS2R39** | NA | NA |
| **TAS2R40** | NA | NA |
| **TAS2R41** | NA | NA |
| **TAS2R42** | 31.03 ± 0.38 | 1.26 ± 0.82 |
| **TAS2R43** | NA | NA |
| **TAS2R45** | 31.79 ± 0.48 | 0.75 ± 0.28 |
| **TAS2R46** | 33.26 ± 0.86 | 0.25 ± 0.05 |
| **TAS2R50** | 33.04 ± 0.57 | 0.26 ± 0.11 |
| **TAS2R60** | NA | NA |
| **GADPH** | 18.76 ± 0.78 | - |
| **HPRT1** | 23.19 ± 0.68 | - |

Tab. 8: TAS2R expression of all human subtype in Caco-2 (DSMZ ACC169; LOT 19). All datas are expressed as mean ($2^{-\Delta Ct}$ * 1000) ± Dev.st or Cq ± Dev.st obtained from 4 biological replicates (n = 3).

In Fig. 37 is reported the overall TAS2R expression in Caco-2 (DSMZ ACC169; LOT 19) and this is the first time that where a complete gene expression of this receptor is

accomplished in this specific line. According to this analysis 13 TAS2Rs are expressed on this specific cell lines, for the other 12 genes was not possible assess their presence.

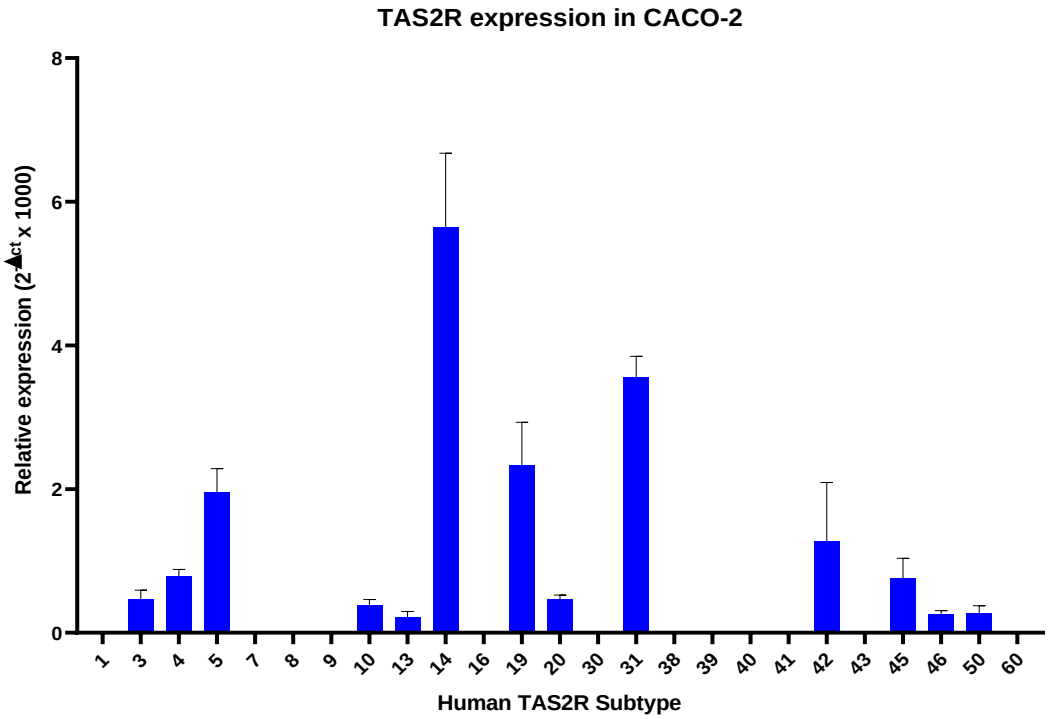


Fig. 37: TAS2R expression of all human subtype in Caco-2 of all human subtype in Caco-2 (DSMZ ACC169; LOT 19). Results are expressed as mean ($2^{-\Delta Ct}$ * 1000) ± Dev.st obtained from 4 biological replicates (n = 3).

The same procedure of screening was followed also for the differentiated Caco-2 cells growth on the transwell filter. The Cq values of several receptor decreased, and the differentiation process seems induced a change in the expression level of TAS2Rs. We found that TAS2R14 and TAS2R31 remain the most expressed with a mean Cq level

of 27.77 and 28.02. The expression levels of TAS2R5, TAS2R19 are similar followed by TAS2R20, TAS2R4, TAS2R46, TAS2R30, TAS2R10, TAS2R50, TAS2R45, TAS2R13, TAS2R1 and TAS2R8. Eleven TAS2R genes (TAS2R3, TAS2R7, TAS2R9, TAS2R16, TAS2R38, TAS2R39, TAS2R40, TAS2R41, TAS2R42, TAS2R43 and TAS2R60) were not expressed according to the experimental conditions used (Tab. 9).

| **Target** | **Cq** | **Mean -ΔCq expression *1000 ± Dev.st** |
|---|---|---|
| **TAS2R1** | 33.96 ± 0.74 | 0.12 ± 0.031 |
| **TAS2R3** | NA | NA |
| **TAS2R4** | 31.28 ± 0.59 | 1.00 ± 0.37 |
| **TAS2R5** | 29.44 ± 0.24 | 2.74 ± 0.44 |
| **TAS2R7** | NA | NA |
| **TAS2R8** | 34.65 ± 0.73 | 0.07 ± 0.014 |
| **TAS2R9** | NA | NA |
| **TAS2R10** | 32.79 ± 0.29 | 0.33 ± 0.09 |
| **TAS2R13** | 33.91 ± 0.50 | 0.13 ± 0.04 |
| **TAS2R14** | 27.77 ± 0.11 | 7.58 ± 0.86 |

| | | |
|---|---|---|
| **TAS2R16** | NA | NA |
| **TAS2R19** | 29.07 ± 0.15 | 3.54 ± 0.36 |
| **TAS2R20** | 30.42 ± 0.53 | 1.37 ± 0.05 |
| **TAS2R30** | 31.75 ± 0.43 | 0.70 ± 0.21 |
| **TAS2R31** | 28.02 ± 0.09 | 9.16 ± 0.73 |
| **TAS2R38** | NA | NA |
| **TAS2R39** | NA | NA |
| **TAS2R40** | NA | NA |
| **TAS2R41** | NA | NA |
| **TAS2R42** | NA | NA |
| **TAS2R43** | NA | NA |
| **TAS2R45** | 33.63 ± 0.21 | 0.83 ± 0.25 |
| **TAS2R46** | 31.69 ± 0.50 | 0.21 ± 0.022 |
| **TAS2R50** | 32.93 ± 0.57 | 0.35 ± 0.11 |
| **TAS2R60** | NA | NA |
| **GADPH** | 18.91 ± 0.63 | - |
| **HPRT1** | 23.20 ± 0.38 | - |

Tab. 9: TAS2R expression of all human subtype in Caco-2 after 21 days. All datas are expressed Cq ± Dev.st obtained 3 biological replicates (n = 3) for the other groups.

It is clear (Fig. 38) how the expression of TAS2Rs in this case is different if compared to the normal cells, this is the first time that a scientific research claim that the differentiation process can induce a change in the TAS2R expression. Moreover, it seems that some receptor after the differentiation process are not expressed anymore (TAS2R3, TA2R42) while other are expressed only after the differentiation process (TAS2R1, TA2R8, TAS2R30). Moreover, the mean of the overall gene expression of TAS2R seems to be reduced, underlying a general overexpression of these receptors.

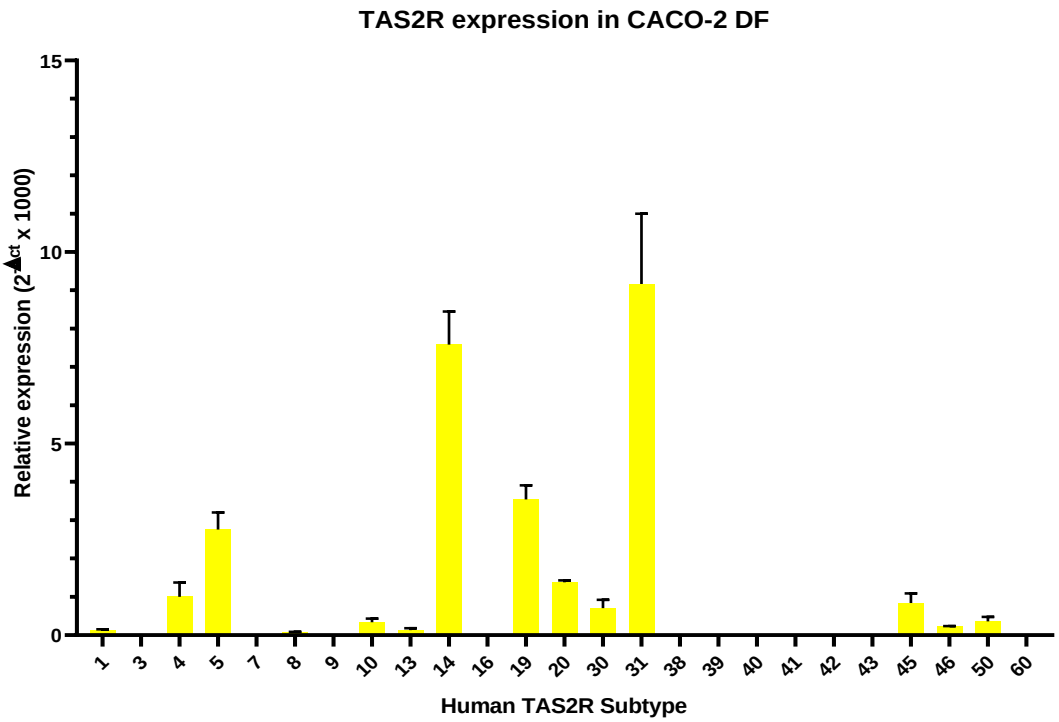


Fig. 38: TAS2R expression of all human subtype in Caco-2 of all human subtype in Caco-2

differentiated after 21 days (DF). Results are expressed as mean ($2^{-\Delta Ct}$ * 1000) ± Dev.st obtained from 3 biological replicates (n = 3).

After the treatment with the bitter melon extract at the concentration of 31.25 µg/mL for 2 hours the gene expression of all TAS2R were repeated again. We found that TAS2R14 and TAS2R31 remain the most expressed with a mean Cq level of 27.65 and 30.11, followed by TAS2R19 20, TAS2R5, TASR20, TAS2R45, TAS2R10, TAS2R50, TAS2R46, TAS2R8, TAS2R1 and TAS2R30. Twelve TAS2R genes (TAS2R3, TAS2R4, TAS2R7, TAS2R9, TAS2R16, TAS2R38, TAS2R39, TAS2R40, TAS2R41, TAS2R42, TAS2R43 and TAS2R60) were not expressed according to the experimental conditions used (Tab. 10).

| **Target** | **Cq** | **Mean -ΔCq expression *1000 ± Dev.st** |
|---|---|---|
| **TAS2R1** | 34.34 ± 0.92 | 0.11 ± 0.04 |
| **TAS2R3** | NA | NA |
| **TAS2R4** | NA | NA |
| **TAS2R5** | 31.70 ± 0.32 | 0.69 ± 0.15 |
| **TAS2R7** | NA | NA |

| | | |
|---|---|---|
| **TAS2R8** | 34.22 ± 0.44 | 0.09 ± 0.03 |
| **TAS2R9** | NA | NA |
| **TAS2R10** | 33.33 ± 0.42 | 0.11 ± 0.03 |
| **TAS2R13** | 35.55 0.13 | 0.04 ± 0.007 |
| **TAS2R14** | 27.65 ± 0.16 | 9.76 ± 3.10 |
| **TAS2R16** | NA | NA |
| **TAS2R19** | 30.11 ± 0.44 | 2.10 ± 0.41 |
| **TAS2R20** | 31.70 ± 0.77 | 0.74 ± 0.26 |
| **TAS2R30** | 34.51 ± 0.24 | 0.14 ± 0.01 |
| **TAS2R31** | 30.11 ± 0.07 | 3.14 ± 0.22 |
| **TAS2R38** | NA | NA |
| **TAS2R39** | NA | NA |
| **TAS2R40** | NA | NA |
| **TAS2R41** | NA | NA |
| **TAS2R42** | NA | NA |
| **TAS2R43** | NA | NA |
| **TAS2R45** | 31.90 ± 0.12 | 0.89 ± 0.34 |

| | | |
|---|---|---|
| **TAS2R46** | 34.19 ± 0.13 | 0.22 ± 0.09 |
| **TAS2R50** | 34.06 ± 0.40 | 0.19 ± 0.05 |
| **TAS2R60** | NA | NA |
| **GADPH** | 18.92 ± 0.65 | - |
| **HPRT1** | 23.22 ± 0.68 | - |

Tab. 10: TAS2R expression of all human subtype in Caco-2 DF treated with bitter melon (BM) from the apical side (A-B). All datas are expressed as mean ($2^{-\Delta Ct}$ * 1000) ± Dev.st or Cq ± Dev.st obtained from 4 biological replicates (n = 3).

The gene expression of TAS2R change after the apical treatment with the bitter melon extract for 2h, is possible to see how TAS2R4 it is not still detectable if compared to the Caco-2 DF group. It is clear how different TAS2R are downregulation if compared to the gene expression of the other groups.

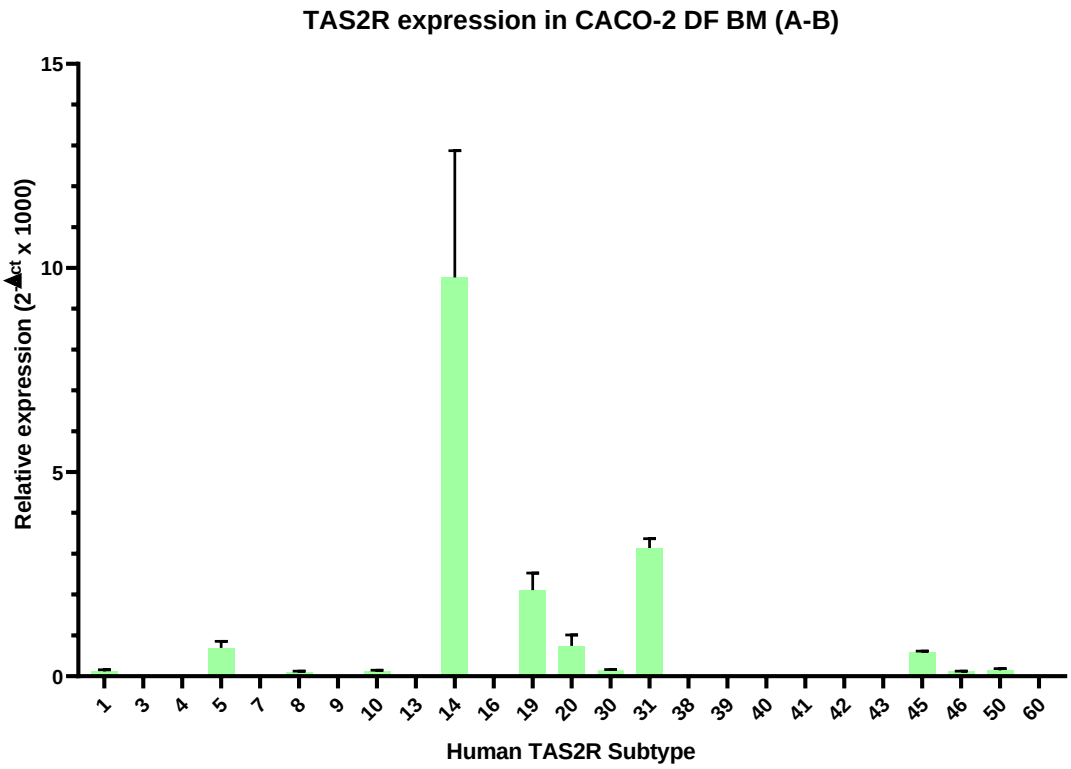


Caco-2 DF treated with bitter melon (BM) from the apical side (A-B). Results are expressed as mean ($2^{-\Delta Ct}$ * 1000) ± Dev.st obtained from 4 biological replicates (n = 3).

The treatment was repeated also for the basolateral compartment at the same concentration of 31.25 µg/mL for 2 hours. We found that TAS2R14 and TAS2R31 remain the most expressed with a mean Cq level of 27.40 and 28.58, followed by TAS2R5, TASR19, TASR45, TAS2R20, TAS2R4, TAS2R30, TAS2R42, TAS2R46, TAS2R50, TAS2R1, TAS2R10, TAS2R8 and TAS2R13. Ten TAS2R genes (TAS2R3, TAS2R7, TAS2R9, TAS2R16, TAS2R38, TAS2R39, TAS2R40, TAS2R41, TAS2R43 and TAS2R60) were not expressed according to the experimental conditions used (Tab. 11).

| Target | Cq | Mean -ΔCq expression *1000 ± Dev.st |
|---|---|---|
| **TAS2R1** | 33.16 ± 0.46 | 0.08 ± 0.03 |
| **TAS2R3** | NA | NA |
| **TAS2R4** | 31.62 ± 0.16 | 0.54 ± 0.08 |
| **TAS2R5** | 29.88 ± 0.11 | 1.98 ± 0.20 |
| **TAS2R7** | NA | NA |
| **TAS2R8** | 33.38 ± 0.39 | 0.07 ± 0.02 |
| **TAS2R9** | NA | NA |
| **TAS2R10** | 33.20 ± 0.52 | 0.08 ± 0.03 |
| **TAS2R13** | 34.87 ± 0.37 | 0.06 ± 0.02 |
| **TAS2R14** | 27.40 ± 0.02 | 7.16 ± 0.59 |
| **TAS2R16** | NA | NA |
| **TAS2R19** | 30.10 ± 0.37 | 1.71 ± 0.26 |
| **TAS2R20** | 31.488 ± 0.16 | 0.66 ± 0.10 |
| **TAS2R30** | 32.06 ± 0.16 | 0.40 ± 0.10 |

| | | |
|---|---|---|
| **TAS2R31** | 28.58 ± 0.18 | 4.56 ± 1.26 |
| **TAS2R38** | NA | NA |
| **TAS2R39** | NA | NA |
| **TAS2R40** | NA | NA |
| **TAS2R41** | NA | NA |
| **TAS2R42** | 32.93 ± 0.10 | 0.21 ± 0.01 |
| **TAS2R43** | NA | NA |
| **TAS2R45** | 30.97 ± 0.11 | 0.28 ± 0.05 |
| **TAS2R46** | 32.99 ± 0.17 | 1.13 ± 0.18 |
| **TAS2R50** | 33.10 ± 0.15 | 0.25 ± 0.01 |
| **TAS2R60** | NA | NA |
| **GADPH** | 17.88 ± 0.71 | - |
| **HPRT1** | 22.73 ± 0.567 | - |

Tab. 11: Caco-2 DF treated with bitter melon (BM) from the apical side (B-A) and Caco 2 DF treated with BM from the basal side (B-A). Results are expressed as mean ($2^{\wedge -\Delta Ct}$ * 1000) ± Dev.st obtained from 4 biological replicates (n = 3).

The gene expression of TAS2R change after the basolateral treatment with the bitter melon extract (31.25 µg/mL) for 2h, is it possible to see an overall downregulation if compared to the Caco-2 DF group. Is possible to see how the mean of the –ΔCt genes follow the same trend of the apical treatment, expect for the TAS2R gene which is overexpressed if compared to the other groups.

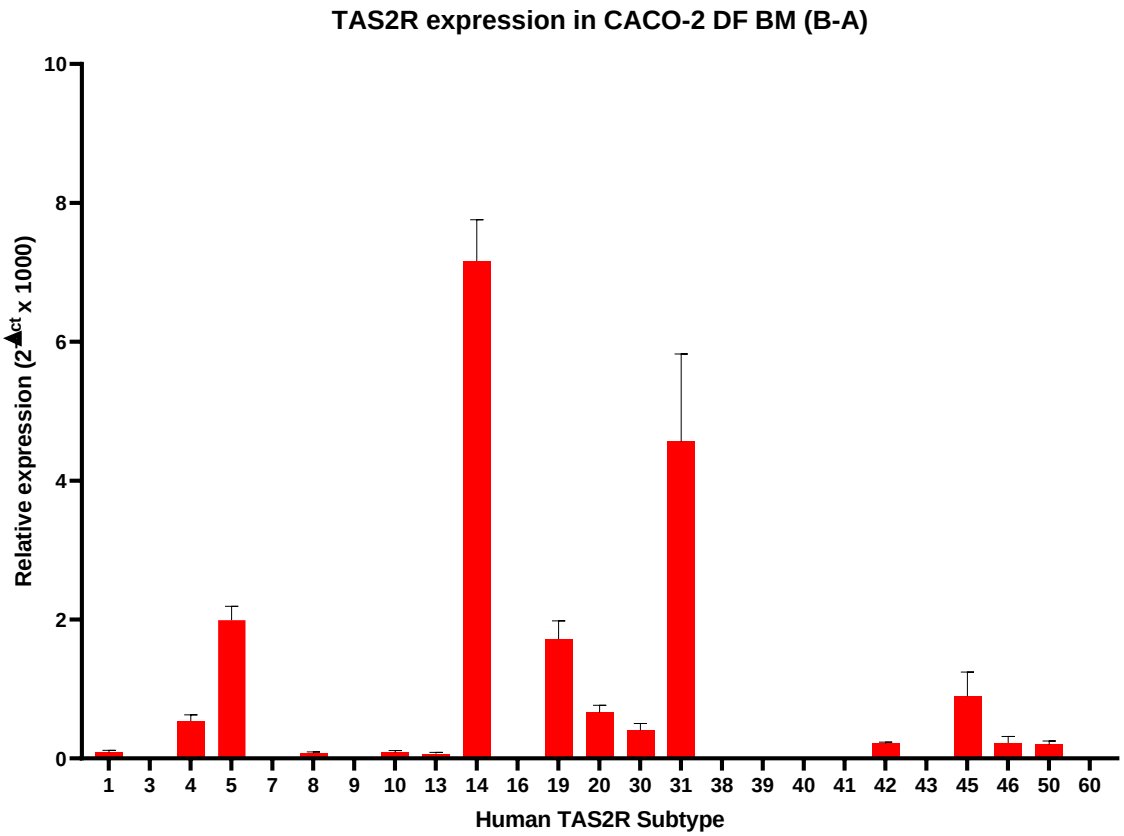


Caco 2 DF treated with bitter melon (BM) from the apical side (B-A). Results are expressed as mean ($2^{-\Delta Ct} * 1000$) ± Dev.st obtained from 4 biological replicates (n = 3).

The overall gene expression, reported in Fig. 39, in the four different group analyzed show that is possible to perform a comparative analysis for the following genes: TAS2R5, TAS2R10, TAS2R14, TAS2R19, TAS2R20, TAS2R31, TAS2R45, TAS2R46 and TAS2R50. After the statistical analysis it was possible to compare see the effect of the differentiation process and of the treatment on the cells on the four groups (Fig. 40):

1) Caco-2

2) Caco-2 DF

3) Caco-2 DF Treated with BM (A-B)

4) Caco-2 DF Treated with BM (B-A)

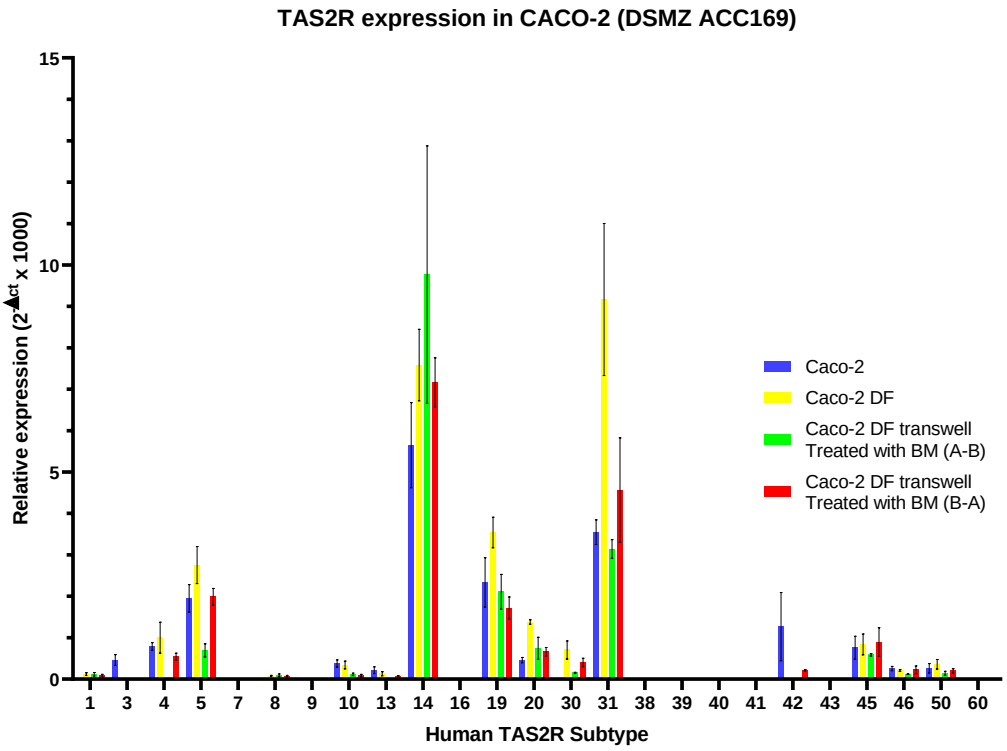

Fig. 40: TAS2R expression of all human subtype in Caco-2 (DSMZ ACC169; LOT 19); Caco-2 differentiated after 21 days (DF), Caco 2 DF treated with bitter melon from the apical side (BM) summary. Results are expressed as mean ($2^{\wedge -\Delta Ct} * 1000$) ± Dev.st. Data were obtained from 4 biological replicates (n = 3) for Caco-2 (DSMZ ACC169; LOT 19) and from 3 biological replicates (n = 3) for the other groups.

The statistical analysis on TAS2R5 (Fig. 41) reveal a statistical difference between the four groups analyzed with a p value < 0.0001 (F = 24.80 < 0.0001). The Tukey test underlines the following differences in the gene expression:

- Caco-2 vs DF Caco-2 BM extract (AB) with a $p < 0.0005$
- DF Caco-2 vs Caco-2 BM extract (AB) with a $p < 0.0001$
- DF Caco-2 BM extract (AB) vs DF Caco-2 BM extract (BA) with a $p < 0.0007$

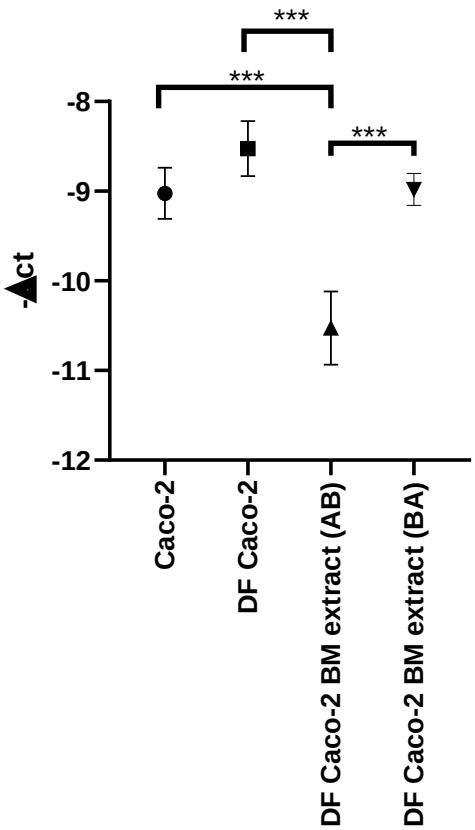


Fig. 41: TAS2R5 expression in Caco-2 (DSMZ ACC169; LOT 19); Caco-2 differentiated after 21 days (DF); Caco 2 DF treated with bitter melon from the apical side (BM) and Caco 2 DF treated with BM from the basal side (B-A). Results are expressed as –Δct ± Dev.st. Data were obtained from 4 biological replicates (n = 3) for Caco-2 (DSMZ ACC169; LOT 19) and from 3 biological replicates (n = 3) for the other groups.

The statistical analysis on TAS2R10 (Fig. 42) reveal a statistical difference between the four groups analyzed with a p value < 0.0001 (F = 13.52 p < 0.0011). The Tukey test underlines the following differences in the gene expression:

- Caco-2 vs DF Caco-2 BM extract (AB) with a p < 0.0138
- DF Caco-2 vs Caco-2 BM extract (BA) with a p < 0.0020
- DF Caco-2 vs DF Caco-2 BM extract (AB) with a p < 0.0344
- DF Caco-2 vs DF Caco-2 BM extract (BA) with a p < 0.0051

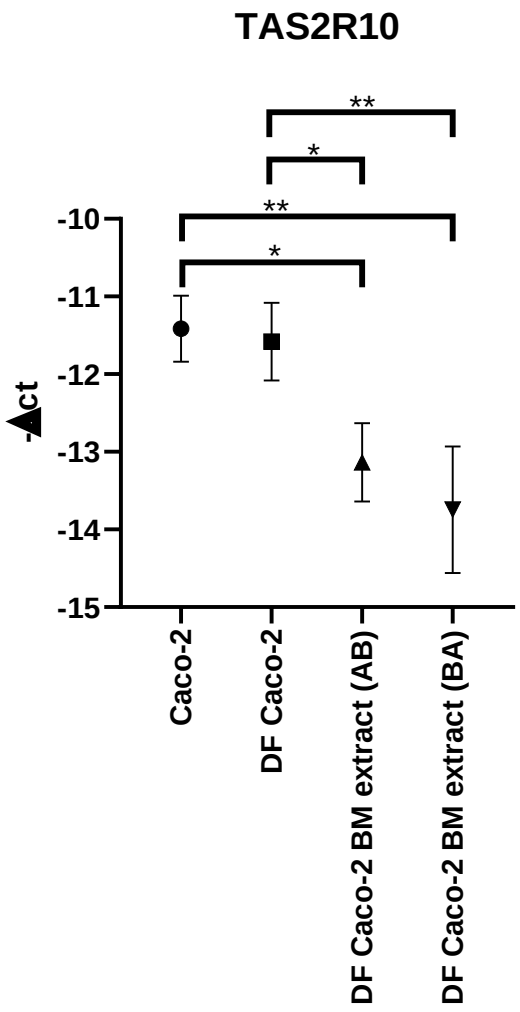

Fig. 42: TAS2R10 expression in Caco-2 (DSMZ ACC169; LOT 19); Caco-2 differentiated after 21 days (DF); Caco 2 DF treated with bitter melon from the apical side (BM) and Caco 2 DF treated with BM from the basal side (B-A). Results are expressed as $-\Delta ct \pm$ Dev.st. Data were obtained from 4 biological replicates (n = 3) for Caco-2 (DSMZ ACC169; LOT 19) and from 3 biological replicates (n = 3) for the other groups. The statistical analysis on TAS2R14 (Fig. 43) reveal that there is no statistical difference between the four groups analyzed with a p value < 0.0001 (F = 2.219 p < 0.153).

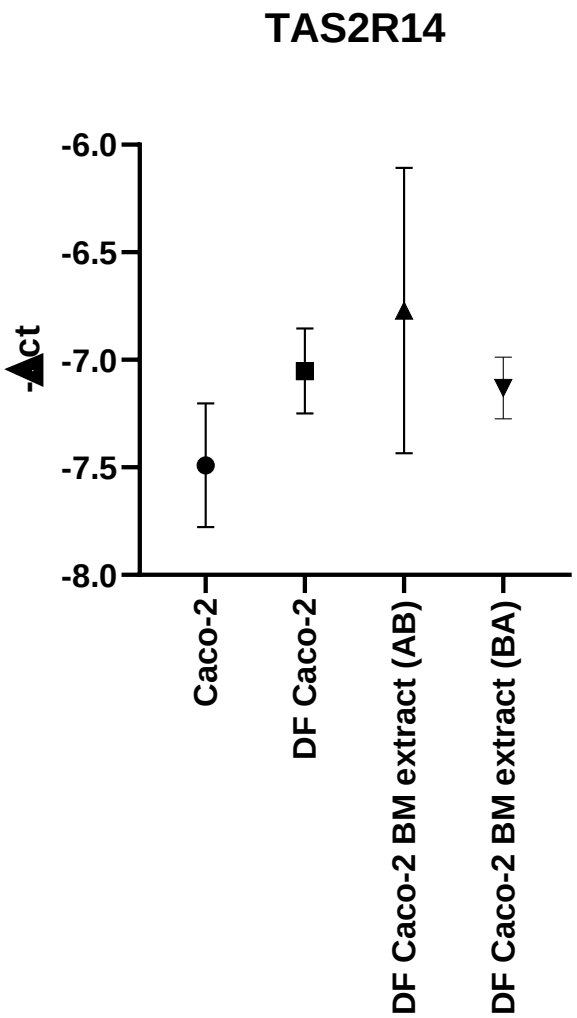


Fig. 43: TAS2R14 expression in Caco-2 (DSMZ ACC169; LOT 19); Caco-2 differentiated after 21 days (DF); Caco 2 DF treated with bitter melon from the apical side (BM) and Caco

2 DF treated with BM from the basal side (B-A). Results are expressed as –Δct ± Dev.st. Data were obtained from 4 biological replicates (n = 3) for Caco-2 (DSMZ ACC169; LOT 19) and from 3 biological replicates (n = 3) for the other groups.

The statistical analysis on TAS2R19 (Fig. 44) reveal a statistical difference between the four groups analyzed with a p value < 0.0001 (F = 5.759 p < 0.017). In particular, the Tukey test underlines the following differences in the gene expression:

- DF Caco-2 vs DF Caco-2 BM extract (BA) with a p < 0.0133

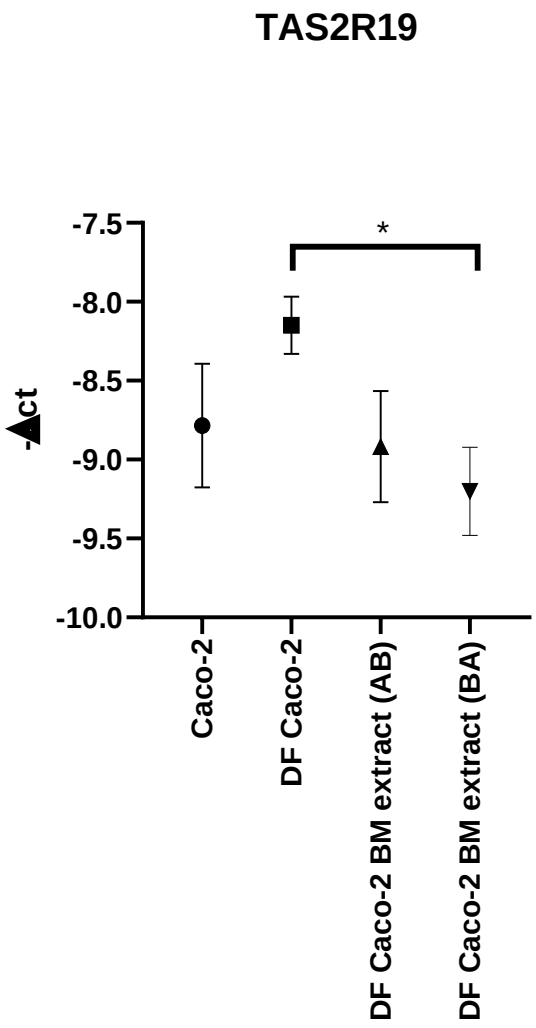

Fig. 44: TAS2R19 expression in Caco-2 (DSMZ ACC169; LOT 19); Caco-2 differentiated after 21 days (DF); Caco 2 DF treated with bitter melon from the apical side (BM) and Caco 2 DF treated with BM from the basal side (B-A). Results are expressed as $-\Delta ct \pm$ Dev.st. Data were obtained from 4 biological replicates (n = 3) for Caco-2 (DSMZ ACC169; LOT 19) and from 3 biological replicates (n = 3) for the other groups.

The statistical analysis on TAS2R20 (Fig. 45) reveal a statistical difference between the four groups analyzed with a p value < 0.0001 ($F = 13.52$ $p < 0.0011$). The Tukey test underlines the following differences in the gene expression:

- Caco-2 vs DF Caco-2 BM extract (AB) with a $p < 0.0029$
- DF Caco-2 vs DF Caco-2 BM extract (BA) with a $p < 0.0424$

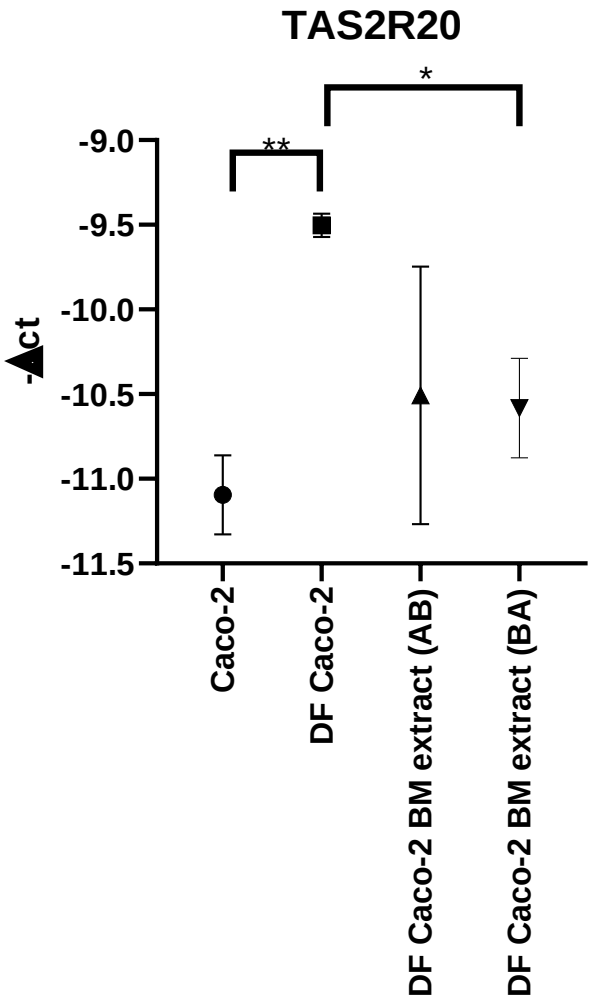


Fig. 45: TAS2R20 expression in Caco-2 (DSMZ ACC169; LOT 19); Caco-2 differentiated after 21 days (DF); Caco 2 DF treated with bitter melon from the apical side (BM) and Caco 2 DF treated with BM from the basal side (B-A). Results are expressed as –Δct ± Dev.st. Data were obtained from 4 biological replicates (n = 3) for Caco-2 (DSMZ ACC169; LOT 19) and from 3 biological replicates (n = 3) for the other groups.

The statistical analysis on TAS2R31 (Fig. 46) reveal a statistical difference between the four groups analyzed with a p value < 0.0001 (F = 16.10 p < 0.0006). In particular the Tukey test underlines the following differences in the gene expression:

- Caco-2 vs DF Caco-2 with a p < 0.0011
- DF Caco-2 vs DF Caco-2 BM extract (AB) with a p < 0.0007
- DF Caco-2 vs DF Caco-2 BM extract (BA) with a p < 0.0096

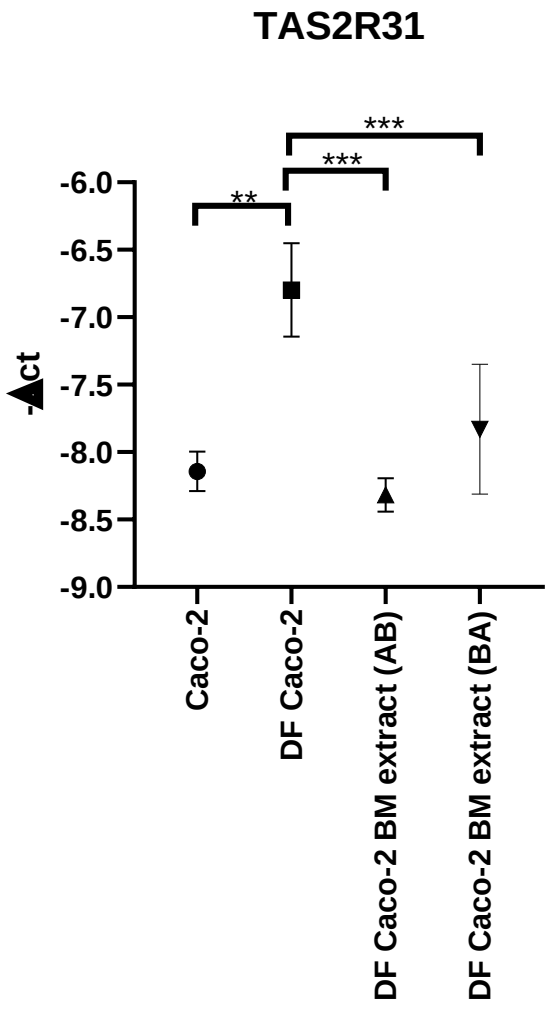


Fig. 46: TAS2R31 expression in Caco-2 (DSMZ ACC169; LOT 19); Caco-2 differentiated after 21 days (DF); Caco 2 DF treated with bitter melon from the apical side (BM) and Caco

2 DF treated with BM from the basal side (B-A). Results are expressed as –Δct ± Dev.st. Data were obtained from 4 biological replicates (n = 3) for Caco-2 (DSMZ ACC169; LOT 19) and from 3 biological replicates (n = 3) for the other groups.

The statistical analysis on TAS2R45 (Fig. 47) reveal that there is no statistical difference between the four groups analyzed with a p value < 0.0001 (F = 0.5598 p < 0.153).

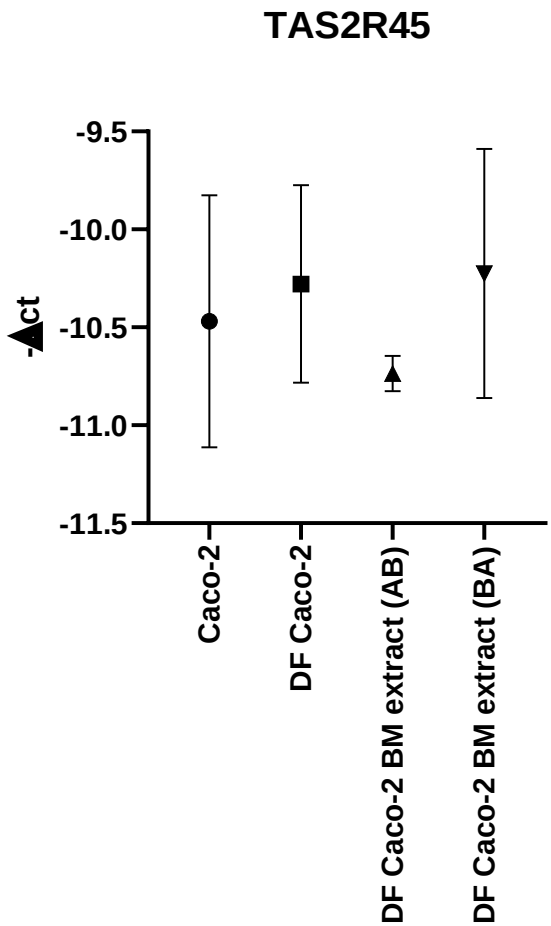


Fig. 47: TAS2R45 expression in Caco-2 (DSMZ ACC169; LOT 19); Caco-2 differentiated after 21 days (DF); Caco 2 DF treated with bitter melon from the apical

side (BM) and Caco 2 DF treated with BM from the basal side (B-A). Results are expressed as $-\Delta ct \pm$ Dev.st. Data were obtained from 4 biological replicates (n = 3) for Caco-2 (DSMZ ACC169; LOT 19) and from 3 biological replicates (n = 3) for the other groups.

The statistical analysis on TAS2R46 (Fig. 48) reveal a statistical difference between the four groups analyzed with a p value < 0.0001 ($F = 4.589$ $p < 0.0032$). In particular, the Tukey test underlines the following differences in the gene expression:

- Caco-2 vs DF Caco-2 BM extract (AB) with a $p < 0.0241$

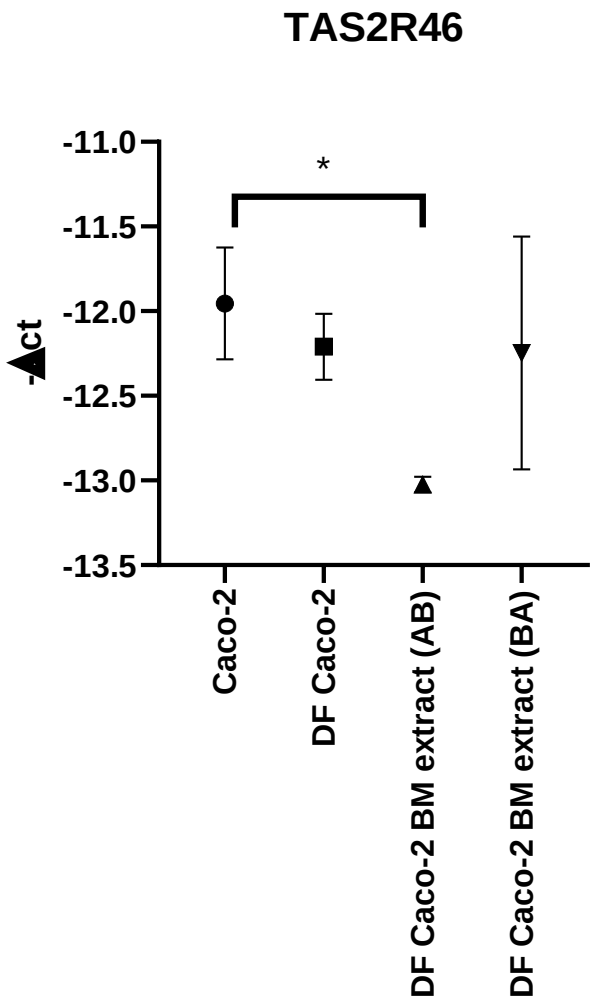


Fig. 48: TAS2R46 expression in Caco-2 (DSMZ ACC169; LOT 19); Caco-2 differentiated after 21 days (DF); Caco 2 DF treated with bitter melon from the apical side (BM) and Caco 2 DF treated with BM from the basal side (B-A). Results are expressed as $-\Delta ct \pm$ Dev.st. Data were obtained from 4 biological replicates (n = 3) for Caco-2 (DSMZ ACC169; LOT 19) and from 3 biological replicates (n = 3) for the other groups.

The statistical analysis on TAS2R50 (Fig. 49) reveal that there is no statistical difference between the four groups analyzed with a p value < 0.0001 (F = 2.219 p < 0.153).

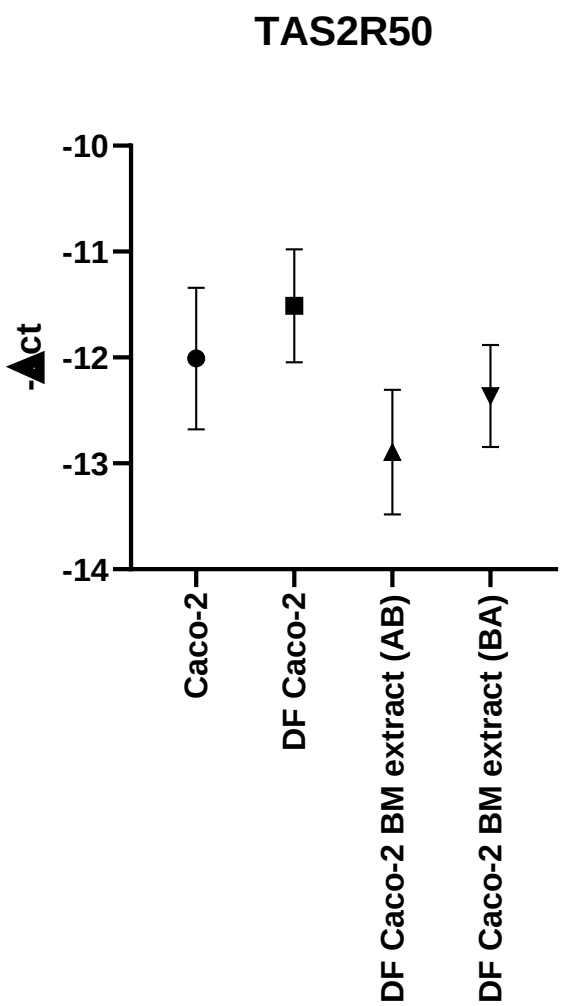


Fig. 49: TAS2R50 expression in Caco-2 (DSMZ ACC169; LOT 19); Caco-2 differentiated after 21 days (DF); Caco 2 DF treated with bitter melon from the apical side (BM) and Caco 2 DF treated with BM from the basal side (B-A). Results are expressed as $-\Delta ct \pm$ Dev.st. Data were obtained from 4 biological replicates (n = 3) for Caco-2 (DSMZ ACC169; LOT 19) and from 3 biological replicates (n = 3) for the other groups.

# 8. Discussion

The transwell assay require a good quality control procedure to assess the right growth of the monolayer. The confocal images at the microscope underline the barrier integrity of the monolayer, which is essential to control the macromolecule absorption through the paracellular space [264]. Another important step was the use of hydrophilic marker (lucifer yellow) due to his transport, which is restricted to the paracellular route. The obtained result at the end of each assay assessed again the integrity of the monolayer and of the tight junctions. Moreover, also media used has a great impact on the monolayer integrity and permeability, Kanyaphat et al. tested the integrity of the monolayer for 3 hours with different medium underlying how the HEPES can impact the integrity and the permeability of the system. Also, the lack of divalent cations like $Ca^{2+}$ and $Mg^{2+}$ increase the paracellular transportation but also affect the success of the experiment especially with a long incubation time [265]**.** Also, in this case the lucifer yellow test after an incubation time of 6 hours using HBSS w $Ca^{2+}$ and $Mg^{2+}$ under gentle shaking (100 rpm) confirmed the integrity of the monolayer. The results obtained from the vitality assay for atropine and digoxin are confirmed from the literature, these molecules are widely used to confirm the cumulative fraction transport in the transwell system after the differentiation process [264]. The case of the cucurbitacin B is different as according to literature this molecule is active also at very low concentration as reported from Prasad Dandawate et al. Cucurbitacin B and I stop the proliferation of colon cancer cell lines (HCT116 and SW480) in a dose-dependent and time-dependent way in a concentration range between 0.5 and 7.8 µM. The antiproliferative action was assessed between the 24 and 72 hours. The antiproliferative effect of cucurbitacin B and I were confirmed using the

flow cytometry. HCT116 and SW480 cells were treated with for 24 h and 48 h and the cells were blocked in G2/M phase till 48 h. All these results were confirmed by western blot analysis cell cycle-associated proteins and after a downregulation of cyclin B1 and cyclin-dependent kinase 1 (CDK1). This compound can also block the cells from S-phase (Cyclin A2, CDK2, Wee1, and CDC25C) to G2/M. However, according to our results a reduced vitality was registered after 1h or 2h of treatment from 1 to 100 µM. Interesting are also the confocal microscope images, there is in fact a good correlation between the reduced viability registered and the alterations of nuclei and monolayer architecture [266]. The work of Xiaojuan et al. sustain that the alterations of microtubule structures in living cells can be induced also only after 2h after the treatment with cucurbitacin B, the study concluded that this molecule could affect the actin filaments promoting depolymerization and aggregation considering a $IC_{50}$ of between 6.43 nM and 64.7 nM on 4 different cell lines [267]. According to Sumana et al. is possible to confirm nuclear condensation, fragmentation, and apoptotic bodies after 24 h of treatment at 50 µg/mL [268]. The microscope confocal images confirm the nuclei morphological alterations are visible also after only 2h of exposure of cucurbitacin especially at 100 and 1000 µM, but a is possible to see a slight effect also at 10 and 1 µM. Considering the presence of cucurbitacins in the fruit it is reasonable see how the skin reduces the vitality of the cells up to the concentration of 31.25 µg/mL together with the pulp, followed by seed extract which affect the vitality starting from 62.5 µg/mL while for the whole extract a vitality reduction is registered from 125 µg/mL. In literature it is not possible to find similar treatment for Caco-2 cells. Yasui et al. used seed oil extract while Kwatra et al. used a methanol extract of the whole fruit [269, 270]. The study of cucurbitane triperpenoids on this cell line was conducted

also by Shi-Biao wu et al., but in this case the cells were treated with a *M. charantia* butanol extract using the transwell system. Unfortunately, they did not report any vitality test even if they decided to treat the cells at the concentration of 200 µg/mL for 2h [271].

The gene expression analysis on Caco-2 cells reveal for the first time the expression of several TAS2R receptors. Until know only the TAS2R38, TAS2R10, TAS2R14 and TAS2R4 were examined in this specific cell line, however in our results we reported the presence of eleven different TAS2Rs confirming the presence of TAS2R10, TAS2R14 and TAS2R4. Jeon et al. found through qRT-PCR the TAS2R38, which can increase the ATP-binding cassette B1 expression also increasing the efflux activity suggesting that this specific receptor limits the absorption of potential tasting/toxic substances [272]. According to our results and the experimental conditions used was not possible to assess the presence of TAS2R38, however the TAS2R10, TAS2R14 and TAS2R4 were found as reported in literature. All three receptors were found by Ting-Ting Huang et al. [273] in 2022, underlying the high expression of TAS2R14 as we also reported in the result section. The considerations related to the relative expression of DF caco-2 and DF caco-2 treated with BM extract are more complex. According to the statistical analysis, the TAS2R5 seems to be downregulated after the apical treatment with BM at the concentration of 31.25 µg/mL for 2h if compared to the other groups. According to the literature and Bitter DB database it is not possible to find any possible interaction between TAS2Rs and cucurbitacins. However, the case of TAS2R10 is different, in fact according to Wolfgang Meyerhof et al. cucurbitacin B can activate this receptor at the concentration of 0.01 µM. The two treated group present a downregulation if compared to the DF caco-2 and caco-2 groups suggesting

that the activation of TAS2R10 could lead to a downregulation of the receptor expression. Is not possible to register the same downregulation for TAS2R10, however the same study assess that the concentration needed, or the activation of this receptor is 100 µM. Also, for TAS2R19 is possible to see how the treatment with bitter melon reduce the expression of the receptor, however in this case the activation of this receptor could be induced also from different chemical compounds present in the BM extract considering that there is no literature to sustain the interaction between the protein and cucurbitacins. The TAS2R20 seems to be overexpressed in the DF Caco-2 group if compared to others, this type of result suggests change in the expression level of the TAS2R after the differentiation process. It is well known that after three weeks the cells start to polarize and express morphological and functional features like the small intestinal enterocytes [274]. The studies which sustain the differential expression of the DF Caco-2 compared to the normal Caco-2 are different. In detail, according to the proteomics analysis the xenobiotic, drug metabolism, extracellular metabolism process was upregulated while the cycle progression, DNA synthesis, RNA processing and protein synthesis were downregulated upon the differentiation of caco-2 cells [275]. A crucial consideration is that the DF-caco-2 cells are very similar to the epithelial cells obtained from primary biopsy, the opposite is instead the comparison between the proliferating caco-2 and the primary cells obtained from patients [276]. For this reason, the DF-caco-2 group can be considered a good model to study the drugs absorption. However, until now no one has studied the possible gene expression change for TAS2R after the differentiation process in this specific cell line. At the same time seems that the apical treatment induces again a down regulation of the TAS2R20 expression as reported in TAS2R19 and TAS2R10. A similar behavior

is registered also for the TAS2R31 where the DF-caco-2 group seems to be overexpressed if compared to the other one. The treatment with BM influence also the expression of TAS2R46 however is not possible to see in literature any proof of the interaction between momordicine or cucurbitacins with this type of receptors.

# 9. Conclusion

UTIs represent the most frequent bacterial infections and the activity of antibiotics is decreasing year after year due to the inappropriate use of antibiotics and to the lack of control and prevention measures. In this context the discovery of new drugs and the research of new non-antibiotics options is essential. The first two years of my research held in Naples have provided a canonical approach widely used in the research for the discovery of new plant extracts which could be used in the prevention of UTIs and management of RUTIs. According to the literature five different plants were selected and screened thanks also to the MBC and MIC determinations. The UHPLC-TOF analysis helped us to determine the chemical profile of the extract, according to the literature different compounds could play and anti-microbial and anti-biofilm activities, also the invasion assay confirmed the potential of *H. Sabdariffa* as new plant which could be used in the management of UTIs. However, more experiments are required to understand which compound is the most active against the uropathogenic *E. coli*. Another important step should be the bioavailability assessment to confirm which compound could be absorbed, metabolized, and excreted following the kidney route maintaining its anti-microbial or anti-biofilm activity. In the year spent abroad it was possible instead to test a new approach thanks to the recent discoveries made in the field of chemoreceptors. In this case the selection of the plant was related to the research of bitter compounds, which can activate the TAS2Rs also expressed in the GU system. The cucurbitacins were the selected target considered the interesting pharmacological properties and the low available information related to the bioavailability of these molecules. The gene expression analysis on caco-2 TAS2Rs confirmed the presence of eleven different type of receptors for the first time in this specific cell line, moreover also the differentiation process seems to play a role in the TAS2Rs expression. All the quality controls sustain the success

of the assay and the correct characterization of the monolayer, which is essential to calculate the prediction bioavailability of the standards compounds and of the extracts used in the assay. The treatment with the BM extracts suggests the capacity of *M. charantia* to modulate the TAS2R expression. This research so it argues how bitter melon extract could modulate the TAS2Rs in intestinal epithelial cells. It is reasonable to think that this response could be determined due to the presence of cucurbitacins and to the consequent activation of TAS2R. This process, according to the literature, could also occur in the GU system. Unfortunately, now the results related to the prediction bioavailability of cucurbitacin B and BM extracts (seed, pulp, skin and whole) are not still available to definitively confirm the possibility of the cucurbitacins to across the intestinal barrier. However, also in possession of these information the following research should be focused also on the possible activation of the TAS2Rs in the GU system using only the compounds able to across the caco-2 monolayer. This type of studies could suggest a new unpublished type of treatment for the prevention of UTIs and management of RUTIs.

# Bibliography


1. Schappert, S. M. & Rechtsteiner, E. A. 2011. Ambulatory medical care utilization estimates for 2007. Vital Health Stat. 13, 1–38.

2. Foxman, B., 2014. Urinary Tract Infection Syndromes. *Infectious Disease Clinics of North America*, 28(1), ,1.

3. Foxman, B., 2010. The epidemiology of urinary tract infection. *Nature Reviews Urology*, 7(12), ,653-660.

4. Flores-Mireles, A., Walker, J., Caparon, M. and Hultgren, S., 2015. Urinary tract infections: epidemiology, mechanisms of infection and treatment options. *Nature Reviews Microbiology*, 13(5), ,269-284.

5. Foxman, B., 2014. Urinary Tract Infection Syndromes. *Infectious Disease Clinics of North America*, 28(1), ,1-

6. Nielubowicz, G. and Mobley, H., 2010. Host–pathogen interactions in urinary tract infection. *Nature Reviews Urology*, 7(8), ,430-441.

7. Kline, K., Schwartz, D., Lewis, W., Hultgren, S. and Lewis, A., 2011. Immune Activation and Suppression by Group B Streptococcus in a Murine Model of Urinary Tract Infection. *Infection and Immunity*, 79(9), ,3588-3595.

8. Ronald, A., 2002. The etiology of urinary tract infection: traditional and emerging pathogens. *The American Journal of Medicine*, 113(1), ,14-19.

9. Foxman, B., 2002. Epidemiology of urinary tract infections: incidence, morbidity, and economic costs. *The American Journal of Medicine*, 113(1), ,5-13.

10. Lichtenberger, P. and Hooton, T., 2008. Complicated urinary tract infections. *Current Infectious Disease Reports*, 10(6), ,499-504.

11. Levison, M. and Kaye, D., 2013. Treatment of Complicated Urinary Tract Infections With an Emphasis on Drug-Resistant Gram-Negative Uropathogens. *Current Infectious Disease Reports*, 15(2), ,109-115.

12. Chenoweth, C., Gould, C. and Saint, S., 2014. Diagnosis, Management, and Prevention of Catheter-Associated Urinary Tract Infections. *Infectious Disease Clinics of North America*, 28(1), ,105-119.

13. Sobel J.D. 1997. Vaginitis. *N. Engl J Med.* 25, 337(26):1896-1903.

14. Roberts, J., 1991. Etiology and Pathophysiology of Pyelonephritis. *American Journal of Kidney Diseases*, 17(1), 1-9.

15. Melican, K., Sandoval, R., Kader, A., Josefsson, L., Tanner, G., Molitoris, B. and Richter-Dahlfors, A., 2011. Uropathogenic Escherichia coli P and Type 1 Fimbriae Act in Synergy in a Living Host to Facilitate Renal Colonization Leading to Nephron Obstruction. *PLoS Pathogens*, 7(2). e1001298.

16. Paxman, J., Lo, A., Sullivan, M., Panjikar, S., Kuiper, M., Whitten, A., Wang, G., Luan, C., Moriel, D., Tan, L., Peters, K., Phan, M., Gee, C., Ulett, G., Schembri, M. and Heras, B., 2019. Unique structural features of a bacterial autotransporter adhesin suggest mechanisms for interaction with host macromolecules. *Nature Communications*, 10(1).

17. Khandelwal, P., Abraham, S. and Apodaca, G., 2009. Cell biology and physiology of the uroepithelium. *American Journal of Physiology-Renal Physiology*, 297(6), F1477-F1501.

18. Lee, G., 2011. Uroplakins in the Lower Urinary Tract. *International Neurourology Journal*, 15(1), 4.

19. Eto, D., Jones, T., Sundsbak, J. and Mulvey, M., 2007. Integrin-Mediated Host Cell Invasion by Type 1–Piliated Uropathogenic Escherichia coli. *PLoS Pathogens*, 3(7), e100.

20. Niveditha, S., 2012. The Isolation and the Biofilm Formation of Uropathogens in the Patients with Catheter Associated Urinary Tract Infections (UTIs). *J. clin. diagn.* 6(9) 1478-1482.

21. Jacobsen, S. and Shirtliff, M., 2011. Proteus mirabilisbiofilms and catheter-associated urinary tract infections. *Virulence*, 2(5), 460-465.

22. Shankar, P., 2016. Book review: Tackling drug-resistant infections globally. *Archives of Pharmacy Practice*, 7(3), 110.

23. O'Brien, V., Hannan, T., Nielsen, H. and Hultgren, S., 2016. Antimicrobial Resistance: Tackling a Crisis for the Health and Drug and Vaccine Development for the Treatment and Prevention of Urinary Tract Infections. *Microbiology Spectrum*, 4(1).

24. Albert X., Pereiró I., Sanfélix J., Gosalbes V., Perrota C. 2004. Antibiotics for preventing recurrent urinary tract infection in non-pregnant women. *Cochrane Database Syst Rev*, 2004(3), CD001209.

25. O'Brien V., Hannan T., Nielsen H., Hultgren S. 2016. Drug and Vaccine Development for the Treatment and Prevention of Urinary Tract Infections. *Microbiol Spectr.* 2016 Feb; 4(1), 10.

26. Aziminia, N., Hadjipavlou, M., Philippou, Y., Pandian, S., Malde, S. and Hammadeh, M., 2018. Vaccines for the prevention of recurrent urinary tract infections: a systematic review. *BJU International*, 123(5), 753-768.

27. Esche, U., Ayoub, M., Pfannes, S., Müller, M., Huber, M., Wiesmüller, K., Loop, T., Humar, M., Fischbach, K., Strünkelnberg, M., Hoffmann, P., Bessler, W. and Mittenbühler, K., 2000. Immunostimulation by bacterial components: I. Activation of macrophages and enhancement of genetic immunization by the lipopeptide P3CSK4. *International Journal of Immunopharmacology*, 22(12), 1093-1102.

28. Uehlingwalter D., Hopkinsjohny J., Elkahwajidianne E., Schmidtglen M., Leverson E. 2003. Phase 2 Clinical Trial of a Vaginal Mucosal Vaccine for Urinary Tract Infections. *The Journal of Urology*, 170, 3, 867-869.

29. Hopkins, W., Elkahwaji, J., Beierle, L., Leverson, G. and Uehling, D., 2007. Vaginal Mucosal Vaccine for Recurrent Urinary Tract Infections in Women: Results of a Phase 2 Clinical Trial. *Journal of Urology*, 177(4), ,1349-1353.

30. Huttner A., Hatz C., Van den Dobbelsteen G., Abbanat D., Hornacek A., Frölich R., Dreyer A.M., Martin P., Davies T., Fae K., Van den Nieuwenhof I., Thoelen S., de Vallière S., Kuhn A., Bernasconi E., Viereck V., Kavvadias T., Kling K., Ryu G., Hülder T., Gröger S., Scheiner D., Alaimo C., Harbarth S., Poolman J., Fonck V.G. Safety, immunogenicity, and preliminary clinical efficacy of a vaccine against extraintestinal pathogenic Escherichia coli in women with a history of recurrent

urinary tract infection: a randomised, single-blind, placebo-controlled phase 1b trial. Lancet Infect Dis. 2017. 17(5):528-537.

31. Vallée M., Bruyère F. Huttner A., Kowalczyk A., Turjeman A 2018. Effect of 5-Day Nitrofurantoin vs Single-dose Fosfomycin on Clinical Resolution of Uncomplicated Lower Urinary Tract Infection in Women: A Randomized Clinical Trial. *JAMA* ;319:1781-9. *Eur Urol.* 74(5) 124.

32. Bruyère F., Azzouzi A.R., Lavigne J.P., Droupy S., Coloby P., Game X., Karsenty G., Issartel B., Ruffion A., Misrai V., Sotto A., Allaert F.A. 2019. A Multicenter, Randomized, Placebo-Controlled Study Evaluating the Efficacy of a Combination of Propolis and Cranberry (*Vaccinium macrocarpon*) (DUAB®) in Preventing Low Urinary Tract Infection Recurrence in Women Complaining of Recurrent Cystitis. *Urol Int.*, 103(1):41-48.

33. Lorenzo-Gómez, M., Padilla-Fernández, B., García-Criado, F., Mirón-Canelo, J., Gil-Vicente, A., Nieto-Huertos, A. and Silva-Abuin, J., 2012. Evaluation of a therapeutic vaccine for the prevention of recurrent urinary tract infections versus prophylactic treatment with antibiotics. *International Urogynecology Journal*, 24(1), 127-134.

34. Yang, B. and Foley, S., 2017. First experience in the UK of treating women with recurrent urinary tract infections with the bacterial vaccine Uromune®. *BJU International*, 121(2), 289-292.

35. Ramírez Sevilla, C., Gómez Lanza, E., Manzanera, J., Martín, J. and Sanz, M., 2019. Active immunoprophyilaxis with uromune® decreases the recurrence of urinary

tract infections at three and six months after treatment without relevant secondary effects. *BMC Infectious Diseases*, 19(1).

36. Sauer, F., Remaut, H., Hultgren, S. and Waksman, G., 2004. Fiber assembly by the chaperone–usher pathway. *Biochimica et Biophysica Acta (BBA) - Molecular Cell Research*, 1694(1-3), 259-267.

37. Wizemann, T., Adamou, J. and Langermann, S., 1999. Adhesins as Targets for Vaccine Development. *Emerging Infectious Diseases*, 5(3), 395-403.

38. Langermann, S., Möllby, R., Burlein, J., Palaszynski, S., Auguste, C., DeFusco, A., Strouse, R., Schenerman, M., Hultgren, S., Pinkner, J., Winberg, J., Guldevall, L., Söderhäll, M., Ishikawa, K., Normark, S. and Koenig, S., 2000. Vaccination with FimH Adhesin Protects Cynomolgus Monkeys from Colonization and Infection by UropathogenicEscherichia coli. *The Journal of Infectious Diseases*, 181(2), 774-778.

39. Poggio, T., La Torre, J. and Scodeller, E., 2006. Intranasal immunization with a recombinant truncated FimH adhesin adjuvanted with CpG oligodeoxynucleotides protects mice against uropathogenic Escherichia coli challenge. *Canadian Journal of Microbiology*, 52(11), 1093-1102.

40. Habibi, M., Asadi Karam, M. and Bouzari, S., 2016. Transurethral instillation with fusion protein MrpH.FimH induces protective innate immune responses against uropathogenicEscherichia coliandProteus mirabilis. *APMIS*, 124(6), 444-452.

41. Riegman N., Kusters R., Van Veggel H., Bergmans H., Van Bergen en Henegouwen P., Hacker J., Van Die I. 1990. F1C fimbriae of a uropathogenic

*Escherichia coli* strain: genetic and functional organization of the foc gene cluster and identification of minor subunits. *J Bacteriol.* 172(2):1114-20.

42. Johnson, J., 1991. Virulence factors in Escherichia coli urinary tract infection. *Clinical Microbiology Reviews*, 4(1), 80-128.

43. Kaijser, B., Larsson, P., Olling, S. and Schneerson, R., 1983. Protection Against Acute, Ascending Pyelonephritis Caused by Escherichia coli in Rats, Using Isolated Capsular Antigen Conjugated to Bovine Serum Albumin. *Infection and Immunity*, 39(1), 142-146.

44. Roberts, I., 1995. Bacterial polysaccharides in sickness and in health. *Microbiology*, 141(9), 2023-2031.

45. Kumar, V., Ganguly, N., Joshi, K., Mittal, R., Harjai, K., Chhibber, S. and Sharma, S., 2005. Protective efficacy and immunogenicity of Escherichia coli K13 diphtheria toxoid conjugate against experimental ascending pyelonephritis. *Medical Microbiology and Immunology*, 194(4), ,211-217.

46. Asadi Karam, M., Habibi, M. and Bouzari, S., 2019. Urinary tract infection: Pathogenicity, antibiotic resistance and development of effective vaccines against Uropathogenic Escherichia coli. *Molecular Immunology*, 108, ,56-67.

47. O'Hanley, P., Lalonde, G. and Ji, G., 1991. Alpha-hemolysin contributes to the pathogenicity of piliated digalactoside-binding Escherichia coli in the kidney: efficacy of an alpha-hemolysin vaccine in preventing renal injury in the BALB/c mouse model of pyelonephritis. *Infection and Immunity*, 59(3), ,1153-1161.

48. Loubet, P., Ranfaing, J., Dinh, A., Dunyach-Remy, C., Bernard, L., Bruyère, F., Lavigne, J. and Sotto, A., 2020. Alternative Therapeutic Options to Antibiotics for the Treatment of Urinary Tract Infections. *Frontiers in Microbiology*, 11.

49. Brumbaugh, A., Smith, S. and Mobley, H., 2013. Immunization with the Yersiniabactin Receptor, FyuA, Protects against Pyelonephritis in a Murine Model of Urinary Tract Infection. *Infection and Immunity*, 81(9), ,3309-3316.

50. Alteri, C., Hagan, E., Sivick, K., Smith, S. and Mobley, H., 2009. Mucosal Immunization with Iron Receptor Antigens Protects against Urinary Tract Infection. *PLoS Pathogens*, 5(9), p.e1000586.

51. Åberg, V. and Almqvist, F., 2007. Pilicides—small molecules targeting bacterial virulence. *Org. Biomol. Chem.*, 5(12), 1827-1834.

52. Svensson, A., Larsson, A., Emtenäs, H., Hedenström, M., Fex, T., Hultgren, S., Pinkner, J., Almqvist, F. and Kihlberg, J., 2001. Design and Evaluation of Pilicides: Potential Novel Antibacterial Agents Directed Against UropathogenicEscherichia coli. *ChemBioChem*, 2(12), 915-918.

53. Greene, S., Pinkner, J., Chorell, E., Dodson, K., Shaffer, C., Conover, M., Livny, J., Hadjifrangiskou, M., Almqvist, F. and Hultgren, S., 2014. Pilicide ec240 Disrupts Virulence Circuits in Uropathogenic Escherichia coli. *mBio*, 5(6).

54. Piatek, R., Zalewska-Piatek, B., Dzierzbicka, K., Makowiec, S., Pilipczuk, J., Szemiako, K., Cyranka-Czaja, A. and Wojciechowski, M., 2013. Pilicides inhibit the FGL chaperone/usher assisted biogenesis of the Dr fimbrial polyadhesin from uropathogenic Escherichia coli. *BMC Microbiology*, 13(1).

55. Pinkner, J., Remaut, H., Buelens, F., Miller, E., Aberg, V., Pemberton, N., Hedenstrom, M., Larsson, A., Seed, P., Waksman, G., Hultgren, S. and Almqvist, F., 2006. Rationally designed small compounds inhibit pilus biogenesis in uropathogenic bacteria. *Proceedings of the National Academy of Sciences*, 103(47), ,17897-17902.

56. Cegelski, L., Pinkner, J., Hammer, N., Cusumano, C., Hung, C., Chorell, E., Åberg, V., Walker, J., Seed, P., Almqvist, F., Chapman, M. and Hultgren, S., 2009. Small-molecule inhibitors target Escherichia coli amyloid biogenesis and biofilm formation. *Nature Chemical Biology*, 5(12), ,913-919.

57. Loubet, P., Ranfaing, J., Dinh, A., Dunyach-Remy, C., Bernard, L., Bruyère, F., Lavigne, J. and Sotto, A., 2020. Alternative Therapeutic Options to Antibiotics for the Treatment of Urinary Tract Infections. *Frontiers in Microbiology*, 11.58. Musher, D., Griffith, D., Yawn, D. and Rossen, R., 1975. Role of Urease in Pyelonephritis Resulting from Urinary Tract Infection with Proteus. *Journal of Infectious Diseases*, 131(2), ,177-181.

59. Jacobsen, S., Stickler, D., Mobley, H. and Shirtliff, M., 2008. Complicated Catheter-Associated Urinary Tract Infections Due to Escherichia coli and Proteus mirabilis. *Clinical Microbiology Reviews*, 21(1), ,26-59.

60. Xu, W., Flores-Mireles, A., Cusumano, Z., Takagi, E., Hultgren, S. and Caparon, M., 2017. Host and bacterial proteases influence biofilm formation and virulence in a murine model of enterococcal catheter-associated urinary tract infection. *npj Biofilms and Microbiomes*, 3(1).

61. Munakata, K., Mochida, H., Kondo, S., Suzuki, Y., 1980. Mutagenicity of N-acylglycinohydroxamic acids and related compounds. *Journal of Pharmacobio-Dynamics*, 3(11), 557-561.

62. Griffith, D., Gleeson, M., Lee, H., Longuet, R., Deman, E. and Earle, N., 1991. Randomized, Double-Blind Trial of Lithostat™ (AcetohydroxamicAcid) in the Palliative Treatment of Infection-Induced Urinary Calculi. *European Urology*, 20(3), 243-247.

63. Pope, A., Toseland, N., Rushant, B., Richardson, S., Mcvey, M. and Hills, J., 1998. *Digestive Diseases and Sciences*, 43(1), 109-119.

64. Llobet, E., Tomás, J. and Bengoechea, J., 2008. Capsule polysaccharide is a bacterial decoy for antimicrobial peptides. *Microbiology*, 154(12), 3877-3886.

65. Anderson, G., Goller, C., Justice, S., Hultgren, S. and Seed, P., 2010. Polysaccharide Capsule and Sialic Acid-Mediated Regulation Promote Biofilm-Like Intracellular Bacterial Communities during Cystitis. *Infection and Immunity*, 78(3), 963-975.

66. Varki, A., 2008. Sialic acids in human health and disease. *Trends in Molecular Medicine*, 14(8), 351-360.

67. Goller, C., Arshad, M., Noah, J., Ananthan, S., Evans, C., Nebane, N., Rasmussen, L., Sosa, M., Tower, N., White, E., Neuenswander, B., Porubsky, P., Maki, B., 2013. Rogers. 3-(2,6-difluorobenzamido)-5-(4-ethoxyphenyl) thiophene-2-carboxylic acid inhibits E.coli UT189 bacterial capsule biogenesis. *Probe Reports from the NIH Molecular Libraries Program.*

68. Mendling, W., 2016. Normal and abnormal vaginal microbiota. *LaboratoriumsMedizin*, 40(4).

69. Dayan N., Dabbah H., Weissman I., Aga I., Even L., Glikman D. Urinary tract infections caused by community-acquired extended-spectrum β-lactamase-producing and nonproducing bacteria: A comparative study. *J Pediatr.* 2013. 163(5):1417-21.

70. Di Cerbo, A., Palmieri, B., Aponte, M., Morales-Medina, J. and Iannitti, T., 2015. Mechanisms and therapeutic effectiveness of lactobacilli. *Journal of Clinical Pathology*, 69(3), ,187-203.

71. Cadieux, P. A., Burton, J., Devillard, E., and Reid, G. 2009. Lactobacillus byproducts inhibit the growth and virulence of uropathogenic Escherichia coli. *J. Physiol. Pharmacol.* 60, 13–18.

72. Chikindas, M., Weeks, R., Drider, D., Chistyakov, V. and Dicks, L., 2018. Functions and emerging applications of bacteriocins. *Current Opinion in Biotechnology*, 49, ,23-28.

73. De Vuyst, L. and Leroy, F., 2007. Bacteriocins from Lactic Acid Bacteria: Production, Purification, and Food Applications. *Journal of Molecular Microbiology and Biotechnology*, 13(4), 194-199.

74. Riaz, S., Nawaz, S. and Hasnain, S., 2010. Bacteriocins produced by L. fermentum and L .acidophilus can inhibit cephalosporin resistant E .coli. *Brazilian Journal of Microbiology*, 41(3), 643-648.

75. Isolauri, E., Sütas, Y., Kankaanpää, P., Arvilommi, H. and Salminen, S., 2001. Probiotics: effects on immunity. *The American Journal of Clinical Nutrition*, 73(2), 444s-450s

76. Beerepoot, M., den Heijer, C., Penders, J., Prins, J., Stobberingh, E. and Geerlings, S., 2012. Predictive value of Escherichia coli susceptibility in strains causing asymptomatic bacteriuria for women with recurrent symptomatic urinary tract infections receiving prophylaxis. *Clinical Microbiology and Infection*, 18(4), E84-E90.

77. Ng, Q., Peters, C., Venkatanarayanan, N., Goh, Y., Ho, C. and Yeo, W., 2018. Use of Lactobacillus s, to prevent recurrent urinary tract infections in females. *Medical Hypotheses*, 114, 49-54.

78. Koradia, P., Kapadia, S., Trivedi, Y., Chanchu, G. and Harper, A., 2019. Probiotic and cranberry supplementation for preventing recurrent uncomplicated urinary tract infections in premenopausal women: a controlled pilot study. *Expert Review of Anti-infective Therapy*, 17(9), 733-740.

79. Sockett, R., 2009. Predatory Lifestyle of Bdellovibrio bacteriovorus. *Annual Review of Microbiology*, 63(1), 523-539.

80. Dashiff, A., Junka, R., Libera, M. and Kadouri, D., 2010. Predation of human pathogens by the predatory bacteria Micavibrio aeruginosavorus and Bdellovibrio bacteriovorus. *Journal of Applied Microbiology*, 110(2), 431-444.

81. Ferry, T., Boucher, F., Fevre, C., Perpoint, T., Chateau, J., Petitjean, C., Josse, J., Chidiac, C., L'hostis, G., Leboucher, G., Laurent, F., Ferry, T., Valour, F., Perpoint,

T., Boibieux, A., Biron, F., Miailhes, P., Ader, F., Becker, A., Roux, S., Triffault-Fillit, C., Conrad, A., Bosch, A., Daoud, F., Lippman, J., Braun, E., Chidiac, C., Lustig, S., Servien, E., Gaillard, R., Schneider, A., Gunst, S., Batailler, C., Fessy, M., Herry, Y., Viste, A., Chaudier, P., Courtin, C., Louboutin, L., Martres, S., Trouillet, F., Barrey, C., Jouanneau, E., Jacquesson, T., Mojallal, A., Braye, F., Boucher, F., Shipkov, H., Chateau, J., Gleizal, A., Aubrun, F., Dziadzko, M., Macabéo, C., Laurent, F., Rasigade, J., Dupieux, C., Craighero, F., Boussel, L., Pialat, J., Morelec, I., Janier, M., Giammarile, F., Tod, M., Gagnieu, M., Goutelle, S. and Mabrut, E., 2018. Innovations for the treatment of a complex bone and joint infection due to XDR Pseudomonas aeruginosa including local application of a selected cocktail of bacteriophages. *Journal of Antimicrobial Chemotherapy*, 73(10), 2901-2903.

82. Jault, P., Leclerc, T., Jennes, S., Pirnay, J., Que, Y., Resch, G., Rousseau, A., Ravat, F., Carsin, H., Le Floch, R., Schaal, J., Soler, C., Fevre, C., Arnaud, I., Bretaudeau, L. and Gabard, J., 2019. Efficacy and tolerability of a cocktail of bacteriophages to treat burn wounds infected by Pseudomonas aeruginosa (PhagoBurn): a randomised, controlled, double-blind phase 1/2 trial. *The Lancet Infectious Diseases*, 19(1), 35-45.

83. Sybesma, W., Zbinden, R., Chanishvili, N., Kutateladze, M., Chkhotua, A., Ujmajuridze, A., Mehnert, U. and Kessler, T., 2016. Bacteriophages as Potential Treatment for Urinary Tract Infections. *Frontiers in Microbiology*, 7.

84. Dufour N., Clermont O., La Combe B., Messika J., Dion S., Khanna V., Denamur E., Ricard J.D., Debarbieux L. ColoColi group. 2016. Bacteriophage LM33_P1, a fast-

acting weapon against the pandemic ST131-O25b:H4 Escherichia coli clonal complex. *J Antimicrob Chemother.* 71(11):3072-3080.

85. Ujmajuridze, A., Chanishvili, N., Goderdzishvili, M., Leitner, L., Mehnert, U., Chkhotua, A., Kessler, T. and Sybesma, W., 2018. Adapted Bacteriophages for Treating Urinary Tract Infections. *Frontiers in Microbiology*, 9.

86. Kuipers, S., Ruth, M., Mientjes, M., de Sévaux, R. and van Ingen, J., 2019. A Dutch Case Report of Successful Treatment of Chronic Relapsing Urinary Tract Infection with Bacteriophages in a Renal Transplant Patient. *Antimicrobial Agents and Chemotherapy*, 64(1).

87. Howell, A., Reed, J., Krueger, C., Winterbottom, R., Cunningham, D. and Leahy, M., 2005. A-type cranberry proanthocyanidins and uropathogenic bacterial anti-adhesion activity. *Phytochemistry*, 66(18), 2281-2291.

88. Ahuja, S., Kaack, B. and Roberts, J., 1998. Loss of fimbrial adhesion with the addition of vaccinum macrocarpon to the growth medium of p-fimbriated Escherchia Coli. *Journal of Urology*, 159(2), 559-562.

89. Liu, Z., Ren, Z., Zhang, J., Chuang, C., Kandaswamy, E., Zhou, T. and Zuo, L., 2018. Role of ROS and Nutritional Antioxidants in Human Diseases. *Frontiers in Physiology*, 9.

90. Chan, M., Hidalgo, G., Asadishad, B., Almeida, S., Muja, N., Mohammadi, M., Nazhat, S. and Tufenkji, N., 2013. Inhibition of bacterial motility and spreading via release of cranberry derived materials from silicone substrates. *Colloids and Surfaces B: Biointerfaces*, 110, 275-280.

91. Ulrey, R., Barksdale, S., Zhou, W. and van Hoek, M., 2014. Cranberry proanthocyanidins have anti-biofilm properties against Pseudomonas aeruginosa. *BMC Complementary and Alternative Medicine*, 14(1).

92. Rodríguez-Pérez, C., Quirantes-Piné, R., Uberos, J., Jiménez-Sánchez, C., Peña, A. and Segura-Carretero, A., 2016. Antibacterial activity of isolated phenolic compounds from cranberry (*Vaccinium macrocarpon*) against Escherichia coli. *Food & Function*, 7(3), 1564-1573.

93. Wojnicz, D., Tichaczek-Goska, D., Korzekwa, K., Kicia, M. and Hendrich, A., 2016. Study of the impact of cranberry extract on the virulence factors and biofilm formation byEnterococcus faecalisstrains isolated from urinary tract infections. *International Journal of Food Sciences and Nutrition*, 67(8), 1005-1016.

94. Jepson, R., Williams, G. and Craig, J., 2012. Cranberries for preventing urinary tract infections. *Cochrane Database of Systematic Reviews*, 7;10(10):CD001321.

95. Stapleton, A., Dziura, J., Hooton, T., Cox, M., Yarova-Yarovaya, Y., Chen, S. and Gupta, K., 2012. Recurrent Urinary Tract Infection and Urinary Escherichia coli in Women Ingesting Cranberry Juice Daily: A Randomized Controlled Trial. *Mayo Clinic Proceedings*, 87(2), 143-150.

96. Anger, J., Lee, U., Ackerman, A., Chou, R., Chughtai, B., Clemens, J., Hickling, D., Kapoor, A., Kenton, K., Kaufman, M., Rondanina, M., Stapleton, A., Stothers, L. and Chai, T., 2019. Recurrent Uncomplicated Urinary Tract Infections in Women: AUA/CUA/SUFU Guideline. *Journal of Urology*, 202(2), 282-289.

97. Ranfaing, J., Dunyach-Remy, C., Louis, L., Lavigne, J. and Sotto, A., 2018. Propolis potentiates the effect of cranberry (Vaccinium macrocarpon) against the virulence of uropathogenic Escherichia coli. *Scientific Reports*, 8(1).

98. Boonsai, P., Phuwapraisirisan, P. and Chanchao, C., 2014. Antibacterial Activity of a Cardanol from Thai Apis mellifera Propolis. *International Journal of Medical Sciences*, 11(4), 327-336.

99. Freitas, S., Shinohara, L., Sforcin, J. and Guimarães, S., 2006. In vitro effects of propolis on Giardia duodenalis trophozoites. *Phytomedicine*, 13(3), 170-175.

100. Pereira, E., da Silva, J., Silva, F., De Luca, M., Ferreira, E., Lorentz, T. and Santos, V., 2011. Clinical Evidence of the Efficacy of a Mouthwash Containing Propolis for the Control of Plaque and Gingivitis: A Phase II Study. *Evidence-Based Complementary and Alternative Medicine*, 2011, 1-7.

101. Olczyk, P., Komosinska-Vassev, K., Wisowski, G., Mencner, L., Stojko, J. and Kozma, E., 2014. Propolis Modulates Fibronectin Expression in the Matrix of Thermal Injury. *BioMed Research International*, 2014, 1-10.

102. Pasupuleti, V., Sammugam, L., Ramesh, N. and Gan, S., 2017. Honey, Propolis, and Royal Jelly: A Comprehensive Review of Their Biological Actions and Health Benefits. *Oxidative Medicine and Cellular Longevity*, 2017, 1-21.

103. Ranfaing, J., Dunyach-Remy, C., Louis, L., Lavigne, J. and Sotto, A., 2018. Propolis potentiates the effect of cranberry (Vaccinium macrocarpon) against the virulence of uropathogenic Escherichia coli. *Scientific Reports*, 8(1).

104. Ranfaing, J., Dunyach-Remy, C., Lavigne, J. and Sotto, A., 2018. Propolis potentiates the effect of cranberry (Vaccinium macrocarpon) in reducing the motility and the biofilm formation of uropathogenic Escherichia coli. *PLOS ONE*, 13(8), .e0202609.

105. Bruyère, F., Azzouzi, A., Lavigne, J., Droupy, S., Coloby, P., Game, X., Karsenty, G., Issartel, B., Ruffion, A., Misrai, V., Sotto, A. and Allaert, F., 2019. A Multicenter, Randomized, Placebo-Controlled Study Evaluating the Efficacy of a Combination of Propolis and Cranberry (*Vaccinium macrocarpon*) (DUAB®) in Preventing Low Urinary Tract Infection Recurrence in Women Complaining of Recurrent Cystitis. *Urologia Internationalis*, 103(1), 41-48.

106. Constantinides, C., Manousakas, T., Nikolopoulos, P., Stanitsas, A., Haritopoulos, K. and Giannopoulos, A., 2004. Prevention of recurrent bacterial cystitis by intravesical administration of hyaluronic acid: a pilot study. *BJU International*, 93(9), 1262-1266.

107. Ciani, O., Arendsen, E., Romancik, M., Lunik, R., Costantini, E., Di Biase, M., Morgia, G., Fragalà, E., Roman, T., Bernat, M., Guazzoni, G., Tarricone, R. and Lazzeri, M., 2016. Intravesical administration of combined hyaluronic acid (HA) and chondroitin sulfate (CS) for the treatment of female recurrent urinary tract infections: a European multicentre nested case–control study. *BMJ Open*, 6(3), e009669.

108. Cicione, A., Cantiello, F., Ucciero, G., Salonia, A., Torella, M., De Sio, M., Autorino, R., Romancik, M., Tomaskin, R. and Damiano, R., 2014. Intravesical treatment with highly-concentrated hyaluronic acid and chondroitin sulphate in

patients with recurrent urinary tract infections: Results from a multicentre survey. *Canadian Urological Association Journal*, 8(9-10), 721.

109. Torella, M., Del Deo, F., Grimaldi, A., Iervolino, S., Pezzella, M., Tammaro, C., Gallo, P., Rappa, C., De Franciscis, P. and Colacurci, N., 2016. Efficacy of an orally administered combination of hyaluronic acid, chondroitin sulfate, curcumin and quercetin for the prevention of recurrent urinary tract infections in postmenopausal women. *European Journal of Obstetrics & Gynecology and Reproductive Biology*, 207, 125-128.

110. Hills, A., Patel, A., Boyd, P. and James, D., 2001. Metabolic control of recombinant monoclonal antibodyN-glycosylation in GS-NS0 cells. *Biotechnology and Bioengineering*, 75(2), 239-251.

111. Pinker 2006

112. Domenici, L., Musella, A., Bracchi, C., Lecce, F., Schiavi, M., Colagiovanni, V., Di Donato, V., Marchetti, C., Tomao, F., Palaia, I., Muzii, L. and Benedetti Panici, P., 2018. Comparison of Anogenital Distance and Correlation with Vulvo-vaginal Atrophy: A Pilot Study on Premenopausal and Postmenopausal Women. *Journal of Menopausal Medicine*, 24(2), 108.

113. Klein, T., Abgottspon, D., Wittwer, M., Rabbani, S., Herold, J., Jiang, X., Kleeb, S., Lüthi, C., Scharenberg, M., Bezençon, J., Gubler, E., Pang, L., Smiesko, M., Cutting, B., Schwardt, O. and Ernst, B., 2010. FimH Antagonists for the Oral Treatment of Urinary Tract Infections: From Design and Synthesis to in Vitro and in Vivo Evaluation. *Journal of Medicinal Chemistry*, 53(24), 8627-8641.

114. Cusumano, C., Pinkner, J., Han, Z., Greene, S., Ford, B., Crowley, J., Henderson, J., Janetka, J. and Hultgren, S., 2011. Treatment and Prevention of Urinary Tract Infection with Orally Active FimH Inhibitors. *Science Translational Medicine*, 3(109).

115. Kranjčec, B., Papeš, D. and Altarac, S., 2013. d-mannose powder for prophylaxis of recurrent urinary tract infections in women: a randomized clinical trial. *World Journal of Urology*, 32(1), 79-84.

116. Larsson, A., Ohlsson, J., Dodson, K., Hultgren, S., Nilsson, U. and Kihlberg, J., 2003. Quantitative studies of the binding of the class II PapG adhesin from uropathogenic Escherichia coli to oligosaccharides. *Bioorganic & Medicinal Chemistry*, 11(10), 2255-2261.

117. Sung, M., Fleming, K., Chen, H. and Matthews, S., 2001. The solution structure of PapGII from uropathogenic Escherichia coli and its recognition of glycolipid receptors. *EMBO reports*, 2(7), 621-627.

118. Habash, M., Van der Mei, H., Busscher, H. and Reid, G., 1999. The effect of water, ascorbic acid, and cranberry derived supplementation on human urine and uropathogen adhesion to silicone rubber. *Canadian Journal of Microbiology*, 45(8), 691-694.

119. Ochoa-Brust, G., Fernández, A., Villanueva-Ruiz, G., Velasco, R., Trujillo-Hernández, B. and Vásquez, C., 2007. Daily intake of 100 mg ascorbic acid as urinary tract infection prophylactic agent during pregnancy. *Acta Obstetricia et Gynecologica Scandinavica*, 86(7), 783-787.

120. Adappa, N., Howland, T., Palmer, J., Kennedy, D., Doghramji, L., Lysenko, A., Reed, D., Lee, R. and Cohen, N., 2013. Genetics of the taste receptor T2R38 correlates with chronic rhinosinusitis necessitating surgical intervention. *International Forum of Allergy & Rhinology*, 3(3), 184-187.

121. Adappa, N., Zhang, Z., Palmer, J., Kennedy, D., Doghramji, L., Lysenko, A., Reed, D., Scott, T., Zhao, N., Owens, D., Lee, R. and Cohen, N., 2013. The bitter taste receptor T2R38 is an independent risk factor for chronic rhinosinusitis requiring sinus surgery. *International Forum of Allergy & Rhinology*, 4(1), 3-7.

122. Behrens, M. and Meyerhof, W., 2010. Oral and Extraoral Bitter Taste Receptors. *Results and Problems in Cell Differentiation*, 87-99.

123. Xu, J., Cao, J., Iguchi, N., Riethmacher, D. and Huang, L., 2012. Functional characterization of bitter-taste receptors expressed in mammalian testis. *Molecular Human Reproduction*, 19(1), 17-28.

124. Wu, S., Rozengurt, N., Yang, M., Young, S., Sinnett-Smith, J. and Rozengurt, E., 2002. Expression of bitter taste receptors of the T2R family in the gastrointestinal tract and enteroendocrine STC-1 cells. *Proceedings of the National Academy of Sciences*, 99(4), 2392-2397.

125. Kautiainen, A., 1992. Determination of hemoglobin adducts from aldehydes formed during lipid peroxidation in vitro. *Chemico-Biological Interactions*, 83(1), ,55-63.

126. Wong, G., Gannon, K. and Margolskee, R., 1996. Transduction of bitter and sweet taste by gustducin. *Nature*, 381(6585), ,796-800.

127. Huang, L., Shanker, Y., Dubauskaite, J., Zheng, J., Yan, W., Rosenzweig, S., Spielman, A., Max, M. and Margolskee, R., 1999. Gγ13 colocalizes with gustducin in taste receptor cells and mediates IP3 responses to bitter denatonium. *Nature Neuroscience*, 2(12), ,1055-1062.

128. Chandrashekar, J., Hoon, M., Ryba, N. and Zuker, C., 2006. The receptors and cells for mammalian taste. *Nature*, 444(7117), ,288-294.

129. Mueller, K., Hoon, M., Erlenbach, I., Chandrashekar, J., Zuker, C. and Ryba, N., 2005. The receptors and coding logic for bitter taste. *Nature*, 434(7030), 225-229.

130. Finger, T., Bottger, B., Hansen, A., Anderson, K., Alimohammadi, H. and Silver, W., 2003. Solitary chemoreceptor cells in the nasal cavity serve as sentinels of respiration. *Proceedings of the National Academy of Sciences*, 100(15), ,8981-8986.

131. Chaudhari, N. and Roper, S., 2010. The cell biology of taste. *Journal of Cell Biology*, 190(3),285-296.

132. Taruno, A., Vingtdeux, V., Ohmoto, M., Ma, Z., Dvoryanchikov, G., Li, A., Adrien, L., Zhao, H., Leung, S., Abernethy, M., Koppel, J., Davies, P., Civan, M., 133. Chaudhari, N., Matsumoto, I., Hellekant, G., Tordoff, M., Marambaud, P. and Foskett, J., 2013. CALHM1 ion channel mediates purinergic neurotransmission of sweet, bitter and umami tastes. *Nature*, 495(7440), 223-226.

133. Peng, Y., Gillis-Smith, S., Jin, H., Tränkner, D., Ryba, N. and Zuker, C., 2015. Sweet and bitter taste in the brain of awake behaving animals. *Nature*, 527(7579), 512-515.

134. Lossow, K., Hübner, S., Roudnitzky, N., Slack, J., Pollastro, F., Behrens, M. and Meyerhof, W., 2016. Comprehensive Analysis of Mouse Bitter Taste Receptors Reveals Different Molecular Receptive Ranges for Orthologous Receptors in Mice and Humans. *Journal of Biological Chemistry*, 291(29),15358-15377.

135. Adler, E., Hoon, M., Mueller, K., Chandrashekar, J., Ryba, N. and Zuker, C., 2000. A Novel Family of Mammalian Taste Receptors. *Cell*, 100(6),693-702.

136 Chandrashekar, J., Mueller, K., Hoon, M., Adler, E., Feng, L., Guo, W., Zuker, C. and Ryba, N., 2000. T2Rs Function as Bitter Taste Receptors. *Cell*, 100(6), 703-711.

137 Matsunami, H., Montmayeur, J. and Buck, L., 2000. A family of candidate taste receptors in human and mouse. *Nature*, 404(6778), 601-604.

138. Salathe, M., 2007. Regulation of Mammalian Ciliary Beating. *Annual Review of Physiology*, 69(1), pp.401-422.

139. Zhang, C., Lifshitz, L., Uy, K., Ikebe, M., Fogarty, K. and ZhuGe, R., 2013. Correction: The Cellular and Molecular Basis of Bitter Tastant-Induced Bronchodilation. *PLoS Biology*, 11(3).

140. Jeon, T., Seo, Y. and Osborne, T., 2011. Gut bitter taste receptor signalling induces ABCB1 through a mechanism involving CCK. *Biochemical Journal*, 438(1), 33-37.

141. Cummings, D. and Overduin, J., 2007. Gastrointestinal regulation of food intake. *Journal of Clinical Investigation*, 117(1), ,13-23.Finger, T., Bottger, B., Hansen, A., Anderson, K., Alimohammadi, H. and Silver, W., 2003. Solitary

chemoreceptor cells in the nasal cavity serve as sentinels of respiration. *Proceedings of the National Academy of Sciences*, 100(15) ,8981-8986.

142. Ogura, T., Krosnowski, K., Zhang, L., Bekkerman, M. and Lin, W., 2010. Chemoreception Regulates Chemical Access to Mouse Vomeronasal Organ: Role of Solitary Chemosensory Cells. *PLoS ONE*, 5(7), e11924.

143. Tizzano, M., Gulbransen, B., Vandenbeuch, A., Clapp, T., Herman, J., Sibhatu, H., Churchill, M., Silver, W., Kinnamon, S. and Finger, T., 2010. Nasal chemosensory cells use bitter taste signaling to detect irritants and bacterial signals. *Proceedings of the National Academy of Sciences*, 107(7), 3210-3215.

144. Krasteva, G., Canning, B., Hartmann, P., Veres, T., Papadakis, T., Muhlfeld, C., Schliecker, K., Tallini, Y., Braun, A., Hackstein, H., Baal, N., Weihe, E., Schutz, B., Kotlikoff, M., Ibanez-Tallon, I. and Kummer, W., 2011. Cholinergic chemosensory cells in the trachea regulate breathing. *Proceedings of the National Academy of Sciences*, 108(23), ,9478-9483.

145. Saunders, C., Christensen, M., Finger, T. and Tizzano, M., 2014. Cholinergic neurotransmission links solitary chemosensory cells to nasal inflammation. *Proceedings of the National Academy of Sciences*, 111(16), 6075-6080.

146. K., Filipski, K., Krasteva-Christ, G., Fronius, M., Althaus, M., Rafiq, A., Papadakis, T., Renno, L., Jurastow, I., Wessels, L., Wolff, M., Schutz, B., Weihe, E., Chubanov, V., Gudermann, T., Klein, J., Bschleipfer, T. and Kummer, W., 2014. Bitter triggers acetylcholine release from polymodal urethral chemosensory cells and bladder reflexes. *Proceedings of the National Academy of Sciences*, 111(22) ,8287-8292.

147. Gerbe, F., Sidot, E., Smyth, D., Ohmoto, M., Matsumoto, I., Dardalhon, V., Cesses, P., Garnier, L., Pouzolles, M., Brulin, B., Bruschi, M., Harcus, Y., Zimmermann, V., Taylor, N., Maizels, R. and Jay, P., 2016. Intestinal epithelial tuft cells initiate type 2 mucosal immunity to helminth parasites. *Nature*, 529(7585), 226-230.

148. Howitt, M., Lavoie, S., Michaud, M., Blum, A., Tran, S., Weinstock, J., Gallini, C., Redding, K., Margolskee, R., Osborne, L., Artis, D. and Garrett, W., 2016. Tuft cells, taste-chemosensory cells, orchestrate parasite type 2 immunity in the gut. *Science*, 351(6279), 1329-1333.

149. von Moltke, J., Ji, M., Liang, H. and Locksley, R., 2015. Tuft-cell-derived IL-25 regulates an intestinal ILC2–epithelial response circuit. *Nature*, 529(7585), 221-225.

150. Zheng, K., Lu, P., Delpapa, E., Bellve, K., Deng, R., Condon, J., Fogarty, K., Lifshitz, L., Simas, T., Shi, F. and ZhuGe, R., 2017. Bitter taste receptors as targets for tocolytics in preterm labor therapy. *The FASEB Journal*, 31(9), 4037-4052.

151. Xu, J., Cao, J., Iguchi, N., Riethmacher, D. and Huang, L., 2012. Functional characterization of bitter-taste receptors expressed in mammalian testis. *Molecular Human Reproduction*, 19(1), 17-28.

152. Liu, S., Lu, S., Xu, R., Atzberger, A., Günther, S., Wettschureck, N. and Offermanns, S., 2017. Members of Bitter Taste Receptor Cluster Tas2r143/Tas2r135/Tas2r126 Are Expressed in the Epithelium of Murine Airways and Other Non-gustatory Tissues. *Frontiers in Physiology*, 8.

153. Avau, B. and Depoortere, I., 2015. The bitter truth about bitter taste receptors: beyond sensing bitter in the oral cavity. *Acta Physiologica*, 216(4), 407-420.

154. Lu, P., Zhang, C., Lifshitz, L. and ZhuGe, R., 2017. Extraoral bitter taste receptors in health and disease. *Journal of General Physiology*, 149(2), ,181-197.

155. Jaggupilli, A., Singh, N., De Jesus, V., Gounni, M., Dhanaraj, P. and Chelikani, P., 2018. Chemosensory bitter taste receptors (T2Rs) are activated by multiple antibiotics. *The FASEB Journal*, 33(1), 501-517.

156. Workman, A., Palmer, J., Adappa, N. and Cohen, N., 2015. The Role of Bitter and Sweet Taste Receptors in Upper Airway Immunity. *Current Allergy and Asthma Reports*, 15(12).

157. Tizzano, M., Gulbransen, B., Vandenbeuch, A., Clapp, T., Herman, J., Sibhatu, H., Churchill, M., Silver, W., Kinnamon, S. and Finger, T., 2010. Nasal chemosensory cells use bitter taste signaling to detect irritants and bacterial signals. *Proceedings of the National Academy of Sciences*, 107(7), 3210-3215.

158. Carey, R., Adappa, N., Palmer, J., Lee, R. and Cohen, N., 2016. Taste Receptors: Regulators of Sinonasal Innate Immunity. *Laryngoscope Investigative Otolaryngology*, 1(4), 88-95.

159. Zheng, K., Lu, P., Delpapa, E., Bellve, K., Deng, R., Condon, J., Fogarty, K., Lifshitz, L., Simas, T., Shi, F. and ZhuGe, R., 2017. Bitter taste receptors as targets for tocolytics in preterm labor therapy. *The FASEB Journal*, 31(9), 4037-4052.

160. Rennemeier, C., Frambach, T., Hennicke, F., Dietl, J. and Staib, P., 2009. Microbial Quorum-Sensing Molecules Induce Acrosome Loss and Cell Death in Human Spermatozoa. *Infection and Immunity*, 77(11), 4990-4997.

161. Rutherford, S. and Bassler, B., 2012. Bacterial Quorum Sensing: Its Role in Virulence and Possibilities for Its Control. *Cold Spring Harbor Perspectives in Medicine*, 2(11), a012427-a012427.

162. Rajput, A., Kaur, K. and Kumar, M., 2015. SigMol: repertoire of quorum sensing signaling molecules in prokaryotes. *Nucleic Acids Research*, 44(D1), D634-D639.

163. Barr, H., Halliday, N., Cámara, M., Barrett, D., Williams, P., Forrester, D., Simms, R., Smyth, A., Honeybourne, D., Whitehouse, J., Nash, E., Dewar, J., Clayton, A., Knox, A. and Fogarty, A., 2015. Pseudomonas aeruginosaquorum sensing molecules correlate with clinical status in cystic fibrosis. *European Respiratory Journal*, 46(4),1046-1054.

164. Deep, A., Chaudhary, U. and Gupta, V., 2011. Quorum sensing and Bacterial Pathogenicity: From Molecules to Disease. *Journal of Laboratory Physicians*, 3(01), 004-011.

165. Miller, M. and Bassler, B., 2001. Quorum Sensing in Bacteria. *Annual Review of Microbiology*, 55(1), 165-199.

166. Zhao, L., Xue, T., Shang, F., Sun, H. and Sun, B., 2010. Staphylococcus aureus AI-2 Quorum Sensing Associates with the KdpDE Two-Component System To Regulate Capsular Polysaccharide Synthesis and Virulence. *Infection and Immunity*, 78(8), 3506-3515.

167. Thalmann, S., Behrens, M. and Meyerhof, W., 2013. Major haplotypes of the human bitter taste receptor TAS2R41 encode functional receptors for chloramphenicol. *Biochemical and Biophysical Research Communications*, 435(2), 267-273.

168. Manson, M., Säfholm, J., Al-Ameri, M., Bergman, P., Orre, A., Swärd, K., James, A., Dahlén, S. and Adner, M., 2014. Bitter taste receptor agonists mediate relaxation of human and rodent vascular smooth muscle. *European Journal of Pharmacology*, 740, 302-311.

169. Pulkkinen, V., Manson, M., Säfholm, J., Adner, M. and Dahlén, S., 2012. The bitter taste receptor (TAS2R) agonists denatonium and chloroquine display distinct patterns of relaxation of the guinea pig trachea. *American Journal of Physiology-Lung Cellular and Molecular Physiology*, 303(11), L956-L966.

170. Tan, X. and Sanderson, M., 2014. Bitter tasting compounds dilate airways by inhibiting airway smooth muscle calcium oscillations and calcium sensitivity. *British Journal of Pharmacology*, 171(3), 646-662.

171. Carey, R., Adappa, N., Palmer, J., Lee, R. and Cohen, N., 2016. Taste Receptors: Regulators of Sinonasal Innate Immunity. *Laryngoscope Investigative Otolaryngology*, 1(4), 88-95.

172. Weaver, J., Porasuphatana, S., Tsai, P., Cao, G., Budzichowski, T., Roman, L. and Rosen, G., 2002. The Activation of Neuronal Nitric-Oxide Synthase by Various Divalent Cations. *Journal of Pharmacology and Experimental Therapeutics*, 302(2), 781-786.

173. Grekov, I., Pombinho, A., Kobets, T., Bartůněk, P. and Lipoldová, M., 2017. Calcium Ionophore, Calcimycin, Kills Leishmania Promastigotes by Activating Parasite Nitric Oxide Synthase. *BioMed Research International*, 2017, 1-6.

174. Wheeler, M., Smith, S., García-Cardeña, G., Nathan, C., Weiss, R. and Sessa, W., 1997. Bacterial infection induces nitric oxide synthase in human neutrophils. *Journal of Clinical Investigation*, 99(1), 110-116.

175. Wölfle, U., Elsholz, F., Kersten, A., Haarhaus, B., Schumacher, U. and Schempp, C., 2016. Expression and Functional Activity of the Human Bitter Taste Receptor TAS2R38 in Human Placental Tissues and JEG-3 Cells. *Molecules*, 21(3), 306.

176. Hristov, K., Chen, M., Kellett, W., Rovner, E. and Petkov, G., 2011. Large-conductance voltage- and Ca2+-activated K+ channels regulate human detrusor smooth muscle function. *American Journal of Physiology-Cell Physiology*, 301(4), C903-C912.

177. Pearson, M., Yep, A., Smith, S. and Mobley, H., 2011. Transcriptome of Proteus mirabilis in the Murine Urinary Tract: Virulence and Nitrogen Assimilation Gene Expression. *Infection and Immunity*, 79(7), ,2619-2631.

178. Ziemba, B. and Falke, J., 2018. A PKC-MARCKS-PI3K regulatory module links Ca2+ and PIP3 signals at the leading edge of polarized macrophages. *PLOS ONE*, 13(5), p.e0196678.

179. Falke, J. and Ziemba, B., 2014. Interplay between phosphoinositide lipids and calcium signals at the leading edge of chemotaxing ameboid cells. *Chemistry and Physics of Lipids*, 182, 73-79.

180. Banadakoppa, M., Goluszko, P., Liebenthal, D., Nowicki, B., Nowicki, S. and Yallampalli, C., 2014. PI3K/Akt pathway restricts epithelial adhesion of Dr+Escherichia coli by down-regulating the expression of decay accelerating factor. *Experimental Biology and Medicine*, 239(5), 581-594.

181. Manning, B. and Cantley, L., 2007. AKT/PKB Signaling: Navigating Downstream. *Cell*, 129(7), 1261-1274.

182. Peixoto, C., Oliveira, W., Araújo, S. and Nunes, A., 2017. AMPK activation: Role in the signaling pathways of neuroinflammation and neurodegeneration. *Experimental Neurology*, 298, 31-41.

183. Guo, Y., Zhang, Y., Hong, K., Luo, F., Gu, Q., Lu, N. and Bai, A., 2014. AMPK Inhibition Blocks ROS-NFκB Signaling and Attenuates Endotoxemia-Induced Liver Injury. *PLoS ONE*, 9(1), e86881.

184. Kamoshita, M., Ozawa, Y., Kubota, S., Miyake, S., Tsuda, C., Nagai, N., Yuki, K., Shimmura, S., Umezawa, K. and Tsubota, K., 2014. AMPK-NF-κB Axis in the Photoreceptor Disorder during Retinal Inflammation. *PLoS ONE*, 9(7), e103013.

185. Yi, C., Jeon, B., Shin, H., Jeong, E., Chang, K., Lee, J., Lee, D., Kim, H., Kang, S., Cho, G., Choi, W. and Roh, G., 2011. Resveratrol activates AMPK and suppresses LPS-induced NF-κB-dependent COX-2 activation in RAW 264.7 macrophage cells. *Anatomy & Cell Biology*, 44(3), 194.

186. Dan, H., Cooper, M., Cogswell, P., Duncan, J., Ting, J. and Baldwin, A., 2008. Akt-dependent regulation of NF-κB is controlled by mTOR and Raptor in association with IKK. *Genes & Development*, 22(11), 1490-1500.

187. Zhou, L., Huang, W., Xu, Y., Gao, C. 2018. Sweet-Taste Receptors Mediated ROS-NLRP3 Inflammasome Signaling Activation—Implications for Diabetic Nephropathy. *Diabetes*, 67(Supplement_1).

188. GA, A., 2015. Isolation of Hexadecanoic Acid Methyl Ester and 1,1,2-Ethanetricarboxylic Acid- 1-Hydroxy-1, 1-Dimethyl Ester from the Calyx of Green Hibiscus Sabdariffa (Linn). *Natural Products Chemistry & Research*, 3(2).

189. R.D. Gautam, Sorrel- a lesser known source of medicinal soft drink and food in India, Nat. Prod. Radiance 3 (5) (2004) 338–341.

190. Okosun, L., ., M. and ., A., 2006. Effect of Sowing Date and Planting Distance on Growth and Yield of Two Cultivars of Roselle (Hibiscus sabdariffa var. sabdariffa). *Journal of Plant Sciences*, 1(4), 297-305.

191. Ali, B., Wabel, N. and Blunden, G., 2005. Phytochemical, pharmacological and toxicological aspects ofHibiscus sabdariffa L.: a review. *Phytotherapy Research*, 19(5), 369-375.

192. A. Ismail, E.H.K. Ikram, H.S.M. Nazril, 2008. Roselle (Hibiscus sabdariffa L.) seeds- nutritional composition, protein quality and health benefits, *Food*, 2 (1), 1–16.

193. R.K. Singh, K.A. Sureja, D. Singh, Amta and Amti, 2006. (Hibiscus sabdariffa L.)-cultural and agricultural dynamics of agrobiodiversity conservation, *Indian J. Tradit.Knowl*, 5 (1), 151–157.

194. Omobuwajo, T., Sanni, L. and Balami, Y., 2000. Physical properties of sorrel (Hibiscus sabdariffa) seeds. *Journal of Food Engineering*, 45(1), ,37-41.

194. D'Heureux-Calix, F. and Badrie, N., 2004. Consumer acceptance and physicochemical quality of processed red sorrel/roselle (Hibiscus sabdariffa L.) sauces from enzymatic extracted calyces. *Food Service Technology*, 4(4), 141-148.

195. Okoro, C., 2010. Production of red wine from roselle (Hibiscus sabdariffa) and pawpaw (Carica papaya) using palm-wine yeast (Saccharomyces cerevisiae). *Nigerian Food Journal*, 25(2).

196. M.K. Bolade, I.B. Oluwalana, O. Ojo, 2009. Commercial practice of roselle (Hibiscus sabdariffa L.) beverage production: optimization of hot water extraction and sweetness level, *World J. Agric. Sci.*, 5 (1), 126–131.

197. J.F. Morton, F.L. Miami, C.F. DowlingJr (Ed.), 1987. Roselle in Fruits of Warm Climates, Media Incorporated, Greensborough, *NC*, 281–286.

198. P.-D. Duh, G.-C. Yen, 1997. Antioxidant activity of three herbal water extracts, *Food Chem.*, 60 (4), 639–645.

199. Da-Costa-Rocha, I., Bonnlaender, B., Sievers, H., Pischel, I. and Heinrich, M., 2014. Hibiscus sabdariffa L. – A phytochemical and pharmacological review. *Food Chemistry*, 165, 424-443.

200. Ali, M., Salih, W., Mohamed, A. and Homeida, A., 1991. Investigation of the antispasmodic potential of Hibiscus sabdariffa calyces. *Journal of Ethnopharmacology*, 31(2), 249-257.

201. Chen, C., Hsu, J., Wang, S., Chiang, H., Yang, M., Kao, E., Ho, Y. and Wang, C., 2003. Hibiscus sabdariffa Extract Inhibits the Development of Atherosclerosis in

Cholesterol-Fed Rabbits. *Journal of Agricultural and Food Chemistry*, 51(18), 5472-5477.

202. Khalid, H., Abdalla, W., Abdelgadir, H., Opatz, T. and Efferth, T., 2012. Gems from traditional north-African medicine: medicinal and aromatic plants from Sudan. *Natural Products and Bioprospecting*, 2(3), 92-103.

203. Chou, S., Lo, H., Li, C., Cheng, L., Chou, P., Lee, Y., Ho, T. and Hsiang, C., 2016. Exploring the effect and mechanism of Hibiscus sabdariffa on urinary tract infection and experimental renal inflammation. *Journal of Ethnopharmacology*, 194, 617-625.

204. Ali, B., Cahliková, L., Opletal, L., Karaca, T., Manoj, P., Ramkumar, A., Al Suleimani, Y., Al Za'abi, M., Nemmar, A., Chocholousova-Havlikova, L., Locarek, M., Siatka, T. and Blunden, G., 2017. Effect of aqueous extract and anthocyanins of calyces of Hibiscus sabdariffa (Malvaceae) in rats with adenine-induced chronic kidney disease. *Journal of Pharmacy and Pharmacology*, 69(9), 1219-1229.

205. Christian, K., Nair, M. and Jackson, J., 2006. Antioxidant and cyclooxygenase inhibitory activity of sorrel (Hibiscus sabdariffa). *Journal of Food Composition and Analysis*, 19(8), 778-783.

206. Chang, Y., 2005. anthocyanins rich extract-induced apoptotic cell death in human promyelocytic leukemia cells. *Toxicology and Applied Pharmacology*, 205(3), 201-212.

207. Murkovic, M., Toplak, H., Adam, U. and Pfannhauser, W., 2000. Analysis of Anthocyanins in Plasma for Determination of their Bioavailability. *Journal of Food Composition and Analysis*, 13(4), 291-296.

208. Tseng, T., Hsu, J., Lo, M., Chu, C., Chou, F., Huang, C. and Wang, C., 1998. Inhibitory effect of Hibiscus protocatechuic acid on tumor promotion in mouse skin. *Cancer Letters*, 126(2), 199-207.

209. Mahadevan N., Shivali, P. K, 2009. *Hibiscus sabdariffa* Linn. An overview, *Nat. Prod. Radiance*, 8 (1), 77–83.

210. Ali, B., Wabel, N. and Blunden, G., 2005. Phytochemical, pharmacological and toxicological aspects of *Hibiscus sabdariffa L.*: a review. *Phytotherapy Research*, 19(5), 369-375.

211. Hirunpanich, V., Utaipat, A., Morales, N., Bunyapraphatsara, N., Sato, H., Herunsale, A. and Suthisisang, C., 2006. Hypocholesterolemic and antioxidant effects of aqueous extracts from the dried calyx of *Hibiscus sabdariffa* L. in hypercholesterolemic rats. *Journal of Ethnopharmacology*, 103(2), 252-260.

212. Jabeur, I., Pereira, E., Barros, L., Calhelha, R., Soković, M., Oliveira, M. and Ferreira, I., 2017. Hibiscus sabdariffa L. as a source of nutrients, bioactive compounds and colouring agents. *Food Research International*, 100, 717-723.

213. Sinela, A., Rawat, N., Mertz, C., Achir, N., Fulcrand, H. and Dornier, M., 2017. Anthocyanins degradation during storage of Hibiscus sabdariffa extract and evolution of its degradation products. *Food Chemistry*, 214, 234-241.

214. Idhm Z., Muhamad I., Mohd Setapar, S. and Sarmidi, M., 2011. Effect of thermal processes on rosselle anthocyanins encapsulated in different polymer matrices. *Journal of Food Processing and Preservation*, 36(2), 176-184.

215. Gradinaru, G., Biliaderis, C., Kallithraka, S., Kefalas, P. and Garcia-Viguera, C., 2003. Thermal stability of Hibiscus sabdariffa L. anthocyanins in solution and in solid state: effects of copigmentation and glass transition. *Food Chemistry*, 83(3), 423-436.

216. Pouget M.P. Vennat B. Lejeune B., Pourrat A. Extraction analysis and study of the stability of Hibiscus anthocyanins. *Lebensm. Technol.*, 23, 103–105.

217. Bridle P., Timberlake C.F. Anthocyanins as natural food colour-selected aspects, 2007. *Food Chem.*, 58 (1-2), 103–109.

218. Tsai P.J. McIntosh P. Pearce B. Camden B.R. Jordan. 2002. Anthocyanin and antioxidant capacity in roselle (Hibiscus sabdariffa L.) extract, *Food Res., Int.* 35, 351–356.

219. Tsai T., Huang H., Chang Y., C.-J. Wang. 2014. An anthocyanin-rich extract from Hibiscus sabdariffa Linnaeus inhibits N-nitrosomethylurea-induced leukemia in rats, *J. Agric. Food Chem*. 62, 1572–1580.

220. Alshami I., Ahmed E. 2014. Hibiscus sabdariffa extract inhibits in vitro biofilm formation capacity of Candida albicans isolated from recurrent urinary tract infections. *Asian Pac. J. Trop. Biomed.* 4(2), 104-108.

221. Borras-Linares I., Fernandez-Arroyo S., Arraez-Roman D., Palmeros-Suarez P.A., Val-Diaz D.R., Andrade-Gonzales I., Fernandez-Gutierrez A., J.F. Gomez-Leyva J.F., Segura-Carretero A. 2015. Characterization of phenolic compounds,

anthocyanidin, antioxidant and antimicrobial activity of 25 varieties of Mexican roselle (Hibiscus sabdariffa), *Ind. Crop Prod.* 69, 385–394.

222. Jabeur I., Pereira E., Barros L., Calhelha R.C., Soković M., Oliveira M.B.P., Ferreira I.C.F.R. 2017. Hibiscus sabdariffa L. as a source of nutrients, bioactive compounds and colouring agents, Food Res. Int. 100, 717–723.

223. Fullerton M., Khatiwada J., Johnson J.U., Davis S., Williams L.L. 2011. Determination of antimicrobial activity of sorrel (Hibiscus sabdariffa) on *Escherichia coli* O157:H7 isolated from food, veterinary, and clinical samples, *J. Med. Food* 14 (9), 950-956.

224. Al-Hashimi A.G., 2012. Antioxidant and antibacterial activities of Hibiscus sabdariffa L. extracts, *Afr. J. Food Sci.* 6 (21), 506–511.

225. Polito, L., Bortolotti, M., Maiello, S., Battelli, M. G., and Bolognesi, A. (2016a). Plants producing ribosome-inactivating proteins in traditional medicine. *Molecules* 21, E1560.

226. Scartezzini, P., and Speroni, E. (2000). Review on some plants of Indian traditional medicine with antioxidant activity. *J. Ethnopharmacol.* 71, 23–43.

227. Gürdal B., Kültür S. 2013. An ethnobotanical study of medicinal plants in Marmaris (Muğla, Turkey). J. Ethnopharmacol. 146 113–126.

228. Saad, D. Y., Soliman, M. M., Baiomy, A. A., Yassin, M. H., and El-Sawy, H. B. 2017. Effects of Karela (Bitter Melon; Momordica charantia) on genes of lipids and carbohydrates metabolism in experimental hypercholesterolemia: biochemical, molecular and histopathological study. *BMC Complement. Altern. Med*. 17:319.

229. Gupta, M., Sharma, S., Gautam, A. K., and Bhadauria, R. (2011). Momordica charantia Linn, (karela): nature's silent healer. *Int. J. Pharm. Sci. Rev. Res.* 11, 32–37.

230. Yoshime, L. T., de Melo, I. L. P., Sattler, J. A. G., de Carvalho, E. B. T., and Mancini-Filho, J. 2016. Bitter gourd (Momordica charantia L.) seed oil as a naturally rich source of bioactive compounds for nutraceutical purposes. *Nutrire.* 41:12.

231. Dinan L., Harmatha J., Lafont R. 2001 Chromatographic procedure for the isolation of plant steroids. *J Chromatogr A,* 935, 105-23.

232. Gamlath C.B., Leslie G.A. 1998. Cucurbitacins of Colocynthis vulgaris. *Phytochem*. 27:3225-3229.

233. Stuppner H., Muller E.P., Wagner H. 1991. Cucurbitacins from Picrorhiza kurrooa. *Phytochem*. 30:305.

234. Subbiah. Method of isolating Cucurbitacin. 1999. US1999/5,925,356. *Jul. 2011*.

235. Meyerhof W., Batram C., Kuhn C., Brockhoff A., Chudoba E., Bufe B., Appendino G., Behrens M. 2010. The molecular receptive ranges of human TAS2R bitter taste receptors. *Chem Senses*. 35(2):157-70.

236. Born S., Levit A., Niv M., Meyerhof W., and Behrens M. 2013. The Human Bitter Taste Receptor TAS2R10 Is Tailored to Accommodate Numerous Diverse Ligands J Neurosci. 33(1): 201–213.

237. Yamamoto K, Ishimaru Y. 2013. Oral and extra-oral taste perception. *Semin Cell Dev Biol.* 24, 240–246.

238. Minihane A. M., Vinoy S., Russell W. R., Baka A., Roche H. M., Tuohy K. M., Teelin J.L., Blaak E. E., Fenech M., Vauzour D., McArdle H., Kremer B. H. A., Sterkman L., Vafeiadou K., Benedetti M., Williams C. M., Calder P.C., 2015. Low-grade inflammation, diet composition and health: current research evidence and its translation. *Br. J. Nutr.* 114, 999–1012.

239. Alam M. A., Uddin R., Subhan N., Rahman M. M., Jain, P., Reza, H. M. 2015. Beneficial role of bitter melon supplementation in obesity and related complications in metabolic syndrome. *J. Lipids*. 496169.

240. Biswas S. K. 2016. Does the interdependence between oxidative stress and inflammation explain the antioxidant paradox? *Oxid. Med. Cell Longev.*:5698931.

241. Chao C. Y., Sung P. J., Wang W. H., Kuo, Y. H. 2014. Anti-inflammatory effect of *Momordica charantia* in sepsis mice. *Molecules*, 19, 12777–12788.

242. Kobori M., Nakayama H., Fukushima K., Ohnishi-Kameyama M., Ono, H.,

Fukushima, T., 2008a. Bitter gourd suppresses lipopolysaccharide induced inflammatory responses. *J. Agric. Food Chem*. 56, 4004–4011.

243. Lii C. K., Chen H. W., Yun W. T., Liu K. L. 2009. Suppressive effects of wild bitter gourd (Momordica charantia Linn. var. abbreviata ser.) fruit extracts on inflammatory responses in RAW264.7 macrophages. J. Ethnopharmacol. 122, 227–233.

244. Svobodova B., Barros L., Calhelha R. C., Heleno S., Alves M. J., Walcott, S. 2017. Bioactive properties and phenolic profile of *Momordica charantia* L. medicinal plant growing wild in Trinidad and Tobago. *Ind. Crops Prod.* 98, 365–373.

245. Hsu C., Fang S., Lju, C., Chen Y. 2013. Inhibitory effects of new varieties of bitter melon on lipopolysaccharide-stimulated inflammatory response in RAW 264.7 cells. *J. Funct. Foods* 5, 1829–1837.

246. Yang W. S., Yang E., Kim M. J., Jeong D., Yoon D. H., Sung G. H., 2018. Momordica charantia inhibits inflammatory responses in murine macrophages via suppression of TAK1. *Am. J. Chin. Med*. 46, 435–452.

247. Cheng H. L., Kuo C. Y., Liao Y. W., Lin C. C. 2012. EMCD, a hypoglycemic triterpene isolated from Momordica charantia wild variant, attenuates TNFalpha-induced inflammation in FL83B cells in an AMP-activated protein kinase-independent manner. *Eur. J. Pharmacol.* 689, 241–248.

248. Xu J., Cao K., Li Y., Zou X., Chen C., Szeto I. M. 2014. Bitter gourd inhibits the development of obesity-associated fatty liver in C57BL/6 mice fed a high-fat diet. *J. Nutr*. 144, 475–483.

249. Bao B., Chen Y. G., Zhang L., Na X. Y., Wang X., Liu J. 2013. *Momordica charantia,* (bitter melon) reduces obesity-associated macrophage and mast cell infiltration as well as inflammatory cytokine expression in adipose tissues. *PLoS One* 8:e84075.

250. Bai J., Zhu Y., Dong Y. 2018. Obese rats supplemented with bitter melon display marked shifts in the expression of genes controlling inflammatory response and lipid metabolism by RNA-Seq analysis of colonic mucosa. *Genes Genomics* 40, 561–567.

251. Bai, J., Zhu, Y., Dong, Y. 2016. Response of gut microbiota and inflammatory status to bitter melon (*Momordica charantia* L.) in high fat diet induced obese rats. J. Ethnopharmacol. 194, 717–726.

252. Sung H. C., Liu C. W., Hsiao C. Y., Lin S. R., Yu I. S., Lin S. W. 2018. The effects of wild bitter gourd fruit extracts on ICAM-1 expression in pulmonary epithelial cells of C57BL/6J mice and microRNA-221/222 knockout mice: involvement of the miR-221/-222/PI3K/AKT/NF-kB pathway. Phytomedicine. 42, 90–99.

253. Kim K. B., Lee S., Kang I., Kim J. H. 2018. *Momordica charantia* ethanol extract attenuates H2O2-induced cell death by its antioxidant and anti-apoptotic properties in human neuroblastoma SK-N-MC cells. *Nutrients*. 10:E1368.

254. Lin Z. Y., Liu X., Yang F., Yu Y. Q. 2012. Structural characterization and identification of five triterpenoid saponins isolated from *Momordica cochinchinensis* extracts by liquid chromatography/tandem mass spectrometry. *Int. J. Mass Spectrom.* 32, 43–66.

255. Liu, C. H., Yen, M. H., Tsang, S. F., Gan, K. H., Hsu, H. Y., and Lin, C. N. 2010. Antioxidant triterpenoids from the stems of Momordica charantia. *Food Chem*. 118, 751–756.

256. Padmashree, A., Sharma, G. K., Semwal, A. D., and Bawa, A. S. 2010. Studies on antioxygenic activity of bitter gourd (Momordica charantia) and its fractions using various in vitro models. *J. Sci. Food Agric.* 91, 776–782.

257. Kim H. Y., Sin S. M., Lee S., Cho K. M., Cho E. J. 2013. The butanol fraction of bitter melon (*Momordica charantia*) scavenges free radicals and attenuates oxidative stress. *Prev. Nutr. Food Sci*. 18, 18–22.

258. Myojin, C., Enami, N., Nagata, A., Yamaguchi, T., Takamura, H., and Matoba, T. 2008. Changes in the radical-scavenging activity of bitter gourd (*Momordica charantia L*.) during freezing and frozen storage with or without blanching. *J. Food Sci.* 73, C546–C550.

259. Soo May, L., Sanip, Z., Ahmed Shokri, A., Abdul Kadir, A., and Md Lazin, M. R. 2018. The effects of *Momordica charantia* (bitter melon) supplementation in patients with primary knee osteoarthritis: a single-blinded, randomized controlled trial. Complement. *Ther. Clin. Pract.* 32, 181–186.

260. Portillo-Torres, L., Bernardino-Nicanor, A., Gómez-Aldapa, C., González-Montiel, S., Rangel-Vargas, E., Villagómez-Ibarra, J., González-Cruz, L., Cortés-López, H. and Castro-Rosas, J., 2019. Hibiscus Acid and Chromatographic Fractions from Hibiscus Sabdariffa Calyces: Antimicrobial Activity against Multidrug-Resistant Pathogenic Bacteria. *Antibiotics*, 8(4), p.218.

261. Lou, Z., Wang, H., Zhu, S., Ma, C. and Wang, Z., 2011. Antibacterial Activity and Mechanism of Action of Chlorogenic Acid. *Journal of Food Science*, 76(6), pp.M398-M403.

262. Pei, K., Ou, J., Huang, J. and Ou, S., 2016. p-Coumaric acid and its conjugates: dietary sources, pharmacokinetic properties and biological activities. *Journal of the Science of Food and Agriculture*, 96(9), pp.2952-2962.

263. Liszt, K., Ley, J., Lieder, B., Behrens, M., Stöger, V., Reiner, A., Hochkogler, C., Köck, E., Marchiori, A., Hans, J., Widder, S., Krammer, G., Sanger, G., Somoza, M., Meyerhof, W. and Somoza, V., 2017. Caffeine induces gastric acid secretion via bitter taste signaling in gastric parietal cells. *Proceedings of the National Academy of Sciences*, 114(30), pp.E6260-E6269.

264. Hubatsch, I., Ragnarsson, E. and Artursson, P., 2007. Determination of drug permeability and prediction of drug absorption in Caco-2 monolayers. *Nature Protocols*, 2(9), pp.2111-2119.

265. Bunchongprasert, K. and Shao, J., 2020. Impact of Media in Transport Study on Cell Monolayer Integrity and Permeability. *Journal of Pharmaceutical Sciences*, 109(2), pp.1145-1152.

266. Dandawate, P., Subramaniam, D., Panovich, P., Standing, D., Krishnamachary, B., Kaushik, G., Thomas, S., Dhar, A., Weir, S., Jensen, R. and Anant, S., 2020. Cucurbitacin B and I inhibits colon cancer growth by targeting the Notch signaling pathway. *Scientific Reports*, 10(1).

267. Wang, X., Tanaka, M., Peixoto, H. and Wink, M., 2017. Cucurbitacins: elucidation of their interactions with the cytoskeleton. *PeerJ*, 5, p.e3357.

268. Dakeng, S., Duangmano, S., Jiratchariyakul, W., U-Pratya, Y., Bögler, O. and Patmasiriwat, P., 2011. Inhibition of Wnt signaling by cucurbitacin B in breast cancer cells: Reduction of Wnt-associated proteins and reduced translocation of galectin-3-mediated β-catenin to the nucleus. *Journal of Cellular Biochemistry*, 113(1), pp.49-60.

269. Yasui, Y., Hosokawa, M., Sahara, T., Suzuki, R., Ohgiya, S., Kohno, H., Tanaka, T. and Miyashita, K., 2005. Bitter gourd seed fatty acid rich in 9c,11t,13t-conjugated linolenic acid induces apoptosis and up-regulates the GADD45, p53 and PPARγ in human colon cancer Caco-2 cells. *Prostaglandins, Leukotrienes and Essential Fatty Acids*, 73(2), pp.113-119.

270. Kwatra, D., Dandawate, P., Padhye, S. and Anant, S., 2016. Bitter Melon as a Therapy for Diabetes, Inflammation, and Cancer: a Panacea?. *Current Pharmacology Reports*, 2(1), pp.34-44.

271. Wu, S., Yue, G., To, M., Keller, A., Lau, C. and Kennelly, E., 2014. Transport in Caco-2 Cell Monolayers of Antidiabetic Cucurbitane Triterpenoids from Momordica charantia Fruits. *Planta Medica*, 80(11), pp.907-911.

272. Jeon, T., Seo, Y. and Osborne, T., 2011. Gut bitter taste receptor signalling induces ABCB1 through a mechanism involving CCK. *Biochemical Journal*, 438(1), pp.33-37.

273. Huang, T., Gu, P., Zheng, T., Gou, L. and Liu, Y., 2022. Piperine, as a TAS2R14 agonist, stimulates the secretion of glucagon-like peptide-1 in the human enteroendocrine cell line Caco-2. *Food & Function*, 13(1), pp.242-254.

274. Ferruzza, S., Rossi, C., Scarino, M. and Sambuy, Y., 2012. A protocol for differentiation of human intestinal Caco-2 cells in asymmetric serum-containing medium. *Toxicology in Vitro*, 26(8), pp.1252-1255.

275. Fleet, J., Wang, L., Vitek, O., Craig, B. and Edenberg, H., 2003. Gene expression profiling of Caco-2 BBe cells suggests a role for specific signaling pathways during intestinal differentiation. *Physiological Genomics*, 13(1), pp.57-68.

276. Tremblay, E., Auclair, J., Delvin, E., Levy, E., Ménard, D., Pshezhetsky, A., Rivard, N., Seidman, E., Sinnett, D., Vachon, P. and Beaulieu, J., 2006. Gene expression profiles of normal proliferating and differentiating human intestinal epithelial cells: A comparison with the Caco-2 cell model. *Journal of Cellular Biochemistry*, 99(4), pp.1175-1186.